Introduction

- The **boundary layer** of a flowing fluid is **the thin layer close to the wall**
- In a flow field, **viscous stresses are very prominent within this layer**.
- Although the layer is thin, it is very important to know the details of flow within it.
- The **main-flow velocity** within this layer **tends to zero** while approaching the wall **(no-slip condition)**.
- Also the gradient of this velocity component in a direction normal to the surface is large as compared to the gradient in the streamwise direction.

Boundary Layer Equations

- In 1904, **Ludwig Prandtl,** the well known German scientist, introduced the concept of boundary layer and **derived the equations for boundary layer flow** by correct reduction of Navier-Stokes equations.
- He hypothesized that **for fluids having relatively small viscosity**, **the effect of internal friction in the fluid is significant only in a narrow region surrounding solid boundaries or bodies over which the fluid flows.**
- Thus, close to the body is the boundary layer where **shear stresses exert an increasingly larger effect** on the fluid **as one moves from free stream towards the solid boundary.**
- However, **outside the boundary layer where the effect of the shear stresses on the flow is small compared to values inside the boundary layer (since the velocity gradient** $\partial u / \partial y$ **is negligible)**,---------

1. the fluid particles experience **no vorticity** and therefore**,**
2. the flow is similar to a **potential flow.**

- Hence, the ***surface*** **at the boundary layer interface** is a rather fictitious one, that **divides rotational and irrotational flow.** Fig 28.1 shows Prandtl's model regarding boundary layer flow.
- Hence with the exception of the immediate vicinity of the surface, the flow is frictionless (inviscid) and the velocity is *U* (the potential velocity).
- In the region, very near to the surface (in the thin layer), there is friction in the flow which signifies that the fluid is retarded until it adheres to the surface (**no-slip condition).**
- The transition of the mainstream velocity from zero at the surface (with respect to the surface) to full magnitude takes place across the boundary layer.

About the boundary layer

- Boundary layer **thickness is** δ which is a **function of** the coordinate direction ***x*** .
- The thickness is considered to be **very small compared to the characteristic length *L*** of the domain.
- In the normal direction, **within this thin layer**, the gradient $\partial u / \partial y$ **is very large compared to** the gradient in the flow direction $\partial u / \partial x$ **.**

Now we take up the Navier-Stokes equations for : steady, two dimensional, laminar, incompressible flows.

Considering the Navier-Stokes equations together with the equation of continuity, the following dimensional form is obtained.

$$u\frac{\partial u}{\partial x}+v\frac{\partial u}{\partial y}=-\frac{1}{\rho}\frac{\partial p}{\partial x}+\frac{\mu}{\rho}\left[\frac{\partial^2 u}{\partial x^2}+\frac{\partial^2 u}{\partial y^2}\right] \quad (28.1)$$

$$u\frac{\partial v}{\partial x}+v\frac{\partial v}{\partial y}=-\frac{1}{\rho}\frac{\partial p}{\partial x}+\frac{\mu}{\rho}\left[\frac{\partial^2 v}{\partial x^2}+\frac{\partial^2 v}{\partial y^2}\right] \quad (28.2)$$

$$\frac{\partial u}{\partial x}+\frac{\partial v}{\partial y}=0 \quad (28.3)$$

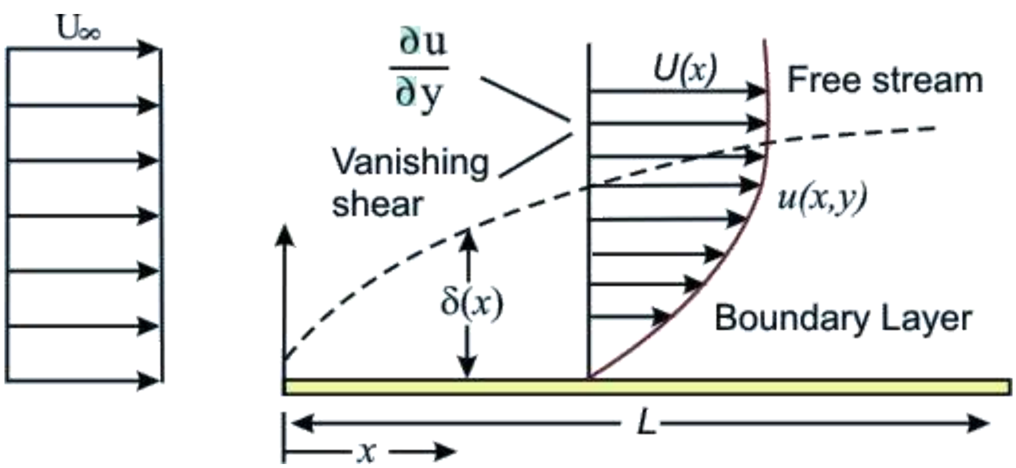

Fig 28.1 Boundary layer and Free Stream for Flow Over a flat plate

- u - velocity component along x direction.
- v - velocity component along y direction
- p - static pressure

- ρ - density.
- μ - dynamic viscosity of the fluid

- The equations are now non-dimensionalised.
- The l**ength and the velocity scales** are chosen as ***L*** **and** U_∞**respectively.**
- The non-dimensional variables are:

$$u* = \frac{u}{U_\infty}, v* = \frac{v}{U_\infty}, p* = \frac{p}{\rho U_\infty^2}$$

$$x* = \frac{x}{L}, y* = \frac{y}{L}$$

where $U_\infty$is the dimensional free stream velocity and the pressure is non-dimensionalised by twice the dynamic pressure $p_d = (1/2)\rho U_\infty^2$.

Using these non-dimensional variables, the Eqs (28.1) to (28.3) become

$u*\frac{\partial u*}{\partial x*} + v*\frac{\partial u*}{\partial y*} = -\frac{\partial p*}{\partial x*} + \frac{1}{\text{Re}}\left[\frac{\partial^2 u*}{\partial x*^2} + \frac{\partial^2 u*}{\partial y*^2}\right]$ click for details	(28.4)
$u*\frac{\partial v*}{\partial x*} + v*\frac{\partial v*}{\partial y*} = -\frac{\partial p*}{\partial x*} + \frac{1}{\text{Re}}\left[\frac{\partial^2 v*}{\partial x*^2} + \frac{\partial^2 v*}{\partial y*^2}\right]$	(28.5)
$\frac{\partial u*}{\partial x*} + \frac{\partial v*}{\partial y*} = 0$	(28.6)

where the Reynolds number,

$$\mathrm{Re} = \frac{\rho U_\infty L}{\mu}$$

Order of Magnitude Analysis

- Let us examine what happens to the *u* velocity as we go across the boundary layer.
  At the **wall** the *u* velocity is **zero** [with respect to the wall and absolute zero for a stationary wall (which is normally implied if not stated otherwise)].
  The value of *u* on the **inviscid side**, that is on the free stream side beyond the boundary layer is ***U***.
  For the case of external flow over a flat plate, this ***U*** is equal to U_∞.
- Based on the above, we can identify the following scales for the boundary layer variables:

Variable	***Dimensional scale***	***Non-dimensional scale***
u	U_∞	1
x	L	1
y	δ	$\varepsilon = \delta / L$

- The **symbol** ε **describes a value much smaller than 1.**
- Now we analyse equations 28.4 - 28.6, and look at the order of magnitude of each individual term

Eq 28.6 - the continuity equation

One **general rule** of incompressible fluid mechanics is that **we are not allowed to drop any term from the continuity equation**.

- From the scales of boundary layer variables, the derivative $\partial u^* / \partial x^*$ is of the order 1.
- The second term in the continuity equation $\partial v^* / \partial y^*$ should also be of the order 1.The reason being v^* has to be of the order ε because y^* becomes $\varepsilon (= \delta / L)$ at its maximum.

Eq 28.4 - x direction momentum equation

- Inertia terms are of the order 1.
- $\partial^2 u / \partial x^2$ is of the order 1
- $\partial^2 u / \partial y^2$ is of the order $(1/\varepsilon^2)$.

However after multiplication with 1/Re, the sum of the two second order derivatives should produce at least one term which is of the same order of magnitude as the inertia terms. This is possible only if the Reynolds number (Re) is of the order of $(1/\varepsilon^2)$.

- It follows from that $-\partial p^* / \partial x^*$ will not exceed the order of 1 so as to be in balance with the remaining term.
- Finally, Eqs (28.4), (28.5) and (28.6) can be rewritten as

$$u^*\frac{\partial u^*}{\partial x^*}+v^*\frac{\partial u^*}{\partial y^*}=-\frac{\partial p^*}{\partial x^*}+\frac{1}{\mathrm{Re}}\left[\frac{\partial^2 u^*}{\partial x^{*2}}+\frac{\partial^2 u^*}{\partial y^{*2}}\right] \tag{28.4}$$

$$(1)\frac{(1)}{(1)} \qquad (\varepsilon)\frac{(1)}{(\varepsilon)}=(1) \qquad (\varepsilon^2)\left[\frac{(1)}{(1)}+\frac{1}{(\varepsilon^2)}\right]$$

$$u^*\frac{\partial v^*}{\partial x^*}+v^*\frac{\partial v^*}{\partial y^*}=-\frac{\partial p^*}{\partial x^*}+\frac{1}{\mathrm{Re}}\left[\frac{\partial^2 v^*}{\partial x^{*2}}+\frac{\partial^2 v^*}{\partial y^{*2}}\right] \tag{28.5}$$

$$(1)\frac{(\varepsilon)}{(1)} \qquad (\varepsilon)\frac{(\varepsilon)}{(\varepsilon)}=(?) \qquad (\varepsilon^2)\left[\frac{(\varepsilon)}{(1)}+\frac{\varepsilon}{(\varepsilon^2)}\right]$$

$$\frac{\partial u^*}{\partial x^*}+\frac{\partial v^*}{\partial y^*}=0 \tag{28.6}$$

$$\frac{(1)}{(1)} \qquad \frac{(\varepsilon)}{(\varepsilon)}$$

As a consequence of the order of magnitude analysis, $\partial^2 u^* / \partial x^{*2}$ can be dropped from the *x* direction momentum equation, because on multiplication with $1/Re$ it assumes the smallest order of magnitude.

Eq 28.5 - *y* direction momentum equation.

- All the terms of this equation are of a smaller magnitude than those of Eq. (28.4).
- This equation can only be balanced if $\partial p^* / \partial y^*$ is of the same order of magnitude as other terms.
- Thus they momentum equation reduces to

$$\frac{\partial p^*}{\partial y^*} = O(\varepsilon) \qquad (28.7)$$

- This means that the **pressure across the boundary layer does not change**. The **pressure is impressed on the boundary layer**, and its value is determined by hydrodynamic considerations.
- This also implies that the **pressure *p* is only a function of *x***. The pressure forces on a body are solely **determined by the inviscid flow outside the boundary layer.**
- The application of Eq. (28.4) at the outer edge of boundary layer gives

$$u^* \frac{\partial u^*}{\partial x^*} = -\frac{\partial p^*}{\partial x^*} \qquad (28.8a)$$

In dimensional form, this can be written as

$$U \frac{dU}{dx} = -\frac{1}{\rho} \frac{\partial p}{\partial x} \qquad (28.8b)$$

On integrating Eq (28.8b) the well known Bernoulli's equation is obtained

$$p + \frac{1}{2} \rho U^2 = \textit{a constant} \qquad (28.9)$$

- Finally, it can be said that by the order of magnitude analysis, the Navier-Stokes equations are simplified into equations given below.

$$u^* \frac{\partial u^*}{\partial x^*} + v^* \frac{\partial u^*}{\partial y^*} = -\frac{\partial p^*}{\partial x^*} + \frac{1}{\mathrm{Re}} \frac{\partial^2 u^*}{\partial y^{*2}} \qquad (28.10)$$

-

$$\frac{\partial p^*}{\partial y^*} = 0 \qquad (28.11)$$

-

$$\frac{\partial u^*}{\partial x^*} + \frac{\partial v^*}{\partial y^*} = 0 \qquad (28.12)$$

-
- These are known as Prandtl's boundary-layer equations.

The available boundary conditions are:

Solid surface $at\ y^* = 0, u^* = 0 = v^*$

or $at\ y = 0, u = 0 = v$ (28.13)

Outer edge of boundary-layer

$$at\ y^* = (\varepsilon) = \frac{\delta}{L}, u^* = 1$$

or $at\ y = \delta, u = U(x)$ (28.14)

- The unknown pressure *p* in the x-momentum equation can be determined from Bernoulli's Eq. (28.9), if the inviscid velocity distribution *U(x)* is also known.

We solve the Prandtl boundary layer equations for $u^*(x,y)$ and $v^*(x,y)$ with *U* obtained from the outer inviscid flow analysis. The equations are solved by commencing at the leading edge of the body and moving downstream to the desired location

- it allows the no-slip boundary condition to be satisfied which constitutes a significant improvement over the potential flow analysis while solving real fluid flow problems.

- The **Prandtl boundary layer equations** are thus a simplification of the Navier-Stokes equations.

Boundary Layer Coordinates

- The boundary layer equations derived are in Cartesian coordinates.
- The Velocity components u and v represent x and y direction velocities respectively.
- For objects with small curvature, these equations can be used with -
  - x coordinate : streamwise direction
  - y coordinate : normal component
- They are called **Boundary Layer Coordinates.**

Application of Boundary Layer Theory

- The Boundary-Layer Theory is not valid beyond the point of separation.
- At the point of separation, boundary layer thickness becomes quite large for the thin layer approximation to be valid.
- It is important to note that boundary layer theory can be used to locate the point of seperation itself.
- In applying the boundary layer theory although U is the free-stream velocity at the outer edge of the boundary layer, it is interpreted as the fluid velocity at the wall calculated from inviscid flow considerations (known as **Potential Wall Velocity**)
- Mathematically, application of the boundary - layer theory converts the character of governing Navier-Stroke equations from elliptic to parabolic
- This allows the marching in flow direction, as the solution at any location is independent of the conditions farther downstream.

Blasius Flow Over A Flat Plate

- The classical problem considered by H. Blasius was
  1. Two-dimensional, steady, incompressible flow over a flat plate at zero angle of incidence with respect to the uniform stream of velocity U_∞.
  2. The fluid extends to infinity in all directions from the plate.

The physical problem is already illustrated in Fig. 28.1

- Blasius wanted to determine
  (a) the velocity field solely within the boundary layer,
  (b) the boundary layer thickness (δ),
  (c) the shear stress distribution on the plate, and
  (d) the drag force on the plate.
- The Prandtl boundary layer equations in the case under consideration are

$$u\frac{\partial u}{\partial x}+\mathrm{v}\frac{\partial u}{\partial y}=\nu\frac{\partial^2 u}{\partial y^2} \quad (28.15)$$

$$\nu=\mu/\rho$$

$$\frac{\partial u}{\partial x}+\frac{\partial u}{\partial y}=0$$

The boundary conditions are

$$at\ y=0,\ u=v=0 \quad (28.16)$$

$$at\quad y=\infty,\quad u=U_\infty$$

- Note that the substitution of the term $-\frac{1}{\rho}\frac{dp}{dx}$ in the original boundary layer momentum equation in terms of the free stream velocity produces $U_\infty\frac{dU_\infty}{dx}$ which is equal to zero.
- Hence the governing Eq. (28.15) does not contain any pressure-gradient term.
- However, the characteristic parameters of this problem are U_∞, ν, x, y that is, $u=u(U_\infty,\nu,x,y)$
- This relation has five variables U_∞, ν, x, y.
- It involves two dimensions, length and time.
- Thus it can be reduced to a dimensionless relation in terms of (5-2) =3 quantities (**Buckingham Pi Theorem**)
- Thus a similarity variables can be used to find the solution

- Such flow fields are called self-similar flow field .

Law of Similarity for Boundary Layer Flows

- It states that the *u* component of velocity with two velocity profiles of *u(x,y)* at different *x* locations differ only by scale factors in *u* and *y* .
- Therefore, the velocity profiles *u(x,y)* at all values of *x* can be made congruent if they are plotted in coordinates which have been made dimensionless with reference to the scale factors.
- The local free stream velocity *U(x)* at section *x* is an obvious scale factor for *u*, because the dimensionless *u(x)* varies between zero and unity with *y* at all sections.
- The scale factor for *y* , denoted by *g(x)* , is proportional to the local boundary layer thickness so that *y* itself varies between zero and unity.
- Velocity at two arbitrary *x* locations, namely x_1 and x_2 should satisfy the equation

$$\frac{u\left[x_1,\{y/g(x_1)\}\right]}{U(x_1)}=\frac{u\left[x_2,\{y/g(x_2)\}\right]}{U(x_2)} \qquad (28.17)$$

- Now, for Blasius flow, it is possible to identify g(x) with the boundary layers thickness δ we know

$$\varepsilon=\frac{\delta}{L}\sim\frac{1}{\sqrt{\mathrm{Re}_L}}$$

Thus in terms of x we get

$$\frac{\delta}{x}\sim\frac{1}{\sqrt{\frac{U_\infty x}{\nu}}}$$

$$\delta\sim\sqrt{\frac{\nu x}{U_\infty}}$$

i.e.,

$$\frac{u}{U_\infty} = F\left(\frac{y}{\sqrt{\frac{\nu x}{U_\infty}}}\right) = F(\eta) \tag{28.18}$$

where $\eta \sim \frac{y}{\delta}$ and $\delta \sim \sqrt{\frac{\nu x}{U_\infty}}$

or more precisely,

$$\eta = \frac{y}{\sqrt{\frac{\nu x}{U_\infty}}} \tag{28.19}$$

$$y = \eta\sqrt{\frac{\nu x}{U_\infty}}$$

$$dy = \sqrt{\frac{\nu x}{U_\infty}}d\eta$$

The stream function can now be obtained in terms of the velocity components as

$$\psi = \int u dy = \int U_\infty F(\eta)\sqrt{\frac{\nu x}{U_\infty}}d\eta = \sqrt{U_\infty \nu x}\int F(\eta)d\eta$$

or

$$\psi = \sqrt{U_\infty \nu x}f(\eta) + D \tag{28.20}$$

where D is a constant. Also $\int F(\eta)d\eta = f(\eta)$ and the constant of integration is zero if the stream function at the solid surface is set equal to zero.

Now, the velocity components and their derivatives are:

$$u = \frac{\partial \psi}{\partial y} = \frac{\partial \psi}{\partial \eta}.\frac{\partial \eta}{\partial y} = U_\infty f'(\eta) \tag{28.21a}$$

$$v = -\frac{\partial \psi}{\partial x} = -\sqrt{U_\infty \nu}\left[\frac{1}{2}.\frac{1}{\sqrt{x}}f(\eta) + \sqrt{x}f'(\eta)\left\{-\frac{1}{2}\frac{y}{\sqrt{\nu x/U_\infty}}\frac{1}{x}\right\}\right]$$

or

$$v = \frac{1}{2}\sqrt{\frac{\nu U_\infty}{x}}\left[\eta f'(\eta) - f(\eta)\right] \qquad (28.21b)$$

$$\frac{\partial u}{\partial x} = U_\infty f''(\eta)\frac{\partial \eta}{\partial x} = U_\infty f''(\eta)\left[-\frac{1}{2}.\frac{y}{\sqrt{\nu x/U_\infty}}\frac{1}{x}\right]$$

$$\frac{\partial u}{\partial x} = -\frac{U_\infty}{2}.\frac{\eta}{x}.f''(\eta) \qquad (28.21c)$$

$$\frac{\partial u}{\partial y} = U_\infty f''(\eta)\frac{\partial \eta}{\partial y} = U_\infty f''(\eta)\left[\frac{1}{\sqrt{\nu x/U_\infty}}\right]$$

$$\frac{\partial u}{\partial y} = U_\infty\sqrt{\frac{U_\infty}{\nu x}}f''(\eta) \qquad (28.21d)$$

$$\frac{\partial^2 u}{\partial y^2} = U_\infty\sqrt{\frac{U_\infty}{\nu x}}f''(\eta)\left\{\frac{1}{\sqrt{\nu x/U_\infty}}\right\}$$

$$\frac{\partial^2 u}{\partial y^2} = \frac{U_\infty^2}{\nu x}f'''(\eta) \qquad (28.21e)$$

 Substituting (28.2) into (28.15), we have

$$-\frac{U_\infty^2}{2}\frac{\eta}{x}.f'(\eta)f''(\eta) + \frac{U_\infty^2}{2x}\left[\eta f'(\eta) - f(\eta)\right]f''(\eta) = \frac{U_\infty^2}{x}f'''(\eta)$$

$$-\frac{1}{2}\frac{U_\infty^2}{x}f(\eta)f''(\eta) = \frac{U_\infty^2}{x}f'''(\eta)$$

or,

$$2f'''(\eta)+f(\eta)f''(\eta)=0 \qquad (28.22)$$

where

$$f(\eta)=\int F(\eta)d\eta+C$$
$$=\int \frac{u}{U_\infty}d\eta+C$$

and

$$\eta=\frac{y}{\sqrt{\frac{\nu x}{U_\infty}}}$$

This is known as Blasius Equation .

Contd. from Previous Slide

- The boundary conditions as in Eg. (28.16), in combination with Eg. (28.21a) and (28.21b) become

at $y=0, u=0$, therefore $\eta=0: f(\eta)=0, f'(\eta)=0$

at $y=\infty, u=U_\infty$ therefore $\eta=\infty: F(\eta)=f'(\eta)=1$ (28.23)

Equation (28.22) is a **third order nonlinear differential equation .**

- Blasius obtained the solution of this equation in the form of series expansion through analytical techniques
- We shall not discuss this technique. However, we shall discuss a numerical technique to solve the aforesaid equation which can be understood rather easily.
- Note that the **equation for** f **does not contain** x .

- **Boundary conditions at $x = 0$ and $y = \infty$ merge into the condition $\eta \to \infty, u / U_\infty = f' = 1$. This is the key feature of similarity solution.**

- We can rewrite Eq. (28.22) as three first order differential equations in the following way

$$f' = G \qquad (28.24a)$$

$$G' = H \qquad (28.24b)$$

$$H' = -\frac{1}{2} fH \qquad (28.24c)$$

- Let us next consider the boundary conditions.

1. The condition $f(0) = 0$ remains valid.
2. The condition $f'(0) = 0$ means that $G(0) = 0$.
3. The condition $f'(\infty) = 1$ gives us $G(\infty) = 1$.

Note that the equations for *f* and *G* have initial values. However, the value for H(0) is not known. Hence, we do not have a usual initial-value problem.

Shooting Technique

We handle this problem as an initial-value problem by choosing values of $H(0)$ and solving by numerical methods $f(\eta), G(\eta)$, and $H(\eta)$.

In general, the condition $G(\infty) = 1$ will not be satisfied for the function G arising from the numerical solution.

We then choose other initial values of H so that eventually we find an $H(0)$ which results in $G(\infty) = 1$.

This method is called the shooting technique **.**

- In Eq. (28.24), the primes refer to differentiation wrt. the similarity variable η. The integration steps following Runge-Kutta method are given below.

$$f_{n+1} = f_n + \frac{1}{6}(k_1 + 2k_2 + 2k_3 + k_4) \qquad (28.25a)$$

$$G_{n+1} = G_n + \frac{1}{6}(l_1 + 2l_2 + 2l_3 + l_4) \qquad (28.25b)$$

$$H_{n+1} = H_n + \frac{1}{6}(m_1 + 2m_2 + 2m_3 + m_4) \qquad (28.25c)$$

- One moves from η_n to $\eta_{n+1} = \eta_n + h$. A fourth order accuracy is preserved if *h* is constant along the integration path, that is, $\eta_{n+1} - \eta_n = h$ for all values of *n* . The values of *k, l* and *m* are as follows.
- For generality let the system of governing equations be

$$f' = F_1(f, G, H, \eta), G' = F_2(f, G, H, \eta) \,\&\, H' = F_3(f, G, H, \eta)$$

$$k_1 = hF_1(f_n, G_n, H_n, \eta_n)$$

$$l_1 = hF_2(f_n, G_n, H_n, \eta_n)$$

$$m_1 = hF_3(f_n, G_n, H_n, \eta_n)$$

$$k_2 = hF_1\left\{\left((f_n + \frac{1}{2}k_1), (G_n + \frac{1}{2}l_1), (H_n + \frac{1}{2}m_1), (\eta_n + \frac{h}{2})\right)\right\}$$

$$l_2 = hF_2\left\{\left((f_n + \frac{1}{2}k_1), (G_n + \frac{1}{2}l_1), (H_n + \frac{1}{2}m_1), (\eta_n + \frac{h}{2})\right)\right\}$$

$$m_2 = hF_3\left\{\left((f_n + \frac{1}{2}k_1), (G_n + \frac{1}{2}l_1), (H_n + \frac{1}{2}m_1), (\eta_n + \frac{h}{2})\right)\right\}$$

In a similar way K_3, l_3, m_3 and k_4, l_4, m_4 mare calculated following standard formulae for the Runge-Kutta integration. For example, K_3 is given by

$$k_3 = hF_1\left\{\left((f_n + \frac{1}{2}k_2), (G_n + \frac{1}{2}l_2), (H_n + \frac{1}{2}m_2), (\eta_n + \frac{h}{2})\right)\right\}$$

The functions F_1, $F_2$and F_3 are G, H , *- f H / 2* respectively. Then at a distance $\Delta\eta$ from the wall, we have

$$f(\Delta\eta) = f(0) + G(0)\Delta\eta \qquad (28.26a)$$

$$G(\Delta\eta) = G(0) + H(0)\Delta\eta \qquad (28.26b)$$

$$H(\Delta\eta) = H(0) + H'(0)\Delta\eta \qquad (28.26c)$$

$$H'(\Delta\eta) = -\frac{1}{2} f(\Delta\eta) H(\Delta\eta) \qquad (28.26d)$$

- As it has been mentioned earlier $f''(0) = H(0) = \lambda$ is unknown. It must be determined such that the condition $f'(\infty) = G(\infty) = 1$ is satisfied.

The condition at infinity is usually approximated at a finite value of η (around $\eta = 10$). The process of obtaining λ accurately involves iteration and may be calculated using the procedure described below.

- For this purpose, consider Fig. 28.2(a) where the solutions of G versus η for two different values of $H(0)$ are plotted.
  The values of $G(\infty)$ are estimated from the G curves and are plotted in Fig. 28.2(b).

- The value of $H(0)$ now can be calculated by finding the value $\tilde{H}(0)$ at which the line 1-2 crosses the line $G(\infty) = 1$ By using similar triangles, it can be said that $\frac{\tilde{H}(0) - H(0)_1}{1 - G(\infty)_1} = \frac{H(0)_2 - H(0)_1}{G(\infty)_2 - G(\infty)_1}$. By solving this, we get $\tilde{H}(0)$.

- Next we repeat the same calculation as above by using $\tilde{H}(0)$ and the better of the two initial values of $H(0)$. Thus we get another improved value $\tilde{\tilde{H}}(0)$. This process may continue, that is, we use $\tilde{\tilde{H}}(0)$ and $\tilde{H}(0)$ as a pair of values to find more improved values for $H(0)$, and so forth. The better guess for H (0) can also be obtained by using the Newton Raphson Method. It should be always kept in mind that for each value of $H(0)$, the curve $G(\eta)$ versus η is to be examined to get the proper value of $G(\infty)$.

- The functions $f(\eta), f'(\eta) = G$ and $f''(\eta) = H$ are plotted in Fig. 28.3.The velocity components, *u* and *v* inside the boundary layer can be computed from Eqs (28.21a) and (28.21b) respectively.

- A sample computer program in FORTRAN follows in order to explain the solution procedure in greater detail. The program uses Runge Kutta integration together with the Newton Raphson method

Download the program

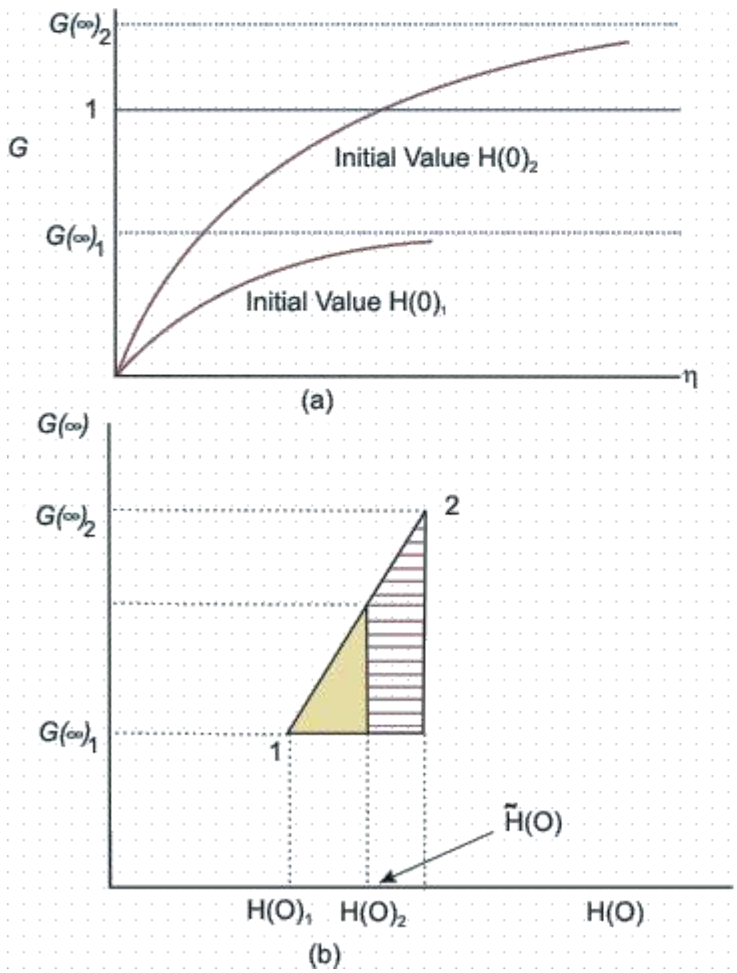

Fig 28.2 Correcting the initial guess for H(O)

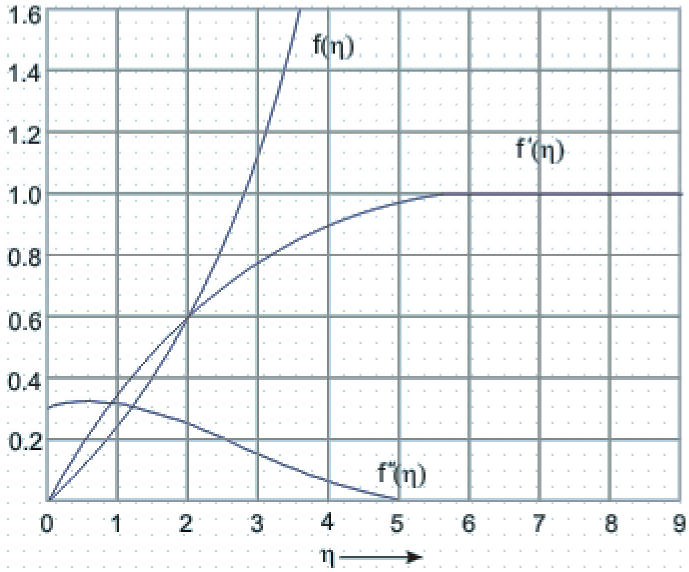

Fig 28.3 f, G and H distribution in the boundary layer

- Measurements to test the accuracy of theoretical results were carried out by many scientists. In his experiments, J. Nikuradse, found excellent agreement with the theoretical results with respect to velocity distribution (u/U_∞) within the boundary layer of a stream of air on a flat plate.
- In the next slide we'll see some values of the velocity profile shape $f'(\eta) = u/U_\infty = G$ and $f''(\eta) = H$ in tabular format.

Values of the velocity profile shape $f'(\eta) = u/U_\infty = G \; and \; f''(\eta) = H$

Table 28.1 The Blasius Velocity Profile $G = u/U_\infty \; f \; and \; H$

η	f	G	H
0	0	0	0.33206
0.2	0.00664	0.006641	0.33199

0.4	0.02656	0.13277	0.33147
0.8	0.10611	0.26471	0.32739
1.2	0.23795	0.39378	0.31659
1.6	0.42032	0.51676	0.29667
2.0	0.65003	0.62977	0.26675
2.4	0.92230	0.72899	0.22809
2.8	1.23099	0.81152	0.18401
3.2	1.56911	0.87609	0.13913
3.6	1.92954	0.92333	0.09809
4.0	2.30576	0.95552	0.06424
4.4	2.69238	0.97587	0.03897
4.8	3.08534	0.98779	0.02187
5.0	3.28329	0.99155	0.01591
8.8	7.07923	1.00000	0.00000

Wall Shear Stress

- With the profile known, wall shear can be evaluated as

$$\tau_w = \mu \frac{\partial u}{\partial y}\bigg|_{y=0}$$

Now, $\frac{\partial u}{\partial y} = U_\infty f'(\eta)\frac{\partial \eta}{\partial y}$

or $\tau_\omega = \mu U_\infty f''(\eta)\frac{\partial \eta}{\partial y}\bigg|_{\eta=0}$

$= \mu U_\infty H \frac{\partial \eta}{\partial y}\bigg|_{\eta=0}$

or $\tau_\omega = \mu U_\infty \times 0.3326 \times \frac{1}{\sqrt{(\nu x)/U_\infty}}$

$[f''(0) = 0.3326]$ from Table 28.1

$$\tau_\omega = \frac{0.332\rho U_\infty^2}{\sqrt{\mathrm{Re}_x}} \quad (29.1a)$$

(Wall Shear Stress)

and the local skin friction coefficient is $C_{fx} = \frac{\tau_\omega}{1/2\rho U_\infty^2}$

- Substituting from (29.1a) we get

$$C_{fx} = \frac{0.664}{\sqrt{\mathrm{Re}_x}} \quad (29.1b)$$

(Skin Friction Coefficient)

-
- In 1951, Liepmann and Dhawan , measured the shearing stress on a flat plate directly. Their results showed a striking confirmation of Eq. (29.1).
- Total frictional force per unit width for the plate of length L is

$$F = \int_0^L \tau_\omega dx$$

$$F = \int_0^L \frac{0.332\rho U_\infty^2}{\sqrt{U_\infty/\nu}}\frac{dx}{\sqrt{x}}$$

or

$$F = \left[\frac{0.332 \rho U_\infty^2}{\sqrt{U_\infty / \nu}} \times \frac{x^{1/2}}{1/2} \right]_0^L$$

or

$$F = 0.664 \times \rho U_\infty^2 \sqrt{\frac{\nu L}{U_\infty}} \qquad (29.2)$$

and the average skin friction coefficient is

$$\overline{C_f} = \frac{F}{1/2\left(\rho U_\infty^2 L\right)} = \frac{1.328}{\sqrt{\mathrm{Re}_L}} \qquad (29.3)$$

where, $\mathrm{Re}_L = U_\infty L / \nu$.

For a flat plate of length L in the streamwise direction and width w perpendicular to the flow, the Drag D would be

$$D = F(2wL) = 0.664(2wL)\rho U_\infty^2 \left(\frac{\nu L}{U_\infty} \right)^{1/2} = 1.328 wL \left(\frac{\rho \mu U_\infty^3}{L} \right)^{1/2} \qquad (29.4)$$

Boundary Layer Thickness

- Since $u / U_\infty \rightarrow 0.99, as \quad y \rightarrow \infty$, it is customary to select the boundary layer thickness δ as that point where u / U_∞ **approaches 0.99.**
- From Table 28.1, u / U_∞ **reaches 0.99 at η= 5.0** and we can write $\delta \Big/ \sqrt{\left(\frac{\nu x}{U_\infty} \right)} \approx 5.0$

$$or \quad \delta \approx 5.0 \sqrt{\left(\frac{\nu x}{U_\infty} \right)} = \frac{5.0 x}{\sqrt{\mathrm{Re}_x}} \qquad (29.5)$$

-
- However, the aforesaid definition of boundary layer thickness is somewhat arbitrary, a physically more meaningful measure of boundary layer estimation is expressed through **displacement** thickness .

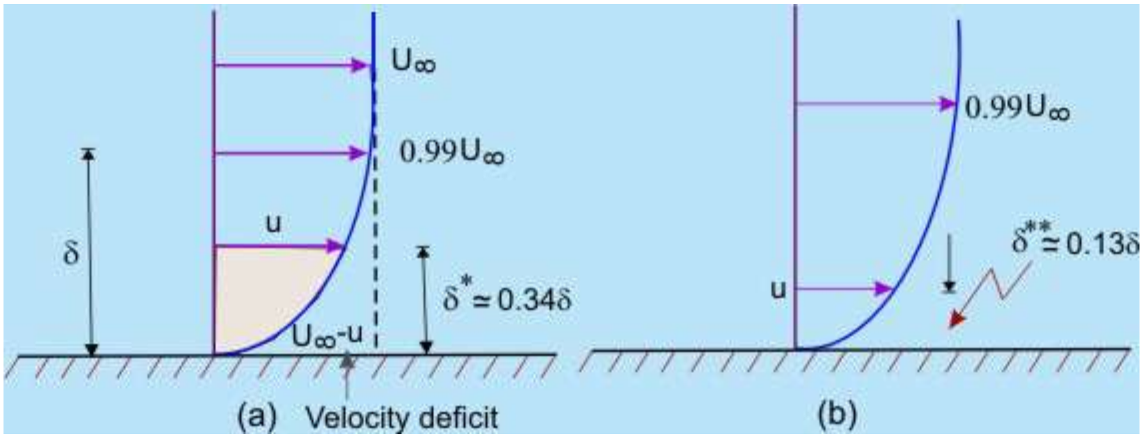

Fig. 29.1 (Displacement thickness) (b) Momentum thickness

- **Displacement thickness** (δ^*) **:** It is defined as the distance by which the external potential flow is displaced outwards due to the decrease in velocity in the boundary layer.

$$U_\infty \delta^* = \int_0^\infty (U_\infty - u)dy$$

Therefore,

$$\delta^* = \int_0^\infty \left(1 - \frac{u}{U_\infty}\right)dy \qquad (29.6)$$

$$dy = \delta d\eta = \sqrt{\frac{\nu x}{U_\infty}}d\eta$$

-
- Substituting the values of u/U_∞ and η from Eqs (28.21a) and (28.19) into Eq.(29.6), we obtain

$$\delta^* = \sqrt{\frac{\nu x}{U_\infty}}\int_0^\infty (1 - f')d\eta = \sqrt{\frac{\nu x}{U_\infty}} \lim_{\eta \to \infty} [\eta - f(\eta)]$$

or,

$$\delta^* = 1.7208\sqrt{\frac{\nu x}{U_\infty}} = \frac{1.7208x}{\sqrt{\mathrm{Re}_x}} \qquad (29.7)$$

Following the analogy of the displacement thickness, a momentum thickness may be defined.

Momentum thickness (δ^{**}): It is defined as the loss of momentum in the boundary layer as compared with that of potential flow. Thus

$$\rho U_\infty^2 \delta^{**} = \int_0^\infty \rho u (U_\infty - u) dy$$

$$\delta^{**} = \int_0^\infty \frac{u}{U_\infty}\left(1 - \frac{u}{U_\infty}\right) dy \qquad (29.8)$$

With the substitution of (u/U_∞) and η from Eg. (28.21a) and (28.19), we can evaluate numerically the value of δ^{**} for a flat plate as

$$\delta^{**} = \sqrt{\frac{\nu x}{U_\infty}} \int_0^\infty f'(1 - f') d\eta$$

$$or \quad \delta^{**} = 0.664 \sqrt{\frac{\nu x}{U_\infty}} = \frac{0.664 x}{\sqrt{\mathrm{Re}_x}} \qquad (29.9)$$

The relationships between $\delta, \delta^{*} and \delta^{**}$ have been shown in Fig. 29.1.

Momentum-Integral Equations For The Boundary Layer

- To employ boundary layer concepts in real engineering designs, we need approximate methods that would quickly lead to an answer even if the accuracy is somewhat less.
- **Karman and Pohlhausen** devised a simplified method by **satisfying only the boundary conditions of the boundary layer flow** rather than satisfying Prandtl's differential equations for each and every particle within the boundary layer. We shall discuss this method herein.
- Consider the case of steady, two-dimensional and incompressible flow, i.e. we shall refer to Eqs (28.10) to (28.14). Upon integrating the dimensional form of Eq. (28.10) with respect to *y = 0* (wall) to *y* = δ (where δ signifies the interface of the free stream and the boundary layer), we obtain

$$\int_0^\delta \left(u \frac{\partial u}{\partial x} + v \frac{\partial u}{\partial y} \right) dy = \int_0^\delta \left(-\frac{1}{\rho} \frac{\partial p}{\partial x} + \nu \frac{\partial^2 u}{\partial y^2} \right) dy$$

or, $$\int_0^{\delta} u\frac{\partial u}{\partial x}dy + \int_0^{\delta} v\frac{\partial u}{\partial y}dy = \int_0^{\delta} -\frac{1}{\rho}\frac{\partial p}{\partial x}dy + \int_0^{\delta} \nu\frac{\partial^2 u}{\partial y^2}dy \tag{29.10}$$

- The second term of the left hand side can be expanded as

$$\int_0^{\delta} v\frac{\partial u}{\partial y}dy = [vu]_0^{\delta} - \int_0^{\delta} u\frac{\partial v}{\partial y}dy$$

or, $$\int_0^{\delta} v\frac{\partial u}{\partial y}dy = U_\infty v_\delta + \int_0^{\delta} u\frac{\partial u}{\partial x}dy\left(\sin ce\frac{\partial u}{\partial x} = -\frac{\partial v}{\partial y}\right)$$ by continuity equation

or, $$\int_0^{\delta} v\frac{\partial u}{\partial y}dy = -U_\infty\int_0^{\delta}\frac{\partial u}{\partial x}dy + \int_0^{\delta} u\frac{\partial u}{\partial x}dy \tag{29.11}$$

- Substituting Eq. (29.11) in Eq. (29.10) we obtain

$$\int_0^{\delta} 2u\frac{\partial u}{\partial x}dy - U_\infty\int_0^{\delta}\frac{\partial u}{\partial x}dy = -\int_0^{\delta}\frac{1}{\rho}\frac{\partial p}{\partial x}dy - \nu\left.\frac{\partial u}{\partial y}\right|_{y=0} \tag{29.12}$$

- Substituting the relation between $\frac{\partial p}{\partial x}$ and the free stream velocity U_∞ for the inviscid zone in Eq. (29.12) we get

$$\int_0^{\delta} 2u\frac{\partial u}{\partial x}dy - U_\infty\int_0^{\delta}\frac{\partial u}{\partial x}dy - \int_0^{\delta} U_\infty\frac{dU_\infty}{dx}dy = -\left(\frac{\mu\left.\frac{\partial u}{\partial y}\right|_{y=0}}{\rho}\right)$$

$$\int_0^{\delta}\left(2u\frac{\partial u}{\partial x} - U_\infty\frac{\partial u}{\partial x} - U_\infty\frac{dU_\infty}{dx}\right)dy = -\frac{\tau_w}{\rho}$$

which is reduced to

$$\int_0^{\delta} \frac{\partial}{\partial x}\left[u\left(U_\infty - u\right)\right]dy + \frac{dU_\infty}{dx}\int_0^{\delta}\left(U_\infty - u\right)dy = \frac{\tau_w}{\rho}$$

- Since the integrals vanish outside the boundary layer, we are allowed to increase the integration limit to infinity (i.e $\delta = \infty$.)

$$\int_0^{\delta} \frac{\partial}{\partial x}\left[u\left(U_\infty - u\right)\right]dy + \frac{dU_\infty}{dx}\int_0^{\delta}\left(U_\infty - u\right)dy = \frac{\tau_w}{\rho}$$

or, $$\frac{d}{dx}\int_0^{\delta}\left[u\left(U_\infty - u\right)\right]dy + \frac{dU_\infty}{dx}\int_0^{\delta}\left(U_\infty - u\right)dy = \frac{\tau_w}{\rho} \qquad (29.13)$$

- Substituting Eq. (29.6) and (29.7) in Eq. (29.13) we obtain

$$\frac{d}{dx}\left[U_\infty^2 \delta^{**}\right] + \delta^{*} U_\infty \frac{dU_\infty}{dx} = \frac{\tau_w}{\rho} \qquad (29.14)$$

where $\delta^{*} = \int_0^{\delta}\left(1 - \frac{u}{U_\infty}\right)dy$ is the displacement thickness

$\delta^{**} = \int_0^{\delta}\frac{u}{U_\infty}\left(1 - \frac{u}{U_\infty}\right)dy$ is momentum thickness

Equation (29.14) is known as momentum integral equation for two dimensional incompressible laminar boundary layer. The same remains valid for turbulent boundary layers as well.

Needless to say, **the wall shear stress** (τ_w) **will be different for laminar and turbulent flows.**

- The term $U_\infty \frac{dU_\infty}{dx}$ signifies space-wise acceleration of the free stream. Existence of this term means that free stream pressure gradient is present in the flow direction.

- For example, we get finite value of $U_\infty \frac{dU_\infty}{dx}$ outside the boundary layer in the entrance region of a pipe or a channel. For external flows, the existence of $U_\infty \frac{dU_\infty}{dx}$ depends on the shape of the body.

- During the flow over a flat plate, $U_\infty \frac{dU_\infty}{dx} = 0$ and the momentum integral equation is reduced to

$$\frac{d}{dx}\left[U_\infty^2 \delta^{**}\right] = \frac{\tau_w}{\rho} \qquad (29.15)$$

Seperation of Boundary Layer

- It has been observed that the **flow is reversed at the vicinity of the wall** under certain conditions.
- The phenomenon is termed as **separation of boundary layer**.
- Separation takes place **due to excessive momentum loss near the wall in a boundary layer trying to move downstream against increasing pressure, i.e.,** $\frac{dp}{dx} > 0$ **, which is called *adverse pressure gradient*.**
- Figure 29.2 shows the flow past a circular cylinder, in an infinite medium.

    1. Up to $\theta = 90^\circ$, the flow area is like a constricted passage and the flow behaviour is like that of a nozzle.
    2. Beyond $\theta = 90^\circ$ the flow area is diverged, therefore, the flow behaviour is much similar to a diffuser

This dictates the inviscid pressure distribution on the cylinder which is shown by a firm line in Fig. 29.2.

Here

p_∞ **: pressure in the free stream**

U_∞ **: velocity in the free stream and**

ρ ***:* is the local pressure on the cylinder.**

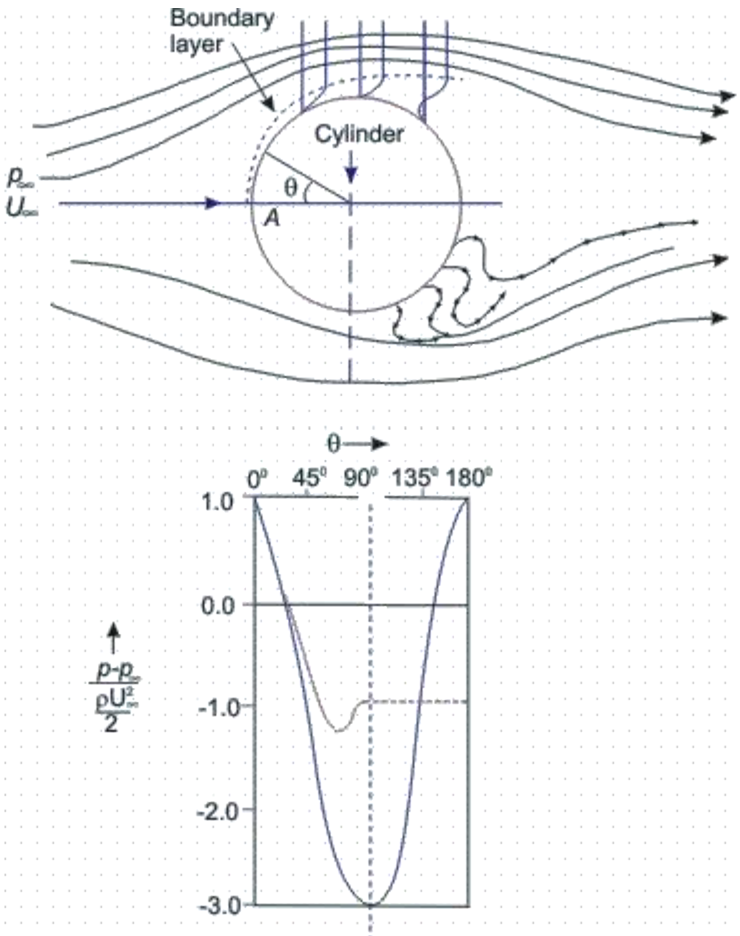

Fig. 29.2 Flow separation and formation of wake behind a circular cylinder

- Consider the forces in the flow field.
  In the **inviscid region,**

  1. **Until** $\theta = 90^\circ$ the pressure force and the force due to streamwise acceleration i.e. inertia forces are acting in the same direction (**pressure gradient** being **negative/favourable**)

  2. **Beyond** $\theta = 90^\circ$, the **pressure gradient is positive or adverse**. Due to the adverse pressure gradient the pressure force and the force due to acceleration will be opposing each other in the in viscid zone of this part.

-

So long as no viscous effect is considered, the situation does not cause any sensation.
In the **viscid region** (near the solid boundary),

1. **Up to** $\theta = 90^\circ$ **, th**e viscous force opposes the combined pressure force and the force due to acceleration. Fluid particles overcome this viscous resistance **due to continuous conversion of pressure force into kinetic energy.**

2. Beyond $\theta = 90^\circ$, within the viscous zone, the flow structure becomes different. It is seen that the force due to acceleration is opposed by both the viscous force and pressure force.

- Depending upon the magnitude of adverse pressure gradient, **somewhere around** $\theta = 90^\circ$ **, the fluid particles, in the** b**oundary layer are separated from the wal**l and driven in the upstream direction. However, the far field external stream pushes back these separated layers together with it and develops **a broad pulsating wake behind the cylinder**.

- **The mathematical explanation of flow-separation :** The point of separation may be defined as the limit between forward and reverse flow in the layer very close to the wall, i.e., at the point of separation

$$\left(\frac{\partial u}{\partial y}\right)_{y=0} = 0 \qquad (29.16)$$

This means that the shear stress at the wall, $\tau_w = 0$. But at this point, the adverse pressure continues to exist and at the downstream of this point the flow acts in a reverse direction resulting in a back flow.

- We can also explain flow separation using the argument about the second derivative of velocity *u* at the wall. From the dimensional form of the momentum at the wall, where *u = v = 0*, we can write

$$\left(\frac{\partial^2 u}{\partial y^2}\right)_{y=0} = \frac{1}{\mu}\frac{dp}{dx} \qquad (29.17)$$

- Consider the situation due to a **favourable pressure gradient** where $\frac{dp}{dx} < 0$ we have,

1. $\left(\partial^2 u / \partial y^2\right)_{wall} < 0$. (From Eq. (29.17))

2. **As we proceed towards the free stream, the velocity *u* approaches** U_∞ **asymptotically,** so $\partial u / \partial y$ decreases at a continuously lesser rate in *y* direction.

3. This means that $\partial^2 u / \partial y^2$ remains less than zero near the edge of the boundary layer.

4. The curvature of a velocity profile $\partial^2 u / \partial y^2$ is always negative as shown in (Fig. 29.3a)

- Consider the case of **adverse pressure gradient**, $\partial p / \partial x > 0$

1. At the boundary, the curvature of the profile must be positive (since $\partial p / \partial x > 0$).

2. Near the interface of boundary layer and free stream the previous argument regarding $\partial u / \partial y$ and $\partial^2 u / \partial y^2$ still holds good and the curvature is negative.

3. Thus we observe that for an adverse pressure gradient, there must exist a point for which $\partial^2 u / \partial y^2 = 0$. This point is known as *point of inflection* of the velocity profile in the boundary layer as shown in Fig. 29.3b

4. However, point of separation means $\partial u / \partial y = 0$ at the wall.

5. $\partial^2 u / \partial y^2 > 0$ at the wall since separation can only occur due to adverse pressure gradient. But we have already seen that at the edge of the boundary layer, $\partial^2 u / \partial y^2 < 0$. It is therefore, clear that **if there is a point of separation, there must exist a point of inflection in the velocity profile.**

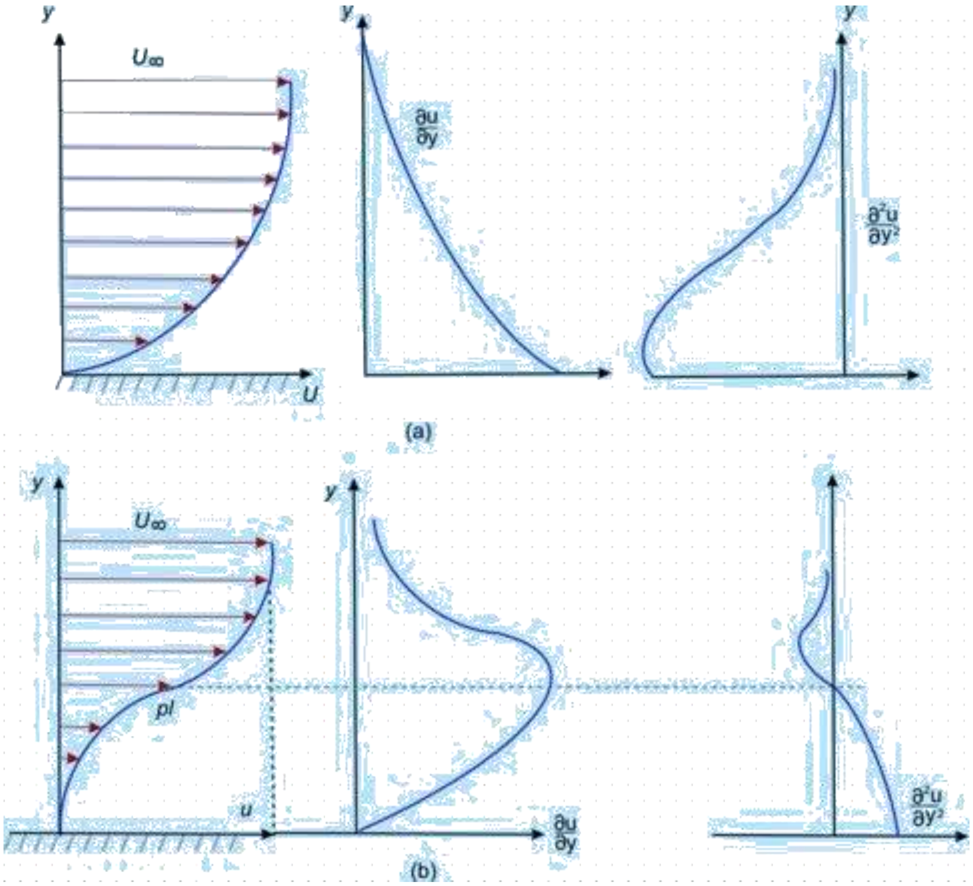

Fig. 29.3 Velocity distribution within a boundary layer

(a) Favourable pressure gradient, $\frac{dp}{dx} < 0$

(b) adverse pressure gradient, $\frac{dp}{dx} > 0$

1. Let us reconsider the flow past a circular cylinder and continue our **discussion on the wake behind a cylinder.** The pressure distribution which was shown by the firm line in Fig. 21.5 is obtained from the potential flow theory. However. somewhere near $\theta = 90^{\circ}$ **(in experiments it has been observed to be at** $\theta = 81^{\circ}$ **) . the boundary layer detaches itself from the wall.**

2. Meanwhile, **pressure in the wake remains close to separation-point-pressure** since the eddies (formed as a consequence of the retarded layers being carried together with the upper layer through the action of shear) cannot convert rotational kinetic energy into pressure head. The actual pressure distribution is shown by the dotted line in Fig. 29.3.

3. Since the **wake zone pressure is less than that of the forward stagnation point** (pressure at point A in Fig. 29.3), the cylinder experiences a drag force which is basically attributed to the pressure difference.

The drag force, brought about by the pressure difference is known as *form drag* whereas the shear stress at the wall gives rise to *skin friction drag*. Generally, these two drag forces together are responsible for resultant drag on a body

Seperation of Boundary Layer

- It has been observed that the **flow is reversed at the vicinity of the wall** under certain conditions.
- The phenomenon is termed as **separation of boundary layer**.
- Separation takes place **due to excessive momentum loss near the wall in a boundary layer trying to move downstream against increasing pressure, i.e.,** $\frac{dp}{dx} > 0$ **, which is called *adverse pressure gradient*.**
- Figure 29.2 shows the flow past a circular cylinder, in an infinite medium.

    1. Up to $\theta = 90^\circ$, the flow area is like a constricted passage and the flow behaviour is like that of a nozzle.
    2. Beyond $\theta = 90^\circ$ the flow area is diverged, therefore, the flow behaviour is much similar to a diffuser

This dictates the inviscid pressure distribution on the cylinder which is shown by a firm line in Fig. 29.2.

Here

p_∞ **: pressure in the free stream**

U_∞ **: velocity in the free stream and**

p ***:* is the local pressure on the cylinder.**

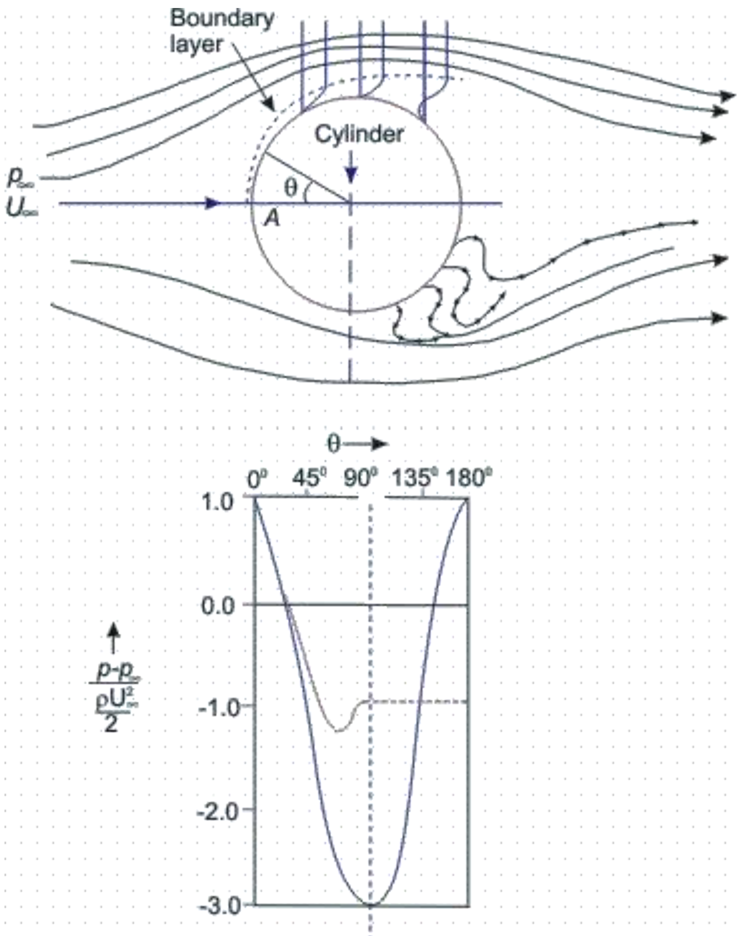

Fig. 29.2 Flow separation and formation of wake behind a circular cylinder

- Consider the forces in the flow field.
  In the **inviscid region,**

  1. **Until** $\theta = 90^\circ$ the pressure force and the force due to streamwise acceleration i.e. inertia forces are acting in the same direction (**pressure gradient** being **negative/favourable**)

  2. **Beyond** $\theta = 90^\circ$, the **pressure gradient is positive or adverse**. Due to the adverse pressure gradient the pressure force and the force due to acceleration will be opposing each other in the in viscid zone of this part.

-

So long as no viscous effect is considered, the situation does not cause any sensation.
In the **viscid region** (near the solid boundary),

1. **Up to** $\theta = 90^\circ$ **, th**e viscous force opposes the combined pressure force and the force due to acceleration. Fluid particles overcome this viscous resistance **due to continuous conversion of pressure force into kinetic energy.**

2. Beyond $\theta = 90^\circ$, within the viscous zone, the flow structure becomes different. It is seen that the force due to acceleration is opposed by both the viscous force and pressure force.

- Depending upon the magnitude of adverse pressure gradient, **somewhere around** $\theta = 90^\circ$ **, the fluid particles, in the** b**oundary layer are separated from the wal**l and driven in the upstream direction. However, the far field external stream pushes back these separated layers together with it and develops **a broad pulsating wake behind the cylinder**.

- **The mathematical explanation of flow-separation :** The point of separation may be defined as the limit between forward and reverse flow in the layer very close to the wall, i.e., at the point of separation

$$\left(\frac{\partial u}{\partial y}\right)_{y=0} = 0 \qquad (29.16)$$

This means that the shear stress at the wall, $\tau_w = 0$. But at this point, the adverse pressure continues to exist and at the downstream of this point the flow acts in a reverse direction resulting in a back flow.

- We can also explain flow separation using the argument about the second derivative of velocity *u* at the wall. From the dimensional form of the momentum at the wall, where *u = v = 0*, we can write

$$\left(\frac{\partial^2 u}{\partial y^2}\right)_{y=0} = \frac{1}{\mu}\frac{dp}{dx} \qquad (29.17)$$

- Consider the situation due to a **favourable pressure gradient** where $\frac{dp}{dx} < 0$ we have,

1. $\left(\partial^2 u / \partial y^2\right)_{wall} < 0$. (From Eq. (29.17))

2. **As we proceed towards the free stream, the velocity *u* approaches** U_∞ **asymptotically,** so $\partial u / \partial y$ decreases at a continuously lesser rate in *y* direction.

3. This means that $\partial^2 u / \partial y^2$ remains less than zero near the edge of the boundary layer.

4. The curvature of a velocity profile $\partial^2 u / \partial y^2$ is always negative as shown in (Fig. 29.3a)

- Consider the case of **adverse pressure gradient**, $\partial p / \partial x > 0$

1. At the boundary, the curvature of the profile must be positive (since $\partial p / \partial x > 0$).
2. Near the interface of boundary layer and free stream the previous argument regarding $\partial u / \partial y$ and $\partial^2 u / \partial y^2$ still holds good and the curvature is negative.
3. Thus we observe that for an adverse pressure gradient, there must exist a point for which $\partial^2 u / \partial y^2 = 0$. This point is known as *point of inflection* of the velocity profile in the boundary layer as shown in Fig. 29.3b
4. However, point of separation means $\partial u / \partial y = 0$ at the wall.
5. $\partial^2 u / \partial y^2 > 0$ at the wall since separation can only occur due to adverse pressure gradient. But we have already seen that at the edge of the boundary layer, $\partial^2 u / \partial y^2 < 0$. It is therefore, clear that **if there is a point of separation, there must exist a point of inflection in the velocity profile.**

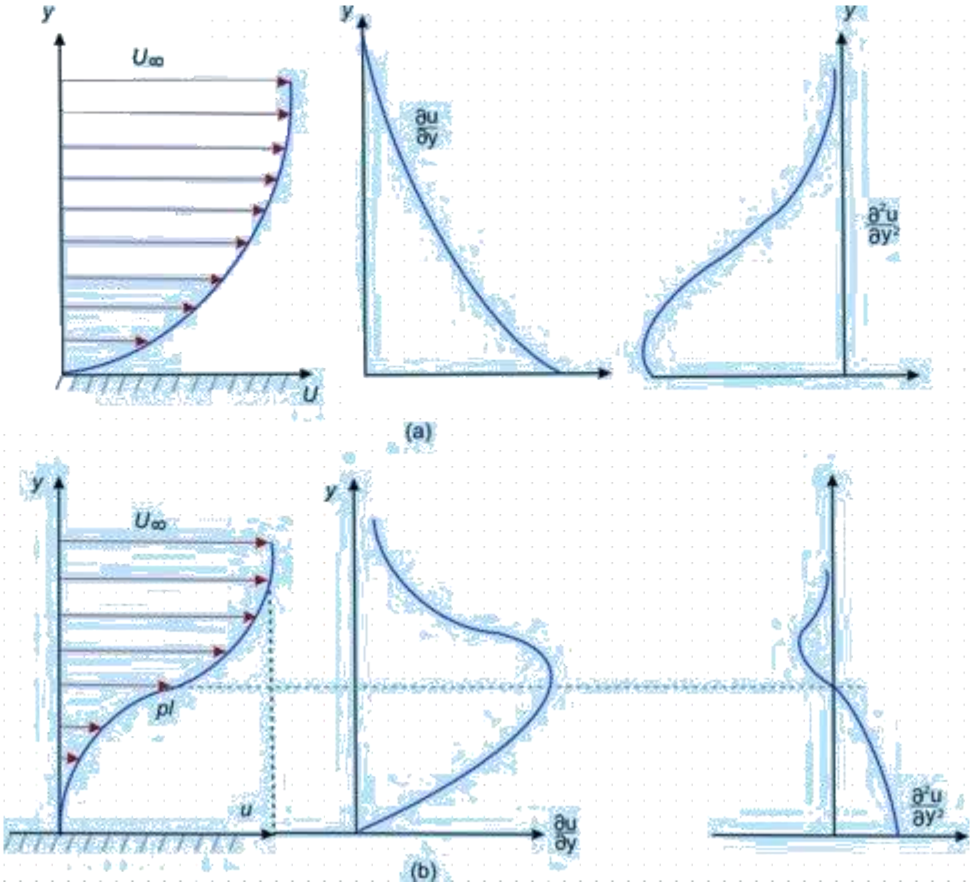

Fig. 29.3 Velocity distribution within a boundary layer

(a) Favourable pressure gradient, $\frac{dp}{dx} < 0$

(b) adverse pressure gradient, $\frac{dp}{dx} > 0$

1. Let us reconsider the flow past a circular cylinder and continue our **discussion on the wake behind a cylinder.** The pressure distribution which was shown by the firm line in Fig. 21.5 is obtained from the potential flow theory. However. somewhere near $\theta = 90^\circ$ **(in experiments it has been observed to be at** $\theta = 81^\circ$ **) . the boundary layer detaches itself from the wall.**

2. Meanwhile, **pressure in the wake remains close to separation-point-pressure** since the eddies (formed as a consequence of the retarded layers being carried together with the upper layer through the action of shear) cannot convert rotational kinetic energy into pressure head. The actual pressure distribution is shown by the dotted line in Fig. 29.3.

3. Since the **wake zone pressure is less than that of the forward stagnation point** (pressure at point A in Fig. 29.3), the cylinder experiences a drag force which is basically attributed to the pressure difference.

The drag force, brought about by the pressure difference is known as *form drag* whereas the shear stress at the wall gives rise to *skin friction drag*. Generally, these two drag forces together are responsible for resultant drag on a body

Karman-Pohlhausen Approximate Method For Solution Of Momentum Integral Equation Over A Flat Plate

- The basic equation for this method is obtained by integrating the *x* direction momentum equation (boundary layer momentum equation) with respect to *y* from the wall (at y = 0) to a distance $\delta(x)$ which is assumed to be outside the boundary layer. Using this notation, we can rewrite the Karman momentum integral equation as

$$U_\infty^2 \frac{d\delta^{**}}{dx} + \left(2\delta^{**} + \delta^{*}\right)U_\infty \frac{dU_\infty}{dx} = \frac{\tau_w}{\rho} \qquad (30.1)$$

- The effect of pressure gradient is described by the second term on the left hand side. For pressure gradient surfaces in external flow or for the developing sections in internal flow, this term contributes to the pressure gradient.

- We assume **a velocity profile which is a polynomial of** $\eta = y/\delta$. η being a form of **similarity variable** , implies that **with the growth of boundary layer as distance *x* varies from the leading edge, the velocity profile** (u/U_∞) **remains geometrically similar.**

- We choose a velocity profile in the form

$$\frac{u}{U_\infty} = a_0 + a_1\eta + a_2\eta^2 + a_3\eta^3 \qquad (30.2)$$

- In order to determine the constants $a_0, a_1, a_2 \;\; and \;\; a_3$ we shall prescribe the following boundary conditions

$$at \;\; y = 0, u = 0 \quad or \quad at \;\; \eta = 0, \frac{u}{U_\infty} = 0 \qquad (30.3a)$$

$$at \;\; y = 0, \frac{\partial^2 u}{\partial y^2} = 0 \quad or \quad at \;\; \eta = 0, \frac{\partial^2}{\partial \eta^2}\left(u/U_\infty\right) = 0 \qquad (30.3b)$$

- at

$$at\ \ y = \delta, u = U_\infty \quad or \quad at\ \ \eta = 1, \frac{u}{U_\infty} = 1 \qquad (30.3c)$$

- at

$$[illegible] \qquad (30.3d)$$

-

- These requirements will yield $a_0 = 0, a_2 = 0, a_1 + a_3 = 1\ \ and\ \ a_1 + 3a_3 = 0$ respectively Finally, we obtain the following values for the coefficients in Eq. (30.2),

$a_0 = 0, a_1 = 3/2, a_2 = 0\ \ and\ \ +a_3 = -1/2$ and the velocity profile becomes

$$\frac{u}{U_\infty} = \frac{3}{2}\eta - \frac{1}{2}\eta^3 \qquad (30.4)$$

- For flow over a flat plate, $\frac{dp}{dx} = 0, \quad hence\ U_\infty \frac{dU_\infty}{dx} = 0$ and the governing Eq. (30.1) reduces to

$$\frac{d\delta^{**}}{dx} = \frac{\tau_w}{\rho U_\infty^2} \qquad (30.5)$$

- Again from Eq. (29.8), the momentum thickness is

$$[illegible] \quad or\ \ \delta^{**} = \int_0^\delta \frac{u}{U_\infty}\left(1 - \frac{u}{U_\infty}\right)dy$$

$$or\ \ \delta^{**} = \delta\int_0^1 \left(\frac{3}{2}\eta - \frac{1}{2}\eta^3\right)\left(1 - \frac{3}{2}\eta + \frac{1}{2}\eta^3\right)d\eta$$

$$or\ \ \delta^{**} = \frac{39}{280}\delta$$

 The wall shear stress is given by

$$\tau_w = \mu \left.\frac{\partial u}{\partial y}\right|_{y=0}$$

$$or\ \tau_w = \mu\left[\frac{\partial}{\delta\partial\eta}\left\{U_\infty\left(\frac{3}{2}\eta - \frac{1}{2}\eta^3\right)\right\}\right]_{\eta=0}$$

$$or\ \tau_w = \frac{3\mu U_\infty}{2\delta}$$

- Substituting the values of δ^{**} and τ_w in Eq. (30.5) we get,

$$\frac{39}{280}\frac{d\delta}{dx} = \frac{3\mu U_\infty}{2\delta\rho U_\infty^2}$$

$$or\ \int \delta d\delta = \int \frac{140}{13}\frac{\mu}{\rho U_\infty}dx + C_1$$

$$or\ \frac{\delta^2}{2} = \frac{140}{13}\frac{\nu x}{U_\infty} + C_1 \qquad (30.6)$$

where C_1 is any arbitrary unknown constant.

- The condition at the leading edge ($at\ \ x = 0, \delta = 0$) yields $C_1 = 0$
  Finally we obtain,

$$\delta^2 = \frac{280}{13}\frac{\nu x}{U_\infty} \qquad (30.7)$$

$$or\ \delta = 4.64\sqrt{\frac{\nu x}{U_\infty}}$$

$$or\ \delta = \frac{4.64x}{\sqrt{\mathrm{Re}_x}} \qquad (30.8)$$

- This is the value of boundary layer thickness on a flat plate. Although, the method is an approximate one, the result is found to be reasonably accurate. The value is slightly lower than the exact solution of laminar flow over a flat plate . As such, **the accuracy depends on the order of the velocity profile.** We could have have used a fourth order polynomial instead --

$$\frac{u}{U_\infty} = a_0 + a_1\eta + a_2\eta^2 + a_3\eta^3 + a_4\eta^4 \qquad (30.9)$$

- In addition to the boundary conditions in Eq. (30.3), we shall require another boundary condition at

$$y = \delta, \frac{\partial^2 u}{\partial y^2} = 0 \;\; or \; at \;\; \eta = 1, \frac{\partial^2 (u / U_\infty)}{\partial \eta^2} = 0$$

- This yields the constants as $a_0 = 0, a_1 = 2, a_3 = -2 \;\; and \;\; a_4 = 1$. Finally the velocity profile will be

$$\frac{u}{U_\infty} = 2\eta - 2\eta^3 + \eta^4$$

Subsequently, for a fourth order profile the growth of boundary layer is given by

$$\delta = \frac{5.83x}{\sqrt{\mathrm{Re}_x}} \qquad (30.10)$$

Integral Method For Non-Zero Pressure Gradient Flows

- A wide variety of "integral methods" in this category have been discussed by Rosenhead . The Thwaites method is found to be a very elegant method, which is an extension of the method due to Holstein and Bohlen . We shall discuss the **Holstein-Bohlen method** in this section**.**
- This is an **approximate method for solving boundary layer equations for two-dimensional generalized flow**. The integrated Eq. (29.14) for laminar flow with pressure gradient can be written as

$$\frac{d}{dx}\left[U^2 \delta^{**}\right] + \delta^* U \frac{dU}{dx} = \frac{\tau_\omega}{\rho}$$

or

$$U^2 \frac{d\delta^{**}}{dx} + \left(2\delta^{**} + \delta^*\right) U \frac{dU}{dx} = \frac{\tau_\omega}{\rho} \qquad (30.11)$$

- The **velocity profile** at the boundary layer is considered to be a **fourth-order polynomial** in terms of the dimensionless distance $\eta = y / \delta$, and is expressed as

$$u/U = a\eta + b\eta^2 + c\eta^3 + d\eta^4$$

The **boundary conditions are**

$$\eta = 0 : u = 0, v = 0 \qquad \frac{\nu}{\delta^2}\frac{\partial^2 u}{\partial \eta^2} = \frac{1}{\rho}\frac{dp}{dx} = -U\frac{dU}{dx}$$

$$\eta = 1 : u = U \qquad \frac{\partial u}{\partial \eta} = 0, \ \frac{\partial^2 u}{\partial \eta^2} = 0$$

- A dimensionless quantity, known as **shape factor** is introduced as

$$\lambda = \frac{\delta^2}{\nu}\frac{dU}{dx} \tag{30.12}$$

- The following relations are obtained

$$a = 2 + \frac{\lambda}{6}, \ b = -\frac{\lambda}{2}, \ c = -2 + \frac{\lambda}{2}, \ d = 1 - \frac{\lambda}{6}$$

- Now, the **velocity profile can be expressed as**

[illegible] (30.13)

where

$$F(\eta) = 2\eta + 2\eta^3 + \eta^4 \, , \ G(\eta) = \frac{1}{6}\eta(1-\eta)^3$$

- The shear stress $\tau_\omega = \mu(\partial u/\partial y)_{y=0}$ is given by

$$\frac{\tau_\omega \delta}{\mu U} = 2 + \frac{\lambda}{6} \tag{30.14}$$

- We use the following dimensionless parameters,

[illegible] (30.15)

[illegible] (30.16)

$$H = \delta^* / \delta^{**} \tag{30.17}$$

- The integrated momentum Eq. (30.10) reduces to

$$U\frac{d\delta^{**}}{dx} + \delta^{**}(2 + H)\frac{dU}{dx} = \frac{\nu L}{\delta^{**}}$$

[illegible] (30.18)

- The parameter ***L* is related to the skin friction**
- The parameter ***K* is linked to the pressure gradient.**
- If we take ***K* as** the **independent variable** . ***L* and *H*** can be shown to be the **functions of *K*** since

$$\frac{\delta^*}{\delta} = \int_0^1 [1 - F(\eta) - \lambda G(\eta)]d\eta = \frac{3}{10} - \frac{\lambda}{120} \quad (30.19)$$

$$\frac{\delta^*}{\delta} = \int_0^1 (F(\eta) + \lambda G(\eta))(1 - F(\eta) - \lambda G(\eta))d\eta$$

$$= \frac{37}{315} - \frac{\lambda}{945} - \frac{\lambda^2}{9072} \quad (30.20)$$

$$K = \frac{[\delta^{**}]^2}{\delta^2}\lambda = \lambda\left(\frac{37}{315} - \frac{\lambda}{945} - \frac{\lambda^2}{9072}\right)^2 \quad (30.21)$$

Therefore,

$$L = \left(2 + \frac{\lambda}{6}\right)\frac{\delta^{**}}{\delta} = \left(2 + \frac{\lambda}{6}\right)\left(\frac{37}{315} - \frac{\lambda}{945} - \frac{\lambda^2}{9072}\right) = f_1(k)$$

$$H = \frac{\delta^*}{\delta^{**}} = \frac{(3/10) - (\lambda/120)}{(37/315) - (\lambda/945) - (\lambda^2/9072)} = f_2(k)$$

- The right-hand side of Eq. (30.18) is thus a function of *K* alone. Walz pointed out that this function can be approximated with a good degree of accuracy by a linear function of *K* so that

$$2[L - K(H - 2)] = a - bK \quad [Walz\text{'s approximation}]$$

[Walz's approximation]

- Equation (30.18) can now be written as

$$\frac{d}{dx}\left(\frac{U[\delta^{**}]^2}{\nu}\right) = a - (b-1)\frac{U[\delta^{**}]^2}{\nu}\frac{1}{U}\frac{dU}{dx}$$

Solution of this differential equation for the dependent variable $U[\delta^{**}]^2/\nu$ subject to the boundary condition *U = 0* when *x = 0* , gives

$$\frac{U[\delta^{**}]^2}{\nu} = \frac{a}{U^{b-1}}\int_0^x U^{b-1}dx$$

- **With *a* = 0.47 and *b* = 6. the approximation is particularly close between the stagnation point and the point of maximum velocity.**
- **Finally the value of the dependent variable is**

[illegible] (30.22)

- By taking the limit of Eq. (30.22), according to L'Hopital's rule, it can be shown that

$$[\delta^{**}]^2 |_{x=0} = 0.47\,\nu/6U'(0)$$

This corresponds to **K = 0.0783.**

- Note that $\left|\delta^{**}\right|$ is not equal to zero at the stagnation point. If $\left([\delta^{**}]^2/\nu\right)$ is determined from Eq. (30.22), *K(x)* can be obtained from Eq. (30.16).
- Table 30.1 gives the necessary parameters for obtaining results, such as velocity profile and shear stress τ_ω The approximate method can be applied successfully to a wide range of problems.

Table 30.1 Auxiliary functions after Holstein and Bohlen

λ	K	$f_1(K)$	$f_2(K)$
12	0.0948	2.250	0.356
10	0.0919	2.260	0.351
8	0.0831	2.289	0.340
7.6	0.0807	2.297	0.337
7.2	0.0781	2.305	0.333
7.0	0.0767	2.309	0.331
6.6	0.0737	2.318	0.328

6.2	0.0706	2.328	0.324
5.0	0.0599	2.361	0.310
3.0	0.0385	2.427	0.283
1.0	0.0135	2.508	0.252
0	0	2.554	0.235
-1	-0.0140	2.604	0.217
-3	-0.0429	2.716	0.179
-5	-0.0720	2.847	0.140
-7	-0.0999	2.999	0.100
-9	-0.1254	3.176	0.059
-11	-0.1474	3.383	0.019
-12	-0.1567	3.500	0

λ	K	$f_1(K)$	$f_2(K)$
0	0	0	0
0.2	0.00664	0.006641	0.006641
0.4	0.02656	0.13277	0.13277
0.8	0.10611	0.26471	0.26471
1.2	0.23795	0.39378	0.39378
1.6	0.42032	0.51676	0.51676

2.0	0.65003	0.62977	0.62977
2.4	0.92230	0.72899	0.72899
2.8	1.23099	0.81152	0.81152
3.2	1.56911	0.87609	0.87609
3.6	1.92954	0.92333	0.92333
4.0	2.30576	0.95552	0.95552
4.4	2.69238	0.97587	0.97587
4.8	3.08534	0.98779	0.98779
5.0	3.28329	0.99155	0.99155
8.8	7.07923	1.00000	1.00000

- As mentioned earlier, *K* and λ are related to the pressure gradient and the shape factor.
- Introduction of *K* and λ in the integral analysis enables extension of Karman-Pohlhausen method for solving flows over curved geometry. However, the **analysis is not valid for the geometries, where** $\lambda < -12$ **and** $\lambda > +12$

Point of Seperation

For point of seperation, $\tau_\omega = 0$

$$\Rightarrow \frac{\mu U}{\delta}\left(2 + \frac{\lambda}{6}\right)$$

or, $$2 + \frac{\lambda}{6} = 0$$

or, $$\lambda = -12$$

Entry Flow In A Duct -

- Growth of boundary layer has a remarkable influence on flow through a constant area duct or pipe.
  Consider a flow entering a pipe with uniform velocity.

  1. The boundary layer starts growing on the wall at the entrance of the pipe.
  2. Gradually it becomes thicker in the downstream.
  3. The flow becomes fully developed when the boundary layers from the wall meet at the axis of the pipe.

- The velocity profile is **nearly rectangular** at the entrance and it gradually changes to a parabolic profile at the fully developed region.
- Before the boundary layers from the periphery meet at the axis, there prevails a core region which is uninfluenced by viscosity.
- Since the volume-flow must be same for every section and the boundary-layer thickness increases in the flow direction, the inviscid core accelerates, and there is a corresponding fall in pressure.
- **Entrance length** : It can be shown that for laminar incompressible flows, the velocity profile approaches the parabolic profile through a distance L_e from the entry of the pipe. This is known as entrance length and is given by

$$\frac{Le}{D} \approx 0.05\mathrm{Re}, \qquad where \quad \mathrm{Re} = \frac{U_{av}D}{\nu}$$

For a Reynolds number of 2000, this distance, the entrance length is about 100 pipe-diameters. For turbulent flows, the entrance region is shorter, since the turbulent boundary layer grows faster.

- **At the entrance region**,

1. The velocity gradient is steeper at the wall, causing a higher value of shear stress as compared to a developed flow.
2. Momentum flux across any section is higher than that typically at the inlet due to the change in shape of the velocity profile.
3. Arising out of these, an additional pressure drop is brought about at the entrance region as compared to the pressure drop in the fully developed region.

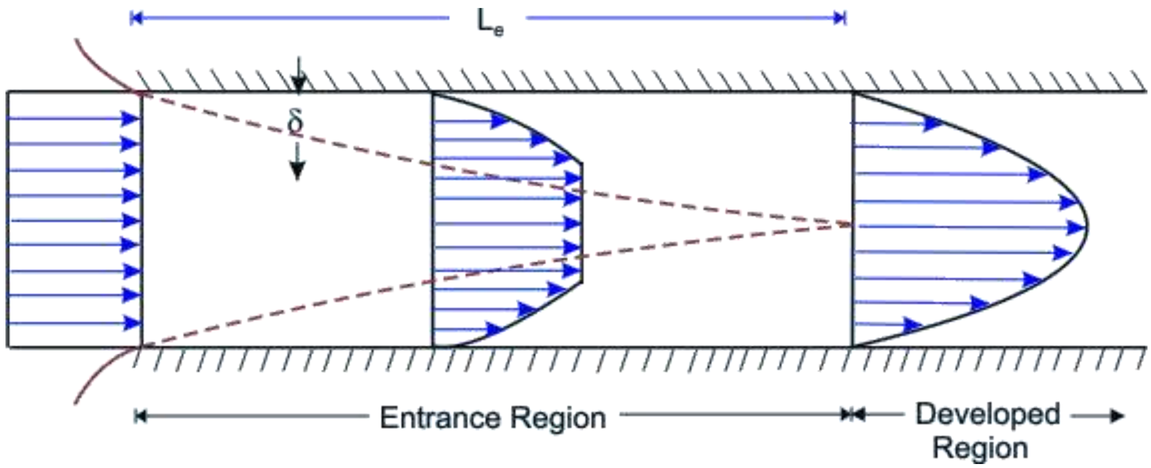

Fig. 31.1 Development of boundary layer in the entrance region of a duct

Control Of Boundary Layer Separation -

- The total drag on a body is attributed to form drag and skin friction drag. In some flow configurations, the contribution of form drag becomes significant.
- In order **to reduce the form drag, the boundary layer separation** should be **prevented or delayed** so that **better pressure recovery takes place** and the form drag is reduced considerably. There are some popular methods for this purpose which are stated as follows.

  i. By giving the profile of the body a streamlined shape(as shown in *Fig. 31.2*).

     1. This has an elongated shape in the rear part to reduce the magnitude of the pressure gradient.
     2. The optimum contour for a streamlined body is the one for which the wake zone is very narrow and the form drag is minimum.

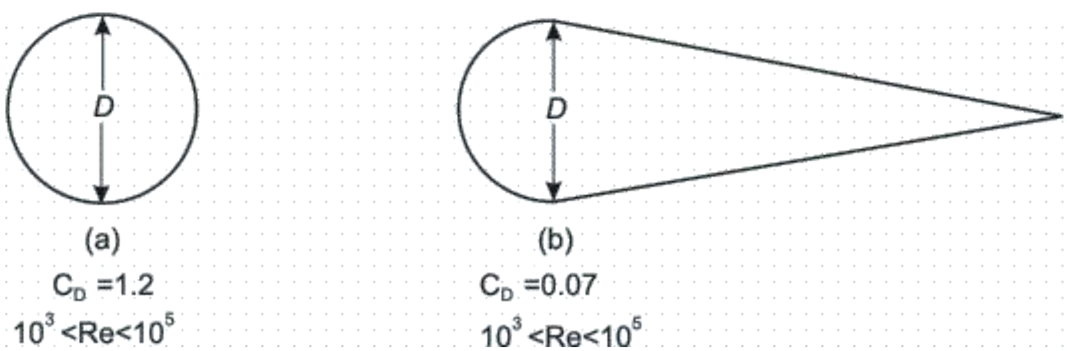

Fig. 31.2 Reduction of drag coefficient (C_D) by giving the profile a streamlined shape

  ii. **The injection of fluid through porous wall can also control the boundary layer separation. This is generally accomplished by** blowing high energy fluid particles tangentially from the location where separation would have taken place otherwise. This is shown in Fig. 31.3.

1. The **injection of fluid promotes turbulence**
2. This **increases skin friction.** But the **form drag is reduced** considerably due to suppression of flow separation
3. The reduction in form drag is quite significant and **increase in skin friction drag can be ignored.**

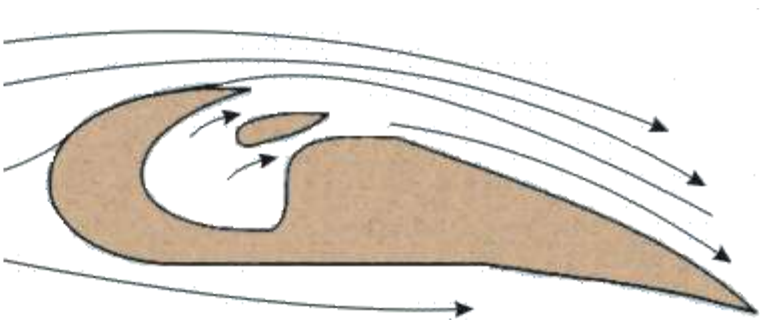

Fig. 31.3 Boundary layer control by blowing

Mechanisms of Boundary Layer Transition

- One of the interesting problems in fluid mechanics is the physical mechanism of transition from laminar to turbulent flow. The problem evolves about the generation of both steady and unsteady vorticity near a body, its subsequent molecular diffusion, its kinematic and dynamic convection and redistribution downstream, and the resulting feedback on the velocity and pressure fields near the body. We can perhaps realise the complexity of the transition problem by examining the behaviour of a real flow past a cylinder.

  Figure 31.4 (a) shows the flow past a cylinder for a very low **Reynolds number** (~ 1). The **flow smoothly divides and reunites around the cylinder.**

- At a **Reynolds number of about 4**, the **flow (boundary layer) separates in the downstream** and the wake is formed by **two symmetric eddies** . The eddies remain steady and **symmetrical** but grow in size **up to a Reynolds number of about 40** as shown in Fig. 31.4(b).

- At a **Reynolds number above 40** , **oscillation in the wake** induces **asymmetry** and finally the wake starts **shedding vortices** into the stream. This situation is termed as **onset of periodicity** as shown in Fig. 31.4(c) and the wake keeps on undulating **up to a Reynolds number of 90** .

- At a **Reynolds number above 90** , the **eddies are shed alternately from a top and bottom** of the cylinder and the regular pattern of **alternately shed clockwise and counterclockwise vortices form *Von Karman vortex street*** as in Fig. 31.4(d).
- Periodicity is eventually induced in the flow field with the vortex-shedding phenomenon.
- The periodicity is characterised by the **frequency of vortex shedding** f
- **In non-dimensional form, the vortex shedding frequency is expressed as** fD/U_{ref} known as the **Strouhal number** named after V. Strouhal, a German physicist who experimented with wires singing in the wind. The Strouhal number shows a slight but continuous variation with Reynolds number around a value of 0.21. The boundary layer on the cylinder surface remains laminar and separation takes placeat about 81^0 from the forward stagnation point.
- **At about Re = 500** , multiple frequencies start showing up and the **wake tends to become Chaotic.**
- As the Reynolds number becomes higher, the boundary layer around the cylinder tends to become turbulent. The wake, of course, shows fully turbulent characters (Fig31.4 (e)).
- For larger Reynolds numbers, the boundary layer becomes turbulent. A turbulent boundary layer offers greater resistance to seperation than a laminar boundary layer. As a consequence the seperation point moves downstream and the seperation angle is delayed to 110^0 from the forward stagnation point (Fig 31.4 (f)).

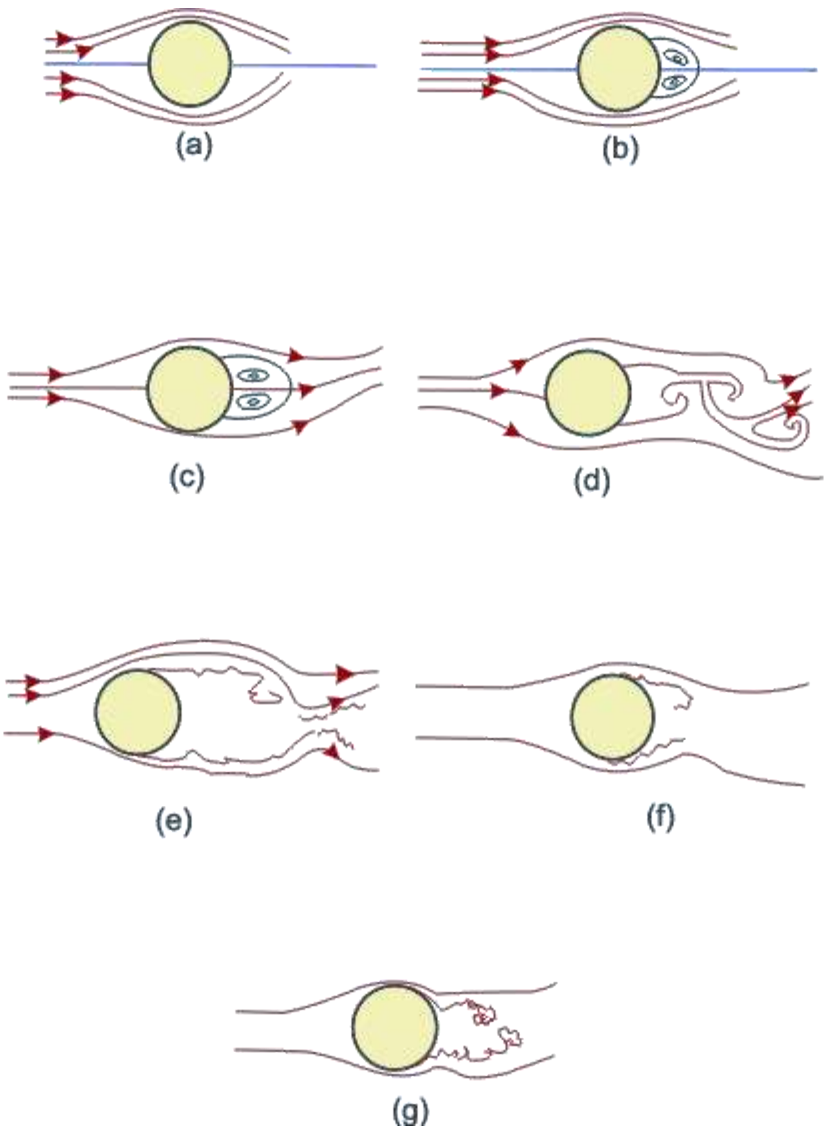

Fig. 31.4 Influence of Reynolds number on wake-zone aerodynamics

- Experimental flow visualizations past a circular cylinder are shown in *Figure 31.5 (a) and (b)*

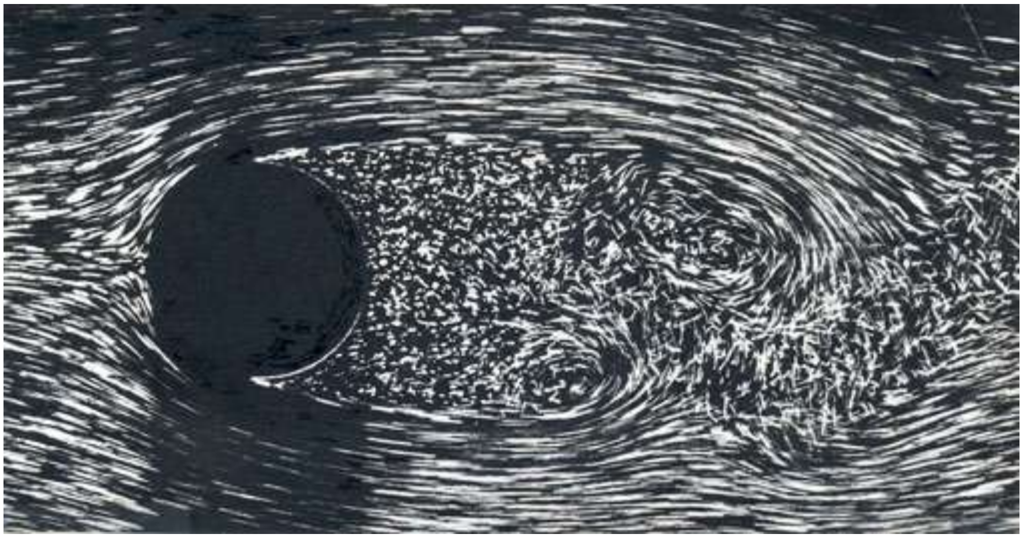

Fig 31.5 (a) Flow Past a Cylinder at Re=2000 [Photograph courtesy Werle and Gallon (ONERA)]

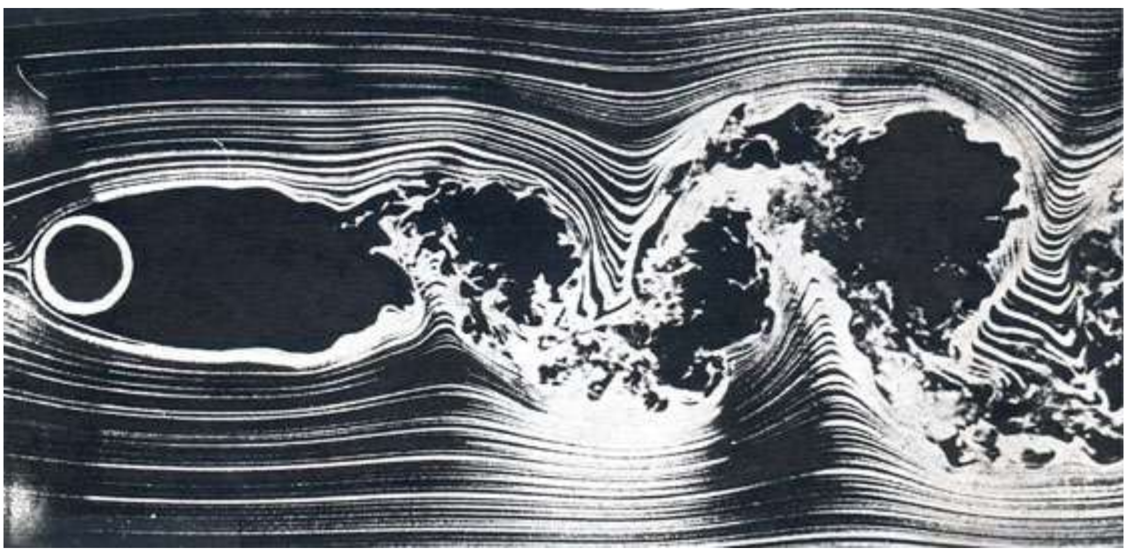

Fig 31.5 (b) Flow Past a Cylinder at Re=10000 [Photograph courtesy Thomas Corke and Hasan Najib (Illinois Institute of Technology, Chicago)]

- A very interesting sequence of events begins to develop when the Reynolds number is increased beyond 40, at which point the wake behind the cylinder becomes unstable. Photographs show that the wake develops a slow oscillation in which the velocity is periodic in time and downstream distance. The amplitude of the oscillation increases downstream. The oscillating wake rolls up into two staggered rows of vortices with opposite sense of rotation.

- Karman investigated the phenomenon and concluded that a nonstaggered row of vortices is unstable, and a staggered row is stable only if the ratio of lateral distance between the vortices to their longitudinal distance is 0.28. Because of the similarity of the wake with footprints in a street, the staggered row of vortices behind a blue body is called a **Karman Vortex Street** . The vortices move downstream at a speed smaller than the upstream velocity *U*.

- In the range $40 < Re < 80$, the vortex street does not interact with the pair of attached vortices. As Re is increased beyond 80 the vortex street forms closer to the cylinder, and the attached eddies themselves begin to oscillate. Finally the attached eddies periodically break off alternately from the two sides of the cylinder.
- While an eddy on one side is shed, that on the other side forms, resulting in an unsteady flow near the cylinder. As vortices of opposite circulations are shed off alternately from the two sides, the circulation around the cylinder changes sign, resulting in an oscillating "lift" or lateral force. If the frequency of vortex shedding is close to the natural frequency of some mode of vibration of the cylinder body, then an appreciable lateral vibration culminates.
- Numerical flow visualizations for the flow past a circular cylinder can be observed in Fig 31.6 and 31.7

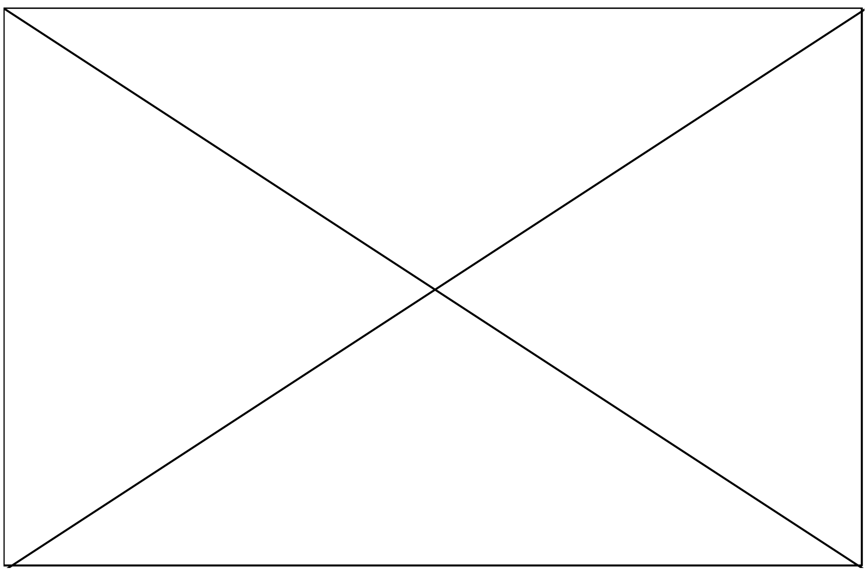

Fig 31.6 Numerical flow visualization (LES results) for a low reynolds number flow past a Circular Cylinder [Animation by Dr.-Ing M. Breuer, LSTM, Univ Erlangen-Nuremberg]

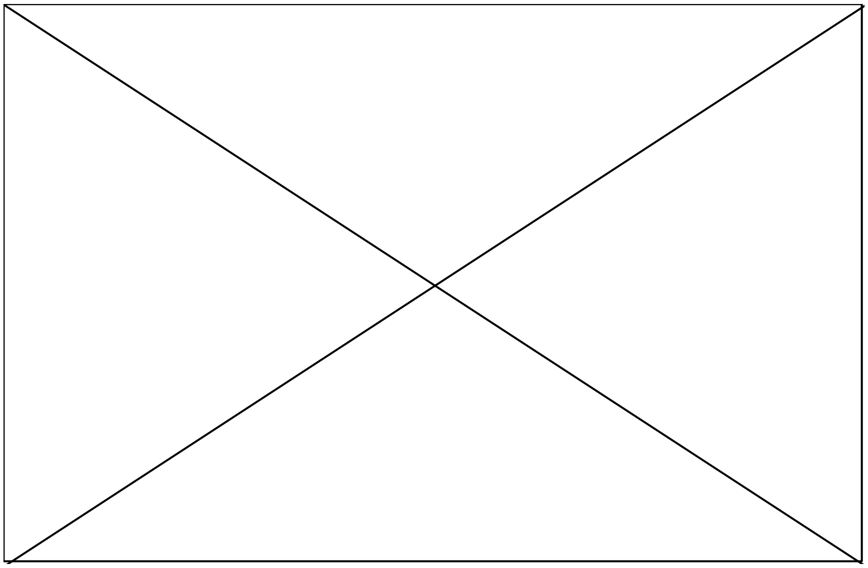

Fig 31.7 Numerical flow visualization (LES results) for a moderately high reynolds number flow past a Circular Cylinder
[Animation by Dr.-Ing M. Breuer, LSTM, Univ Erlangen-Nuremberg]

- An understanding of the transitional flow processes will help in practical problems either by improving procedures for predicting positions or for determining methods of advancing or retarding the transition position.

- The **critical value at which the transition occurs in pipe flow is** $\mathrm{Re}_{cr} = 2300$. The actual value depends upon the disturbance in flow. Some experiments have shown the critical Reynolds number to reach as high as 10,000. The precise upper bound is not known, but the lower bound appears to be $\mathrm{Re}_{cr} = 2300$. **Below this value, the flow remains laminar even when subjected to strong disturbances.**

- In the case of flow through a channel, $2300 \le \mathrm{Re}_{cr} \le 2600$, the flow alternates randomly between laminar and partially turbulent. **Near the centerline, the flow is more laminar than turbulent, whereas near the wall, the flow is more turbulent than laminar.** For flow over a flat plate, turbulent regime is observed between Reynolds numbers $U_\infty x/\nu$ of 3.5×10^5 and 10^6.

Several Events Of Transition -

Transitional flow consists of several events as shown in *Fig. 31.8*. Let us consider the events one after another.

1. Region of instability of small wavy disturbances-

Consider a laminar flow over a flat plate aligned with the flow direction (*Fig. 31.8*).

- In the presence of an adverse pressure gradient, at a high Reynolds number (water velocity approximately 9-cm/sec), **two-dimensional waves appear.**
- **These waves are called *Tollmien-Schlichting* wave(** In 1929, Tollmien and Schlichting predicted that the waves would form and grow in the boundary layer).
- These waves can be made visible by a method known as tellurium method.

2. Three-dimensional waves and vortex formation-

- Disturbances in the free stream or **oscillations in the upstream boundary layer can generate wave growth,** which has a variation **in the span wise direction.**
- This leads an initially two-dimensional wave to **a three-dimensional form.**
- In many such transitional flows, periodicity is observed in the span wise direction.
- This is accompanied by the appearance of vortices whose axes lie in the direction of flow.

3. Peak-Valley development with streamwise vortices-

- As the three-dimensional wave propagates downstream, the **boundary layer flow develops into a complex stream wise vortex system.**
- Within this vortex system, **at some spanwise location, the velocities fluctuate violently** .
- These locations are **called peaks and the neighbouring locations of the peaks are valleys (***Fig. 31.9***).**

4. Vorticity concentration and shear layer development-

At the spanwise locations corresponding to the peak, the instantaneous streamwise velocity profiles demonstrate the following

- Often, an inflexion is observed on the velocity profile.
- The inflectional profile appears and disappears once after each cycle of the basic wave.

5. Breakdown-

The instantaneous velocity profiles produce high shear in the outer region of the boundary layer.

- The velocity fluctuations develop from the shear layer at a higher frequency than that of the basic wave.

- These velocity fluctuations have a strong ability to amplify any slight three-dimensionality, which is already present in the flow field.
- As a result, **a staggered vortex pattern evolves with the streamwise wavelength twice the wavelength of Tollmien-Schlichting wavelength .**
- The span wise wavelength of these structures is about one-half of the stream wise value.
- The high frequency fluctuations are referred as **hairpin eddies.**

This is known as breakdown.

6. Turbulent-spot development-

- The hairpin-eddies travel at a speed grater than that of the basic (primary) waves.
- As they travel downstream, eddies spread in the spanwise direction and towards the wall.
- The vortices begin a cascading breakdown into smaller vortices.
- In such a fluctuating state, intense local changes occur at random locations in the shear layer near the wall in the form of turbulent spots.
- Each spot grows almost linearly with the downstream distance.

The creation of spots is considered as the main event of transition .

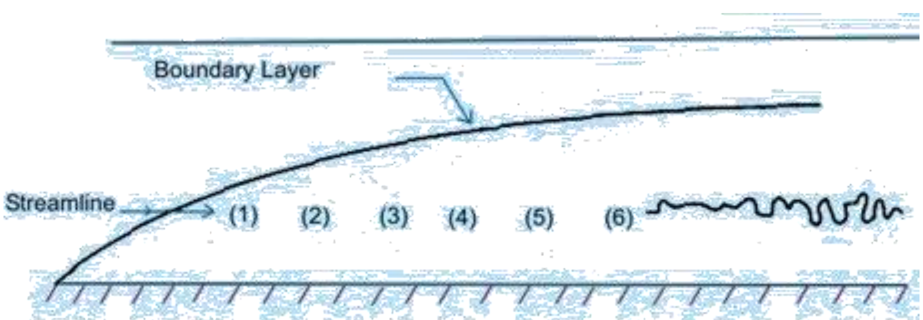

Fig. 31.8 Sequence of event involved in transition

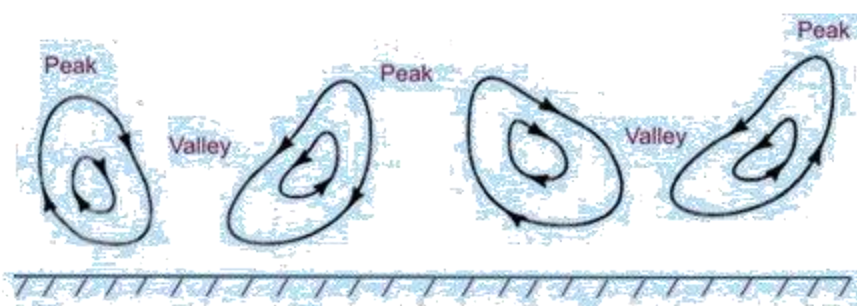

Fig. 31.9 Cross-stream view of the streamwise vortex system

Exercise Problems - Chapter 9

1.Two students are asked to solve the Blasius flow over a flat plate to determine the variation of boundary layer thickness as a function of the Reynolds number. One student solves the problem by similarity method and arrives at the result $\frac{\delta}{x} = \frac{5 \cdot 0}{\sqrt{Re_x}}$. The other student chooses to solve the problem by using the momentum-integer equation and Karman-Pohlhausen method and funds that $\frac{\delta}{x} = \frac{4 \cdot 64}{\sqrt{Re_x}}$. Which of the two results is expected to be closer to the experimental results and why?

2. A scientist claims that a highly viscous flow around a body can generate the same flow patterns as the flow of an inviscid and incompressible fluid around that body. According to our understanding, the Reynolds number for the first flow is very small, while the Reynolds number for the second flow can be taken to be ∞ (infinity). Do you think it is possible to get the same flow patterns for the two extreme values of Reynolds number? Please use mathematical analysis to prove or disprove the scientist's claim.

3. In boundary layer theory, a boundary layer can be characterized by any of the following quantities (i) Boundary layer thickness (ii) Displacement thickness (iii) Momentum thickness.

How do these quantities differ in their physical as well as mathematical definitions? For the flow over a flat plate, which of these is expected to have the highest value at a given location on the wall, and which the lowest?

4. What do you mean by the "point of separation" of a boundary layer? How will the velocity gradient $\frac{\partial u}{\partial y}$ and the second gradient $\frac{\partial^2 u}{\partial y^2}$ .Vary within the boundary layer at the point of separation? Please show the variation graphically. Here u is the velocity along the wall and y is the co-ordinate perpendicular to the wall.

5. Reduce the Prandtl's boundary layer equations to a simpler form than that given by equations (28.10) - (28.12) for -

(a) Flow over a flat plate.
(b) The case $\tau_{yx} = C_1$ (a constant)
(c) The case where velocity (v) is directly proportional to kinematic viscosity (ν)
(d) Also solve the Prandtl's boundary layer equations for v = ν assuming pressure gradient $\frac{\partial p}{\partial x}$ =0.

6. Water of kinematic viscosity (ν) equal to 9.29×10^{-7} m^2 /s is flowing steadily over a smooth flat plate at zero angle of incidence, with a velocity of 1.524 m/s. The length of the plate is 0.3048 m. Calculate-

(a) The thickness of the boundary layer at 0.1524 m from the leading edge.

(b) Boundary layer rate of growth at 0.1524 m from the leading edge.
(c) Total drag coefficient on the plate.

7. Use the Prandtl's boundary layer equations and show that the velocity profile for a laminar flow past a flat plate has an infinite radius of curvature on the surface of the plate.

8. Air is flowing over a smooth flat plate at a velocity of 4.39 m/s. The density of air is 1.031 Kg/m^3 and the kinematic viscosity is 1.34×10^{-5} m^2 /s. The length of the plate is 12.2 m in the direction of the flow. Find-

(a) The boundary layer thickness at 15.24 cm from the leading edge.
(b) The drag coefficient (C_{Df}).

9. Show that the shape factor (H) has the value $\approx$ 2.6 for the boundary layer flow over a flat plate. Also calculate the position where the flow is critical for flow velocity of 3.048 m/s and kinematic viscosity 9.29×10^{-7} m^2 /s.
Given that at the critical location Reynold's Number (based on distance from the leading edge surface) is related to shape factor (H) by-

log(R critical) =H.

10. Determine the distance downstream from the bow of a ship moving at 3.9 m/s relative to still water at which the boundary layer will become turbulent. Also find the boundary layer thickness and total friction drag coefficient for this portion of the surface of the ship. Given the kinematic viscosity = 1.124×10^{-6} m^2 /s.

Turbulent Flow

Introduction

- The turbulent motion is an **irregular** motion.
- Turbulent fluid motion can be considered as an irregular condition of flow in which various quantities (such as velocity components and pressure) show a **random variation with time and space** in such a way that the statistical average of those quantities can be quantitatively expressed.
- It is postulated that the fluctuations inherently come from **disturbances** (such as roughness of a solid surface) and they may be either dampened out due to viscous damping or may grow by drawing energy from the free stream.

- At a **Reynolds number less than the critical**, the kinetic energy of flow is not enough to sustain the random fluctuations against the viscous damping and in such cases **laminar flow** continues to exist.
- At somewhat **higher Reynolds number** than the critical Reynolds number, the kinetic energy of flow supports the growth of fluctuations and **transition to turbulence** takes place.

Characteristics Of Turbulent Flow

- The most important characteristic of turbulent motion is the fact that **velocity and pressure** at a point **fluctuate with time** in a random manner.

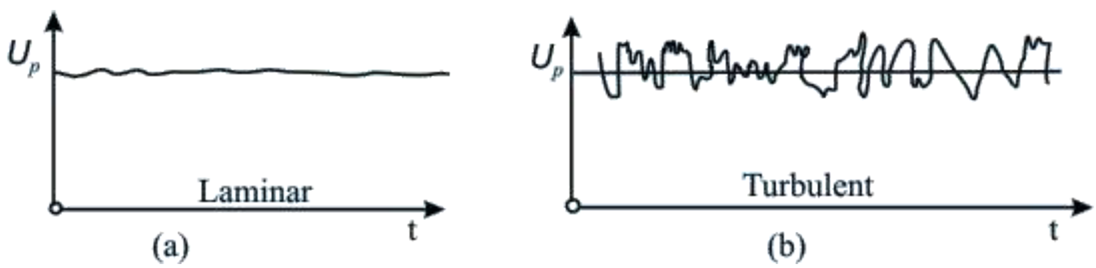

Fig. 32.1 Variation of horizontal components of velocity for laminar and turbulent flows at a point P

- The mixing in turbulent flow is more due to these fluctuations. As a result we can see more uniform velocity distributions in turbulent pipe flows as compared to the laminar flows .

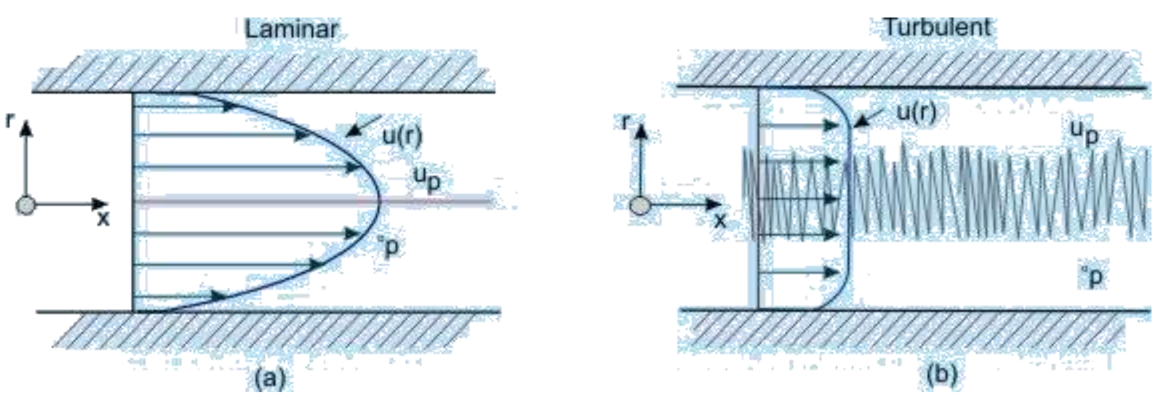

Fig. 32.2 Comparison of velocity profiles in a pipe for (a) laminar and (b) turbulent flows

- **Turbulence can be generated by** -
    1. frictional forces at the confining solid walls
    2. the flow of layers of fluids with different velocities over one another

The turbulence generated in these two ways are considered to be different.

Turbulence generated and continuously affected by fixed walls is designated as **wall turbulence** , and turbulence generated by two adjacent layers of fluid in absence of walls is termed as **free turbulence** . One of the effects of viscosity on turbulence is to make the flow more homogeneous and less dependent on direction.

- Turbulence can be categorised as below -
- **Homogeneous Turbulence**: Turbulence has the same structure quantitatively in all parts of the flow field.
- **Isotropic Turbulence**: The statistical features have no directional preference and perfect disorder persists.
- **Anisotropic Turbulence**: The statistical features have directional preference and the mean velocity has a gradient.

- **Homogeneous Turbulence** : The term homogeneous turbulence implies that the velocity fluctuations in the system are random but the average turbulent characteristics are independent of the position in the fluid, i.e., invariant to axis translation.

Consider the root mean square velocity fluctuations

$u' = \sqrt{\overline{u^2}}$, $v' = \sqrt{\overline{v^2}}$, $w' = \sqrt{\overline{w^2}}$

In homogeneous turbulence, the rms values of *u', v'* and *w'* can all be different, but each value must be constant over the entire turbulent field. Note that even if the rms fluctuation of any component, say *u'* s are constant over the entire field the instantaneous values of u necessarily differ from point to point at any instant.

- **Isotropic Turbulence**: The velocity fluctuations are independent of the axis of reference, i.e. invariant to axis rotation and reflection. <u>Isotropic turbulence is by its definition always homogeneous</u> . In such a situation, the gradient of the mean velocity does not exist, the mean velocity is either zero or constant throughout.

In isotropic turbulence fluctuations are independent of the direction of reference and

$\sqrt{\overline{u^2}} = \sqrt{\overline{v^2}} = \sqrt{\overline{w^2}}$ or $u' = v' = w'$

It is re-emphasised that even if the rms fluctuations at any point are same, their instantaneous values necessarily differ from each other at any instant.

- **Turbulent flow is diffusive and dissipative** . In general, turbulence brings about better mixing of a fluid and produces an additional diffusive effect. Such a diffusion is termed as "Eddy-diffusion

".(Note that this is different from molecular diffusion)
At a large Reynolds number there exists a continuous transport of energy from the free stream to the large eddies. Then, from the large eddies smaller eddies are continuously formed. Near the wall smallest eddies destroy themselves in dissipating energy, i.e., converting kinetic energy of the eddies into intermolecular energy.

Laminar-Turbulent Transition

- For a turbulent flow over a flat plate,

Boundary layer starts as laminar flow at leading edge —subsequently→ Flow turns into transition flow —shortly thereafter→ turns into turbulent flow

- The turbulent boundary layer continues to grow in thickness, with a small region below it called a **viscous sublayer**. In this sub layer, the flow is well behaved,just as the laminar boundary layer (Fig. 32.3)

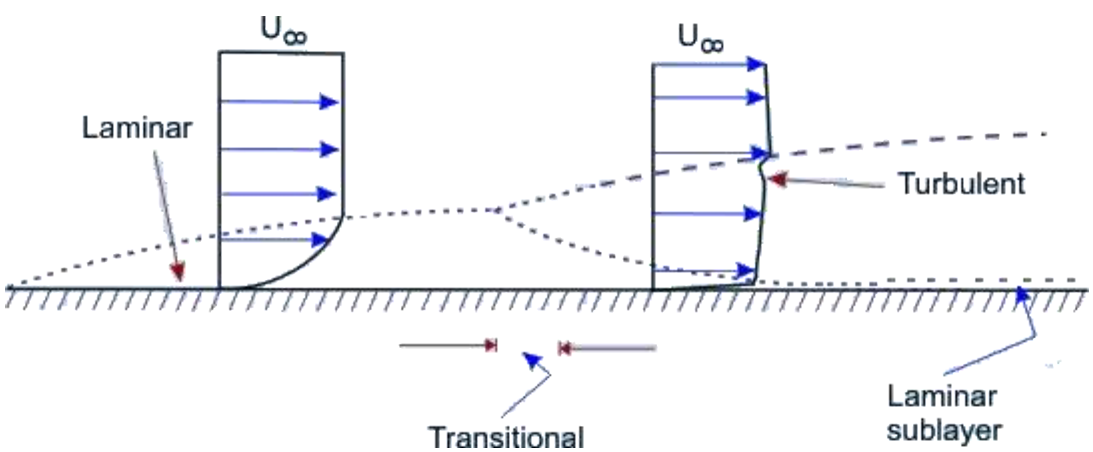

Fig. 32.3 Laminar - turbulent transition

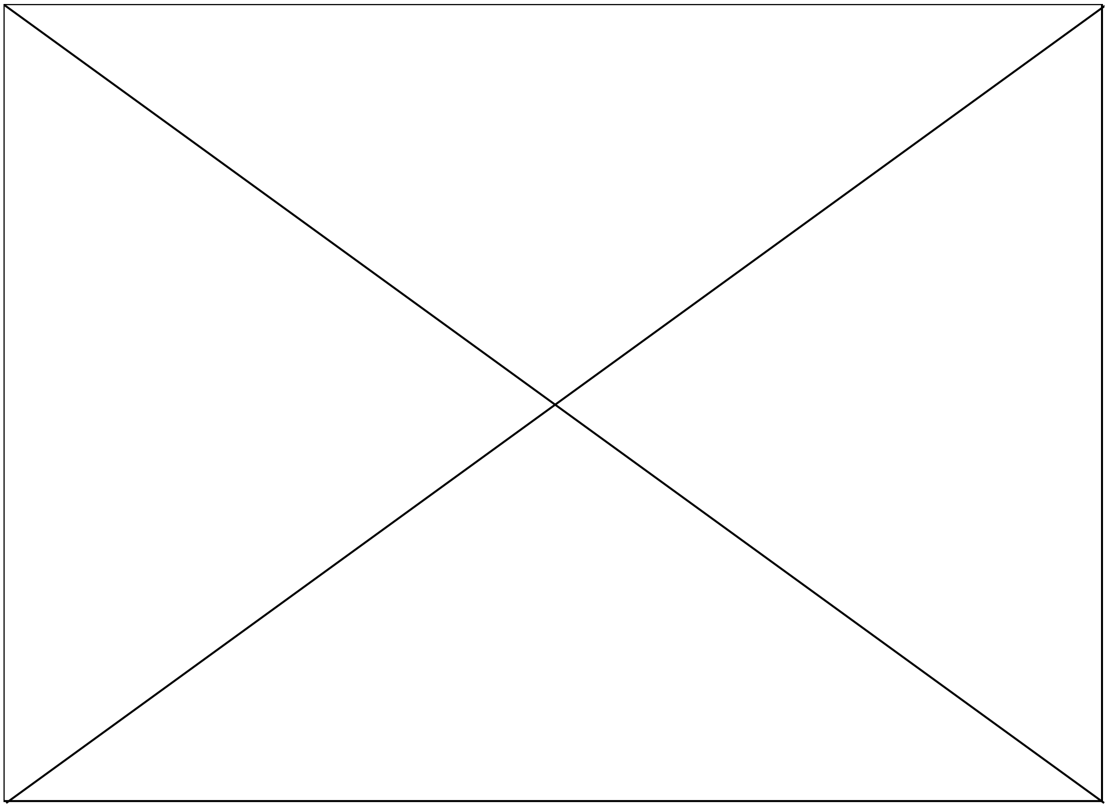

Illustration

- Observe that at a certain axial location, the laminar boundary layer tends to become unstable. Physically this means that the disturbances in the flow grow in amplitude at this location.

Free stream turbulence, wall roughness and acoustic signals may be among the sources of such disturbances. **Transition to turbulent flow is thus initiated with the instability in laminar flow**

- The possibility of instability in boundary layer was felt by **Prandtl** as early as 1912.The theoretical analysis of **Tollmien and Schlichting** showed that unstable waves could exist if the **Reynolds number was 575**.

The Reynolds number was defined as

$$\mathrm{Re} = U_{\infty}\delta^{*}/\nu$$

where U_{∞} is the free stream velocity , δ^{*} is the displacement thickness and ν is the kinematic viscosity .

- **Taylor** developed an alternate theory, which assumed that the transition is caused by a momentary separation at the boundary layer associated with the free stream turbulence.

  In a pipe flow the initiation of turbulence is usually observed at **Reynolds numbers (**$U_{\infty}D/\nu$ **)in the range of 2000 to 2700**.

The development starts with a laminar profile, undergoes a transition, changes over to turbulent profile and then stays turbulent thereafter (Fig. 32.4). The length of development is of the order of 25 to 40 diameters of the pipe.

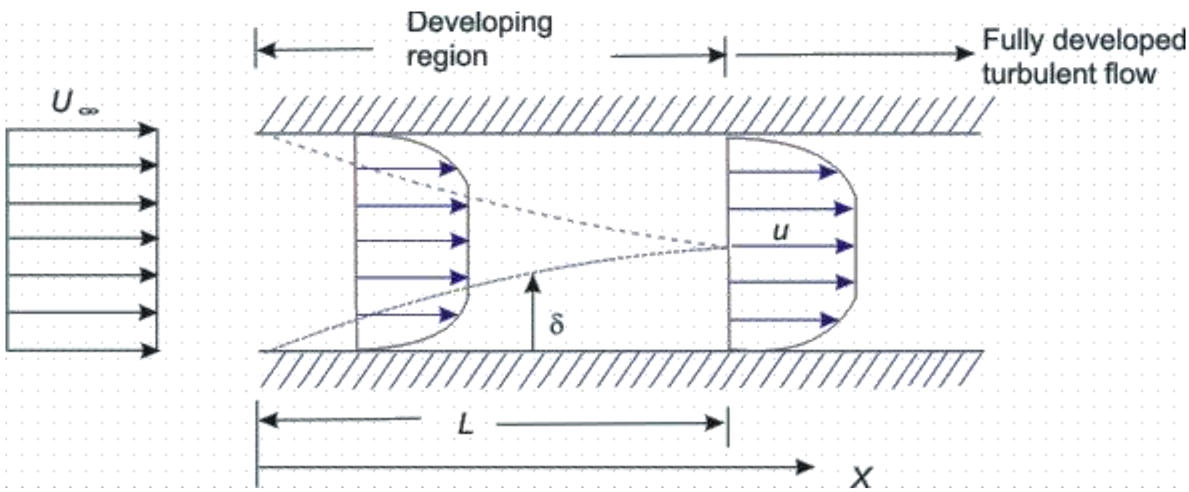

Fig. 32.4 Development of turbulent flow in a circular duct

Correlation Functions

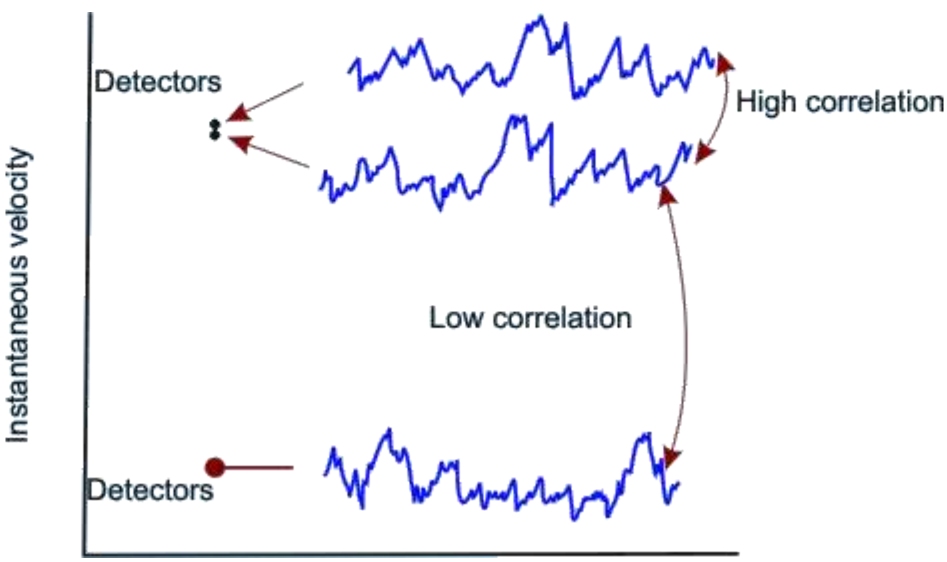

Fig 32.5 Velocity Correlation

- A statistical correlation can be applied to fluctuating velocity terms in turbulence. Turbulent motion is by definition eddying motion. Not withstanding the circulation strength of the individual eddies, a high degree of correlation exists between the velocities at two points in space, if the distance between the points is smaller than the diameter of the eddy. Conversely, if the points are so far apart that the space, in between, corresponds to many eddy diameters (Figure 32.5), little correlation can be expected.

- Consider a statistical property of a random variable (velocity) at two points separated by a distance r. An Eulerian correlation tensor (nine terms) at the two points can be defined by

$$Q = \overline{u(x)u(x+r)}$$

In other words, the dependence between the two velocities at two points is measured by the correlations, i.e. the time averages of the products of the quantities measured at two points. The correlation of the u' components of the turbulent velocity of these two points is defined as

$$\overline{u'(x)u'(x+r)}$$

It is conventional to work with the non-dimensional form of the correlation, such as

$$R(r) = \frac{\overline{u'(x)u'(x+r)}}{\left(\overline{u'^2}(x)\overline{u'^2}(x+r)\right)^{1/2}}$$

A value of **R(r) of unity signifies a perfect correlation** of the two quantities involved and their motion is in phase**.** Negative value of the correlation function implies that the time averages of the velocities in the two correlated points have different signs. Figure 32.6 shows typical variations of the correlation R with increasing separation r .

The positive correlation indicates that the fluid can be modelled as travelling in lumps. Since swirling motion is an essential feature of turbulent motion, these lumps are viewed as eddies of various sizes. The correlation R(r) is a measure of the strength of the eddies of size larger than r. Essentially the velocities at two points are correlated if they are located on the same eddy

- To describe the evolution of a fluctuating function *u'(t)*, we need to know the manner in which the value of *u'* at different times are related. For this purpose the correlation function

$$R(\tau) = \frac{\overline{u'(t)u'(t+\tau)}}{u'^2}$$

between the values of *u'* at different times is chosen and is called **autocorrelation function.**

- The correlation studies reveal that the turbulent motion is composed of eddies which are convected by the mean motion . The eddies have a wide range variation in their size. The size of the large eddies is comparable with the dimensions of the neighbouring objects or the dimensions of the flow passage.

The size of the smallest eddies can be of the order of 1 mm or less. However, the smallest eddies are much larger than the molecular mean free paths and the turbulent motion does obey the principles of continuum mechanics.

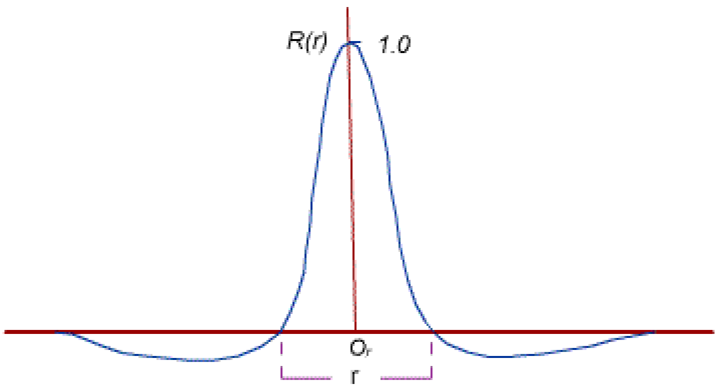

Fig 32.6 Variation of R with the distance of separation, r

Reynolds decomposition of turbulent flow :

- **The Experiment:** In 1883, O. Reynolds conducted experiments with pipe flow by feeding into the stream a thin thread of liquid dye. For low Reynolds numbers, the dye traced a straight line and did not disperse. With increasing velocity, the dye thread got mixed in all directions and the flowing fluid appeared to be uniformly colored in the downstream flow.

The Inference: It was conjectured that on the main motion in the direction of the pipe axis, there existed a superimposed motion all along the main motion at right angles to it. The superimposed motion causes exchange of momentum in transverse direction and the velocity distribution over the cross-section is more uniform than in laminar flow. This description of turbulent flow which consists of superimposed streaming and fluctuating (eddying) motion is well known as **Reynolds decomposition of turbulent flow.**

- Here, we shall discuss different descriptions of mean motion. Generally, for Eulerian velocity *u* , the following two methods of averaging could be obtained.

(i) Time average for a stationary turbulence:

$$\bar{u}^t(x_0) = \lim_{t_1 \to \infty} \frac{1}{2t_1} \int_{-t_1}^{t_1} u(x_0, t)dt$$

(ii) Space average for a homogeneous turbulence:

$$\bar{u}^s(t_0) = \lim_{x \to \infty} \frac{1}{2x} \int_{-x}^{x} u(x, t_0)dx$$

For a stationary and homogeneous turbulence, it is assumed that the two averages lead to the same result: $\bar{u}^t = \bar{u}^s$ and the assumption is known as the **ergodic hypothesis**.

- In our analysis, average of any quantity will be evaluated as a *time average* . Take a finite time interval t_1. This interval must be larger than the time scale of turbulence. Needless to say that it must be small compared with the period t_2 of any slow variation (such as periodicity of the mean flow) in the flow field that we do not consider to be chaotic or turbulent **.**

Thus, for a parallel flow, it can be written that the axial velocity component is

$$u(y,t) = \bar{u}(y) + u'(\Gamma, t) \qquad (32.1)$$

As such, the time mean component $\bar{u}(y)$ determines whether the turbulent motion is steady or not. The symbol Γ signifies any of the space variables.

- While the motion described by Fig.32.6(a) is for a turbulent flow with steady mean velocity the Fig.32.6(b) shows an example of turbulent flow with unsteady mean velocity. The time period of the high frequency fluctuating component is t_1 whereas the time period for the unsteady mean motion is t_2 and for obvious reason $t_2 >> t_1$. Even if the bulk motion is parallel, the fluctuation *u* ' being random varies in all directions.

- The continuity equation, gives us

$$\frac{\partial u}{\partial x} + \frac{\partial v}{\partial y} + \frac{\partial w}{\partial z} = 0$$

Invoking Eq.(32.1) in the above expression, we get

$$\frac{\partial \bar{u}}{\partial x} + \frac{\partial u'}{\partial x} + \frac{\partial v}{\partial y} + \frac{\partial w}{\partial z} = 0 \qquad (32.2)$$

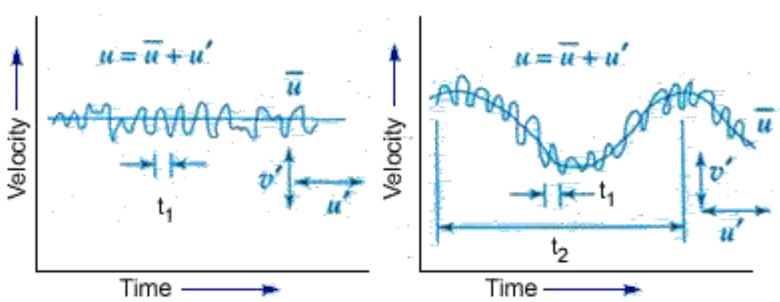

Fig 32.6 Steady and unsteady mean motions in a turbulent flow

Since $\frac{\partial u'}{\partial x} \neq 0$, Eq.(32.2) depicts that *y* and *z* components of velocity exist even for the parallel flow if the flow is turbulent. We have-

$$\begin{aligned} u(y,t) &= u(y) + u'(\Gamma,t) \\ v &= 0 + v'(\Gamma,t) \\ w &= 0 + w'(\Gamma,t) \end{aligned} \qquad (32.3)$$

Contd. from Previous slide

- However, the fluctuating components do not bring about the bulk displacement of a fluid element. The instantaneous displacement is $u'dt$ **,** and that is not responsible for the bulk motion**.** We can conclude from the above

$$\int_{-T}^{T} u'dt = 0 \quad (t_1 < T \leq t_2)$$

Due to the interaction of fluctuating components, macroscopic momentum transport takes place. Therefore, interaction effect between two fluctuating components over a long period is non-zero and this can be expressed as

$$\int_{-T}^{T} u'v'dt \neq 0$$

Taking time average of these two integrals and write

$$\bar{u}' = \frac{1}{2T}\int_{-T}^{T} u'dt = 0 \qquad (32.4a)$$

and

$$\overline{u'v'} = \frac{1}{2T}\int_{-T}^{T} u'v'dt \neq 0 \qquad (32.4b)$$

- Now, we can make a general statement with any two fluctuating parameters, say, with *f* ' and *g*' as

$$\bar{f}' = \bar{g}' = 0 \qquad (32.5a)$$

$$\overline{f'g'} \neq 0 \qquad (32.5b)$$

The time averages of the spatial gradients of the fluctuating components also follow the same laws, and they can be written as

$$\left.\begin{aligned}\overline{\frac{\partial f'}{\partial s}} = \overline{\frac{\partial^2 f'}{\partial s^2}} = 0 \\ \overline{\frac{\partial (f'g')}{\partial s}} \neq 0\end{aligned}\right\} \qquad (32.6)$$

- The **intensity of turbulence** or **degree of turbulence** in a flow is described by the relative magnitude of the root mean square value of the fluctuating components with respect to the time averaged main velocity. The mathematical expression is given by

$$\text{Tu} = \frac{1}{U_\infty}\sqrt{\frac{1}{3}(\overline{u'^2} + \overline{v'^2} + \overline{w'^2})} \qquad (32.7a)$$

The degree of turbulence in a wind tunnel can be brought down by introducing screens of fine mesh at the bell mouth entry. In general, at a certain distance from the screens, the turbulence in a wind tunnel becomes isotropic, i.e. the mean oscillation in the three components are equal,

$$\overline{u'^2} = \overline{v'^2} = \overline{w'^2}$$

In this case, it is sufficient to consider the oscillation u' in the direction of flow and to put

$$\text{Tu} = \frac{1}{U_\infty}\sqrt{\overline{u'^2}} \qquad (32.7b)$$

This simpler definition of turbulence intensity is often used in practice even in cases when turbulence is not isotropic.

Following Reynolds decomposition, it is suggested to separate the motion into a mean motion and a fluctuating or eddying motion. Denoting the time average of the u component of velocity by $\bar{u}$ and fluctuating component as u', we can write down the following,

$$u = \bar{u} + u', v = \bar{v} + v', w = \bar{w} + w', p = \bar{p} + p'$$

By definition, the time averages of all quantities describing fluctuations are equal to zero.

$$\bar{u'} = 0, \bar{v'} = 0, \bar{w'} = 0, \bar{p'} = 0 \qquad (32.8)$$

The fluctuations *u', v'* , and *w'* influence the mean motion $\bar{u}$, $\bar{v}$ and $\bar{w}$ in such a way that the mean motion exhibits an apparent increase in the resistance to deformation. In other words, the effect of fluctuations is an apparent increase in viscosity or macroscopic momentum diffusivity .

- **Rules of mean time - averages**

If *f* and *g* are two dependent variables and if *s* denotes anyone of the independent variables x, y

$$\overline{\overline{f}} = \overline{f}; \overline{f+g} = \overline{f} + \overline{g}; \overline{\overline{f}.g} = \overline{f}.\overline{g};$$

$$\overline{\frac{\partial f}{\partial s}} = \frac{\partial \overline{f}}{\partial s}; \int \overline{f ds} = \int \overline{f} ds$$

Intermittency

- Consider a turbulent flow confined to a limited region. To be specific we shall consider the example of a wake (Figure 33.1a), but our discussion also applies to a jet (Figure 33.1b), a shear layer (Figure 33.1c), or the outer part of a boundary layer on a wall.
- The fluid outside the turbulent region is either in irrotational motion (as in the case of a wake or a boundary layer), or nearly static (as in the case of a jet). Observations show that the instantaneous interface between the turbulent and nonturbulent fluid is very sharp.
- The thickness of the interface must equal the size of the smallest scales in the flow, namely the **Kolmogorov microscale**.

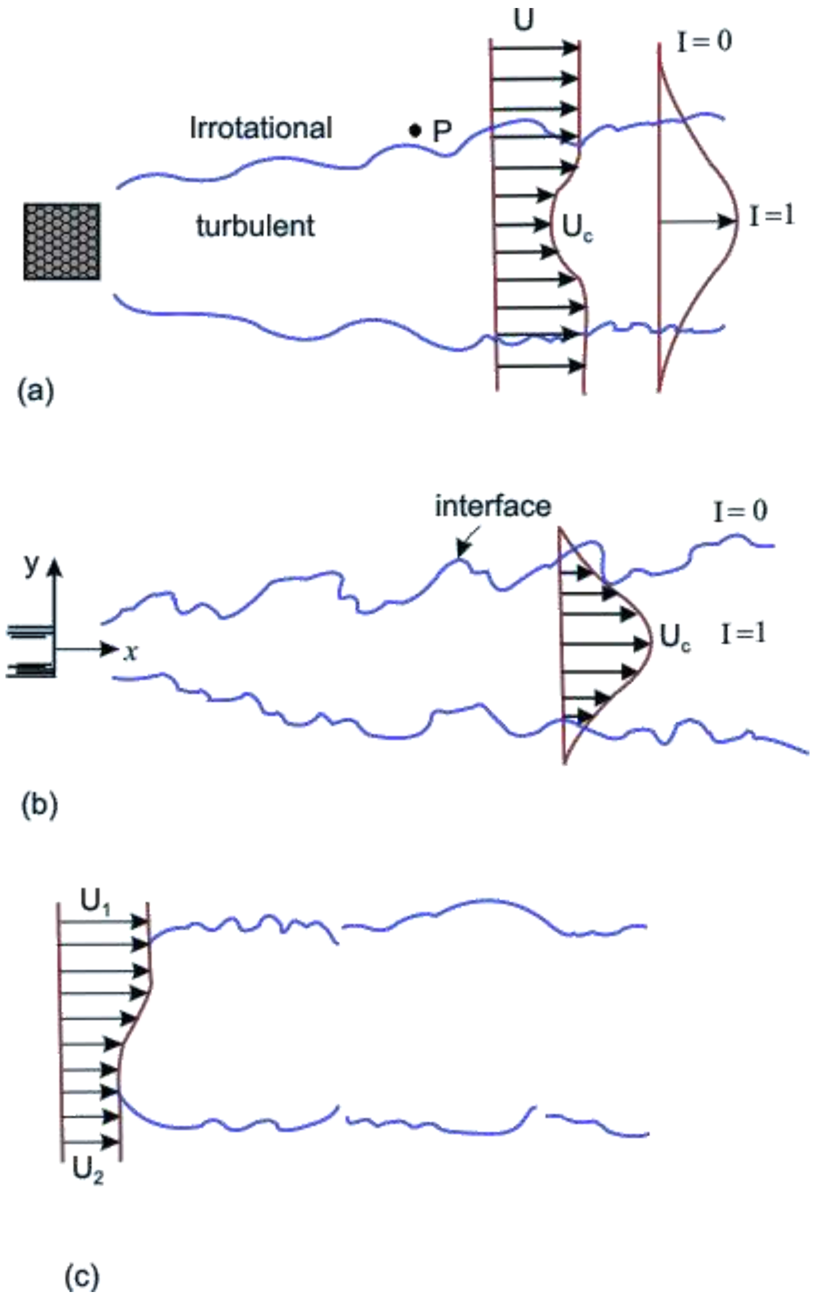

Figure 33.1 Three types of free turbulent flows; (a) wake (b) jet and (c) shear layer **[after P.K. Kundu and I.M. Cohen, Fluid Mechanics, Academic Press, 2002]**

- Measurement at a point in the outer part of the turbulent region (say at point P in Figure 33.1a) shows periods of high-frequency fluctuations as the point P moves into the turbulent flow and low-frequency periods as the point moves out of the turbulent region. Intermittency I is defined as the fraction of time the flow at a point is turbulent.

- The variation of I across a wake is sketched in Figure 33.1a, showing that I =1 near the center where the flow is always turbulent, and I = 0 at the outer edge of the flow domain.

Derivation of Governing Equations for Turbulent Flow

- For **incompressible flows**, the Navier-Stokes equations can be rearranged in the form

(33.1a)

(33.1b)

(33.1c)

and

(33.2)

- Express the velocity components and pressure in terms of time-mean values and corresponding fluctuations. In **continuity equation**, this substitution and subsequent time averaging will lead to

or,
$$\left(\frac{\partial \bar{u}}{\partial x}+\frac{\partial \bar{v}}{\partial y}+\frac{\partial \bar{w}}{\partial z}\right)+\left(\frac{\partial \overline{u'}}{\partial x}+\frac{\partial \overline{v'}}{\partial y}+\frac{\partial \overline{w'}}{\partial z}\right)=0$$

Since,
$$\frac{\partial \overline{u'}}{\partial x}=\frac{\partial \overline{v'}}{\partial y}=\frac{\partial \overline{w'}}{\partial z}=0$$

We can write
$$\frac{\partial \bar{u}}{\partial x}+\frac{\partial \bar{v}}{\partial y}+\frac{\partial \bar{w}}{\partial z}=0 \qquad (33.3a)$$

From Eqs (33.3a) and (33.2), we obtain

$$\frac{\partial u'}{\partial x}+\frac{\partial v'}{\partial y}+\frac{\partial w'}{\partial z}=0 \qquad (33.3b)$$

- It is evident that **the time-averaged velocity components** and **the fluctuating velocity components**, each satisfy the continuity equation for incompressible flow.
- Imagine a two-dimensional flow in which the turbulent components are independent of the *z* -direction. Eventually, Eq.(33.3b) tends to

$$\frac{\partial u'}{\partial x}=-\frac{\partial v'}{\partial y} \qquad (33.4)$$

On the basis of condition (33.4), it is postulated that if at an instant there is an increase in u' in the *x* -direction, it will be followed by an increase in v' in the negative *y* -direction. In other words, $\overline{u'v'}$ **is non-zero and negative**. (see Figure 33.2)

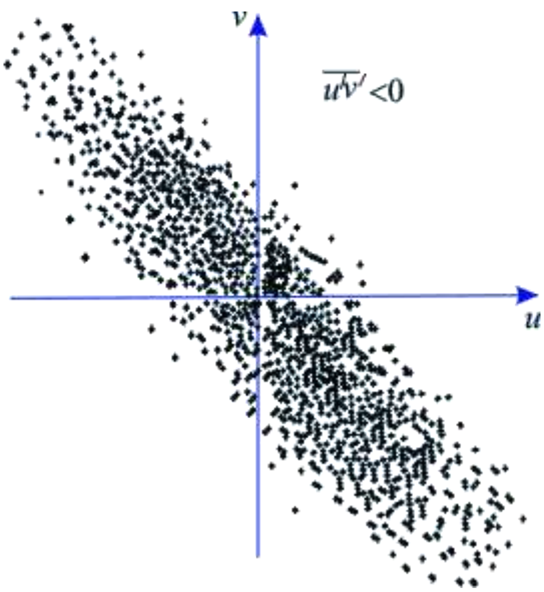

Fig 33.2 Each dot represents uv pair at an instant

- Invoking the concepts of eqn. (32.8) into the equations of motion eqn (33.1 a, b, c), we obtain expressions in terms of mean and fluctuating components. Now, forming time averages and considering the rules of averaging we discern the following. The terms which are linear, such as $\frac{\partial u'}{\partial t}$ and $\frac{\partial^2 u'}{\partial x^2}$ vanish when they are averaged [from (32.6)]. The same is true for the mixed terms like $\overline{u}\cdot u'$, or $\overline{u}\cdot v'$, but the quadratic terms in the fluctuating components remain in the equations. After averaging, they form $\overline{u'^2}$, $\overline{u'v'}$ etc.

- If we perform the aforesaid exercise on the x-momentum equation, we obtain

$$\rho\left\{\frac{\partial \overline{u}}{\partial t}+\frac{\partial \overline{u'}}{\partial t}^{\,0}+\frac{\partial\left(\overline{u}^2+\overline{u'^2}\right)}{\partial x}+\frac{\partial\left(\overline{u\cdot v}+\overline{u'v'}\right)}{\partial y}+\frac{\partial\left(\overline{u}\cdot\overline{w}+\overline{u'w'}\right)}{\partial z}\right\}$$

$$=-\frac{\partial \overline{p}}{\partial x}-\frac{\partial \overline{p'}}{\partial x}^{\,0}+\mu\left[\frac{\partial^2\overline{u}}{\partial x}+\frac{\partial^2\overline{u}}{\partial y}+\frac{\partial^2\overline{u}}{\partial z}+\left(\frac{\partial^2\overline{u'}}{\partial x^2}^{\,0}+\frac{\partial^2\overline{u'}}{\partial y}^{\,0}+\frac{\partial^2\overline{u'}}{\partial z^2}^{\,0}\right)\right]$$

using rules of time averages,

$$\frac{\partial \overline{u}'}{\partial t}=0,\frac{\partial \overline{p}'}{\partial x}=0,\frac{\partial^2 \overline{u}'}{\partial x^2}=\frac{\partial^2 \overline{u}'}{\partial y^2}=\frac{\partial^2 \overline{u}'}{\partial z^2}=0$$

We obtain

$$\rho\left\{\frac{\partial \overline{u}}{\partial t}+\frac{\partial\left(\overline{u}^2\right)}{\partial x}+\frac{\partial\left(\overline{u}\cdot\overline{v}\right)}{\partial y}+\frac{\partial\left(\overline{u}\cdot\overline{w}\right)}{\partial z}\right\}=-\frac{\partial \overline{p}}{\partial x}+\mu\nabla^2\overline{u}-\rho\left[\frac{\partial}{\partial x}\overline{u'^2}+\frac{\partial}{\partial y}\overline{u'v'}+\frac{\partial}{\partial z}\overline{u'w'}\right]$$

- Introducing simplifications arising out of continuity Eq. (33.3a), we shall obtain.

$$\rho\left\{\frac{\partial \overline{u}}{\partial t}+\overline{u}\frac{\partial \overline{u}}{\partial x}+\overline{v}\frac{\partial \overline{u}}{\partial y}+\overline{w}\frac{\partial \overline{u}}{\partial z}\right\}=-\frac{\partial \overline{p}}{\partial x}+\mu\nabla^2\overline{u}-\rho\left[\frac{\partial}{\partial x}\overline{u'^2}+\frac{\partial}{\partial y}\overline{u'v'}+\frac{\partial}{\partial z}\overline{u'w'}\right]$$

- Performing a similar treatment on y and z momentum equations, finally we obtain the momentum equations in the form.

In x direction,

$$\rho\left\{\frac{\partial \overline{u}}{\partial t}+\overline{u}\frac{\partial \overline{u}}{\partial x}+\overline{v}\frac{\partial \overline{u}}{\partial y}+\overline{w}\frac{\partial \overline{u}}{\partial z}\right\}=-\frac{\partial \overline{p}}{\partial x}+\mu\nabla^2\overline{u}-\rho\left[\frac{\partial}{\partial x}\overline{u'^2}+\frac{\partial}{\partial y}\overline{u'v'}+\frac{\partial}{\partial z}\overline{u'w'}\right] \qquad (33.5a)$$

In y direction,

$$\rho\left\{\frac{\partial \bar{v}}{\partial t}+\bar{u}\frac{\partial \bar{v}}{\partial x}+\bar{v}\frac{\partial \bar{v}}{\partial y}+\bar{w}\frac{\partial \bar{v}}{\partial z}\right\}=-\frac{\partial \bar{p}}{\partial y}+\mu\nabla^2\bar{v}-\rho\left[\frac{\partial}{\partial x}\overline{u'v'}+\frac{\partial}{\partial y}\overline{v'^2}+\frac{\partial}{\partial z}\overline{v'w'}\right] \qquad (33.5b)$$

In z direction,

$$\rho\left\{\frac{\partial \bar{w}}{\partial t}+\bar{u}\frac{\partial \bar{w}}{\partial x}+\bar{v}\frac{\partial \bar{w}}{\partial y}+\bar{w}\frac{\partial \bar{w}}{\partial z}\right\}=-\frac{\partial \bar{p}}{\partial z}+\mu\nabla^2\bar{w}-\rho\left[\frac{\partial}{\partial x}\overline{u'w'}+\frac{\partial}{\partial y}\overline{v'w'}+\frac{\partial}{\partial z}\overline{w'^2}\right] \qquad (33.5c)$$

- Comments on the governing equation :

  1. The left hand side of Eqs (33.5a)-(33.5c) are essentially similar to the steady-state Navier-Stokes equations if the velocity components *u, v* and *w* are replaced by $\bar{u}$, $\bar{v}$ and $\bar{w}$.
  2. The same argument holds good for the first two terms on the right hand side of Eqs (33.5a)-(33.5c).
  3. However, the equations contain some additional terms which depend on turbulent fluctuations of the stream. **These additional terms can be interpreted as components of a stress tensor.**

- Now, the resultant surface force per unit area due to these terms may be considered as

In x direction,

$$\rho\left\{\frac{\partial \bar{u}}{\partial t}+\bar{u}\frac{\partial \bar{u}}{\partial x}+\bar{v}\frac{\partial \bar{u}}{\partial y}+\bar{w}\frac{\partial \bar{u}}{\partial z}\right\}=-\frac{\partial \bar{p}}{\partial x}+\mu\nabla^2\bar{u}+\left[\frac{\partial}{\partial x}\sigma'_{xx}+\frac{\partial}{\partial y}\tau'_{yx}+\frac{\partial}{\partial z}\tau'_{zx}\right] \qquad (33.6a)$$

In y direction,

$$\rho\left\{\frac{\partial \bar{v}}{\partial t}+\bar{u}\frac{\partial \bar{v}}{\partial x}+\bar{v}\frac{\partial \bar{v}}{\partial y}+\bar{w}\frac{\partial \bar{v}}{\partial z}\right\}=-\frac{\partial \bar{p}}{\partial y}+\mu\nabla^2\bar{v}+\left[\frac{\partial}{\partial x}\tau'_{xy}+\frac{\partial}{\partial y}\sigma'_{yy}+\frac{\partial}{\partial z}\tau'_{zy}\right] \qquad (33.6b)$$

In z direction,

$$\rho\left\{\frac{\partial \bar{w}}{\partial t}+\bar{u}\frac{\partial \bar{w}}{\partial x}+\bar{v}\frac{\partial \bar{w}}{\partial y}+\bar{w}\frac{\partial \bar{w}}{\partial z}\right\}=-\frac{\partial \bar{p}}{\partial z}+\mu\nabla^2\bar{w}+\left[\frac{\partial}{\partial x}\tau'_{xz}+\frac{\partial}{\partial y}\tau'_{yz}+\frac{\partial}{\partial z}\sigma'_{zz}\right] \qquad (33.6c)$$

- Comparing Eqs (33.5) and (33.6), we can write

$$\begin{bmatrix} \sigma'_{xx} & \tau'_{xy} & \tau'_{xz} \\ \tau'_{xy} & \sigma'_{yy} & \tau'_{yz} \\ \tau'_{xz} & \tau'_{yz} & \sigma'_{zz} \end{bmatrix} = -\rho \begin{bmatrix} \overline{u'^2} & \overline{u'v'} & \overline{u'w'} \\ \overline{u'v'} & \overline{v'^2} & \overline{v'w'} \\ \overline{u'w'} & \overline{v'w'} & \overline{w'^2} \end{bmatrix} \qquad (33.7)$$

- It can be said that the mean velocity components of turbulent flow satisfy the same Navier-Stokes equations of laminar flow. However, for the turbulent flow, the laminar stresses must be increased by additional stresses which are given by the stress tensor (33.7). These additional stresses are known as **apparent stresses of turbulent flow** or **Reynolds stresses** . Since turbulence is considered as eddying motion and the aforesaid additional stresses are added to the viscous stresses due to mean motion in order to explain the complete stress field, it is often said that the apparent stresses are caused by eddy viscosity . The total stresses are now

$$\left.\begin{aligned} \sigma_{xx} &= -\overline{p} + 2\mu \frac{\partial \overline{u}}{\partial x} - \overline{\rho u'^2} \\ \tau_{xy} &= \mu\left(\frac{\partial \overline{u}}{\partial y} + \frac{\partial \overline{v}}{\partial x}\right) - \overline{\rho u'v'} \end{aligned}\right] \qquad (33.8)$$

and so on. The apparent stresses are much larger than the viscous components, and the viscous stresses can even be dropped in many actual calculations .

Turbulent Boundary Layer Equations

- For a two-dimensional flow (w = 0)over a flat plate, the thickness of turbulent boundary layer is assumed to be much smaller than the axial length and the **order of magnitude analysis** may be applied. As a consequence, the following inferences are drawn:

$$(a) \quad \frac{\partial \overline{p}}{\partial y} = 0,$$

$$(b) \quad \frac{\partial \overline{p}}{\partial x} = \frac{d\overline{p}}{dx}$$

$$(c) \quad \frac{\partial^2 \overline{u}}{\partial x^2} << \frac{\partial^2 \overline{u}}{\partial y^2},$$

$$(d) \quad \frac{\partial}{\partial x}\left(-\overline{\rho u'^2}\right) << \frac{\partial}{\partial y}\left(-\overline{\rho u'v'}\right),$$

- The turbulent boundary layer equation together with the equation of continuity becomes

$$\frac{\partial \bar{u}}{\partial x} + \frac{\partial \bar{v}}{\partial y} = 0 \qquad (33.9)$$

-

$$\bar{u}\frac{\partial \bar{u}}{\partial x} + \bar{v}\frac{\partial \bar{u}}{\partial y} = -\frac{1}{\rho}.\frac{\partial \bar{p}}{\partial x} + \frac{\partial}{\partial y}\left\{\nu\frac{\partial \bar{u}}{\partial y} - \overline{u'v'}\right\} \qquad (33.10)$$

- A comparison of Eq. (33.10) with laminar boundary layer Eq. (23.10) depicts that: *u, v* and *p* are replaced by the time average values $\bar{u}, \bar{v}$ and $\bar{p}$, and laminar viscous force per unit volume $\frac{\partial(\tau_l)}{\partial y}$ is replaced by $\frac{\partial}{\partial y}(\tau_l + \tau_t)$ where $\tau_l = \mu\frac{\partial \bar{u}}{\partial y}$ is the laminar shear stress and $\tau_t = -\rho\overline{u'v'}$ is the turbulent shear stress.

Boundary Conditions

- All the components of apparent stresses vanish at the solid walls and only stresses which act near the wall are the viscous stresses of laminar flow. The boundary conditions, to be satisfied by the mean velocity components, are similar to laminar flow.
- A very thin layer next to the wall behaves like a near wall region of the laminar flow. This layer is known as **laminar sublayer** and its velocities are such that the viscous forces dominate over the inertia forces. No turbulence exists in it (see Fig. 33.3).
- For a developed turbulent flow over a flat plate, in the near wall region, inertial effects are insignificant, and we can write from Eq.33.10,

$$\nu\frac{\partial^2 \bar{u}}{\partial y^2} - \frac{\partial\left(\overline{u'v'}\right)}{\partial y} = 0$$

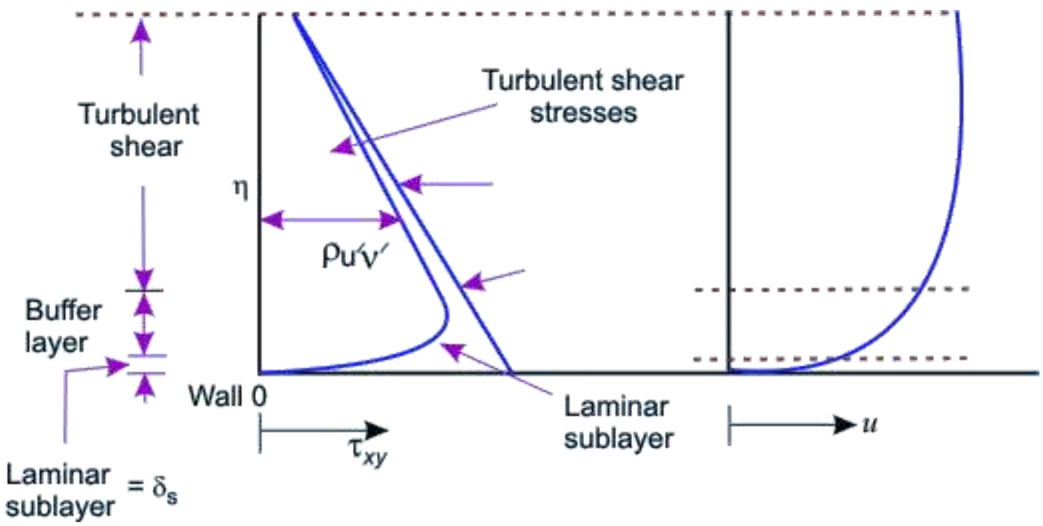

Fig 33.3 Different zones of a turbulent flow past a wall

which can be integrated as , $\frac{\nu \partial \bar{u}}{\partial y} - \overline{u'v'}$ =constant

- We know that the fluctuating components, do not exist near the wall, the shear stress on the wall is purely viscous and it follows

$$\nu \frac{\partial \bar{u}}{\partial y}\bigg|_{y=0} = \frac{\tau_w}{\rho}$$

However, the wall shear stress in the vicinity ofthe laminar sublayer is estimated as

$$\tau_w = \mu \left[\frac{U_s - 0}{\delta_s - 0}\right] = \mu \frac{U_s}{\delta_s} \qquad (33.11a)$$

where U_s is the fluid velocity at the edge of the sublayer. The flow in the sublayer is specified by a velocity scale (characteristic of this region).

- We define the **friction velocity**,

$$u_\tau = \left[\frac{\tau_w}{\rho}\right]^{1/2} \qquad (33.11b)$$

as our velocity scale. Once $u_\tau$is specified, the structure of the sub layer is specified. It has been confirmed experimentally that the turbulent intensity distributions are scaled with u_τ. For example, maximum value of the $\overline{u'^2}$ is always about $8u_\tau^2$. The relationship between u_τ and the U_s can be determined from Eqs (33.11a) and (33.11b) as

$$u_\tau^2 = \nu \frac{U_s}{\delta_s}$$

Let us assume $U_s = \overline{C} U_\infty$. Now we can write

$$u_\tau^2 = \overline{C} \nu \frac{U_\infty}{\delta_s} \qquad (33.12a)$$

where $\overline{C}$ is a proportionality constant

or

$$\frac{\delta_s u_\tau}{\nu} = \overline{C} \left[\frac{U_\infty}{u_\tau} \right] \qquad (33.12b)$$

Hence, a non-dimensional coordinate may be defined as, $\eta = \frac{y u_\tau}{\nu}$ which will help us estimating different zones in a turbulent flow. **The thickness** of **laminar sublayer or viscous sublayer is considered to be** $\eta \approx 5$.

Turbulent effect starts in the zone of $\eta > 5$ and in a zone of $5 < \eta < 70$, laminar and turbulent motions coexist. This domain is termed as **buffer zone**. Turbulent effects far outweight the laminar effect in the zone beyond $\eta = 70$ and this regime is termed as turbulent core .

- For flow over a flat plate, the turbulent shear stress ($-\rho \overline{u'v'}$) is constant throughout in the y direction and this becomes equal to τ_w at the wall. In the event of flow through a channel, the turbulent shear stress ($-\rho \overline{u'v'}$) varies with *y* and it is possible to write

$$\frac{\tau_t}{\tau_w} = \frac{\zeta}{h} \qquad (33.12c)$$

where the channel is assumed to have a height ***2h*** and ζ is the distance measured from the centreline of the channel $(= h - y)$. Figure 33.1 explains such variation of turbulent stress.

Shear Stress Models

- In analogy with the coefficient of viscosity for laminar flow, J. Boussinesq introduced a **mixing coefficient** μ_τ for the Reynolds stress term, defined as

$$\tau_t = -\rho\overline{u'v'} = \mu_t \frac{\partial \bar{u}}{\partial y}$$

- Using μ_τ the shearing stresses can be written as

$$\tau_l = \rho\nu\frac{\partial u}{\partial y}, \tau_t = \mu_t \frac{\partial \bar{u}}{\partial y} = \rho\nu_t\frac{\partial \bar{u}}{\partial y}$$

such that the equation

$$\bar{u}\frac{\partial \bar{u}}{\partial x} + \bar{v}\frac{\partial \bar{u}}{\partial y} = -\frac{1}{\rho}.\frac{\partial p}{\partial x} + \frac{\partial}{\partial y}\left\{\nu\frac{\partial \bar{u}}{\partial y} - \overline{u'v'}\right\}$$

may be written as

$$\bar{u}\frac{\partial \bar{u}}{\partial x} + \bar{v}\frac{\partial \bar{u}}{\partial y} = \frac{1}{\rho}.\frac{\partial p}{\partial x} + \frac{\partial}{\partial y}\left\{(\nu + \nu_t)\frac{\partial \bar{u}}{\partial y}\right\} \quad (33.13)$$

The term v_t is known as **eddy viscosity** and the model is known as **eddy viscosity model** .

- Unfortunately the value of v_t is not known. The term v is a property of the fluid whereas v_t is attributed to random fluctuations and is not a property of the fluid. However, it is necessary to find out empirical relations between v_t, and the mean velocity. The following section discusses relation between the aforesaid apparent or eddy viscosity and the mean velocity components

Prandtl's Mixing Length Hypothesis

- Consider a fully developed turbulent boundary layer . The stream wise mean velocity varies only from streamline to streamline. The main flow direction is assumed parallel to the x-axis (Fig. 33.4).

- The time average components of velocity are given by $\bar{u} = \bar{u}(y), \bar{v} = 0, \bar{w} = 0$. The fluctuating component of transverse velocity v'transports mass and momentum across a plane at y_1 from the wall. The shear stress due to the fluctuation is given by

$$\tau_t = -\rho\overline{u'v'} = \mu_t \frac{\partial \bar{u}}{\partial y} \tag{33.14}$$

- Fluid, which comes to the layer y_1 from a layer $(y_1 - l)$ has a positive value of v'. If the lump of fluid retains its original momentum then its velocity at its current location y_1 is smaller than the velocity prevailing there. The difference in velocities is then

$$\Delta u_1 = \bar{u}(y_1) - \bar{u}(y_1 - l) \approx l\left(\frac{\partial \bar{u}}{\partial y}\right)_{y1} \tag{33.15}$$

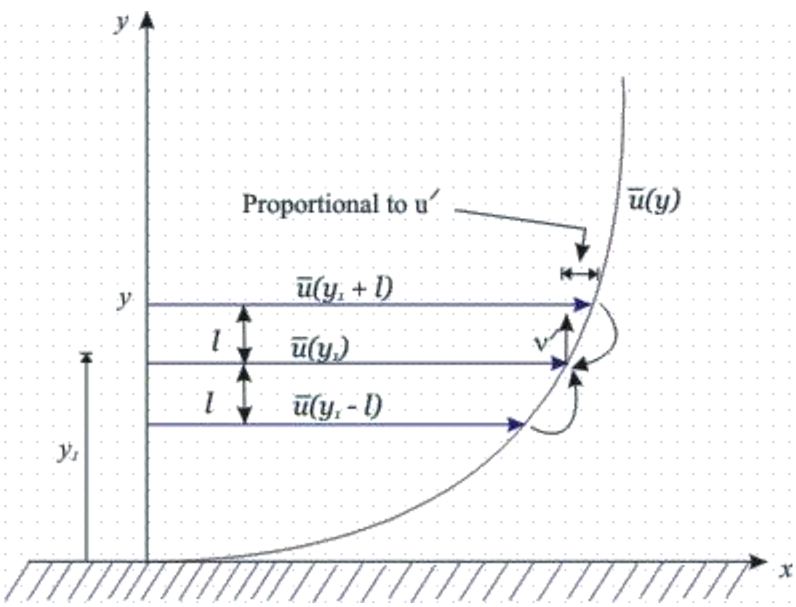

Fig. 33.4 One-dimensional parallel flow and Prandtl's mixing length hypothesis

The above expression is obtained by expanding the function $\bar{u}(y_1 - l)$ in a Taylor series and neglecting all higher order terms and higher order derivatives. l is a small length scale known as Prandtl's mixing length . Prandtl proposed that the transverse displacement of any fluid particle is, on an average, 'l' .

continued..

- Consider another lump of fluid with a negative value of v' . This is arriving at $y_1$from $(y_1 + l)$. If this lump retains its original momentum, its mean velocity at the current lamina $y_1$will be somewhat more than the original mean velocity of y_1. This difference is given by

$$\Delta u_2 = \bar{u}(y_1 + l) - \bar{u}(y_1) \approx l\left(\frac{\partial \bar{u}}{\partial y}\right)_{y1} \quad (33.16)$$

- The velocity differences caused by the transverse motion can be regarded as the turbulent velocity components at y_1.
- We calculate the time average of the absolute value of this fluctuation as

$$\left|\overline{u'}\right| = \frac{1}{2}\left(\left|\Delta u_1\right| + \left|\Delta u_2\right|\right) = l\left|\left(\frac{\partial \bar{u}}{\partial y}\right)\right|_{y1} \quad (33.17)$$

- Suppose these two lumps of fluid meet at a layer y_1The lumps will collide with a velocity $2u'$ and diverge. This proposes the possible existence of transverse velocity component in both directions with respect to the layer at y_1. Now, suppose that the two lumps move away in a reverse order from the layer $y_1$with a velocity $2u'$. The empty space will be filled from the surrounding fluid creating transverse velocity components which will again collide at y_1. Keeping in mind this argument and the physical explanation accompanying Eqs (33.4), we may state that

$$\left|\overline{v'}\right| \sim \left|\overline{u'}\right|$$

or, $$\left|\overline{v'}\right| = (const)\left|\overline{u'}\right| = (const)l\left|\left(\frac{\partial \bar{u}}{\partial y}\right)\right|$$

along with the condition that the moment at which u' is positive, v' is more likely to be negative and conversely when u' is negative. Possibly, we can write at this stage

$$\overline{u'v'} = -C_1\left|\overline{u'}\right|\left|\overline{v'}\right|$$

$$\overline{u'v'} = -C_2 l^2\left(\frac{\partial \bar{u}}{\partial y}\right)^2 \quad (33.18)$$

where C_1 and C_2 are different proportionality constants. However, the constant C_2 can now be included in still unknown mixing length and Eg. (33.18) may be rewritten as

$$\overline{u'v'} = -l^2\left(\frac{\partial \bar{u}}{\partial y}\right)^2$$

- For the expression of turbulent shearing stress τ_t we may write

$$\mu_t = \rho l^2\left|\frac{\partial \bar{u}}{\partial y}\right| \qquad (33.19)$$

- After comparing this expression with the eddy viscosity Eg. (33.14), we may arrive at a more precise definition,

$$\tau_t = \rho l^2\left|\frac{\partial \bar{u}}{\partial y}\right|\left(\frac{\partial \bar{u}}{\partial y}\right) = \mu_t\frac{\partial \bar{u}}{\partial y} \qquad (33.20a)$$

where the apparent viscosity may be expressed as

$$\mu_t = \rho l^2\left|\frac{\partial \bar{u}}{\partial y}\right| \qquad (33.20b)$$

and the apparent kinematic viscosity is given by

$$\nu_t = l^2\left|\frac{\partial \bar{u}}{\partial y}\right| \qquad (33.20c)$$

- The decision of expressing one of the velocity gradients of Eq. (33.19) in terms of its modulus as $\left|\frac{\partial \bar{u}}{\partial y}\right|$ was made in order to assign a sign to τ_t according to the sign of $\frac{\partial \bar{u}}{\partial y}$.
- Note that the apparent viscosity and consequently,the mixing length are not properties of fluid. They are dependent on turbulent fluctuation.
- But how to determine the value of "l" the mixing length? Several correlations, using experimental results for τ_t have been proposed to determine l.

However, so far the most widely used value of mixing length in the regime of isotropic turbulence is given by

$$l = \chi y \quad (33.21)$$

where y is the distance from the wall and χ is known as **von Karman constant** (≈ 0.4).

Universal Velocity Distribution Law And Friction Factor In Duct Flows For Very Large Reynolds Numbers

- For flows in a rectangular channel at very large Reynolds numbers the laminar sublayer can practically be ignored. The channel may be assumed to have a width *2h* and the *x* axis will be placed along the bottom wall of the channel.
- Consider a turbulent stream along a smooth flat wall in such a duct and denote the distance from the bottom wall by *y*, while *u(y)* will signify the velocity. In the neighbourhood of the wall, we shall apply

$$l = \chi y$$

- According to Prandtl's assumption, the turbulent shearing stress will be

$$\tau_t = \rho \chi^2 y^2 \left(\frac{\partial \bar{u}}{\partial y} \right)^2 \quad (34.1)$$

At this point, Prandtl introduced an additional assumption which like a plane Couette flow takes a constant shearing stress throughout, i.e

$$\tau_t = \tau_w \quad (34.2)$$

where τ_w denotes the shearing stress at the wall.

- Invoking once more the friction velocity $u_\tau = \left[\frac{\tau_w}{\rho}\right]^{1/2}$, we obtain

$$u_\tau^2 = \chi^2 y^2 \left(\frac{\partial \overline{u}}{\partial y}\right)^2 \tag{34.3}$$

$$\frac{\partial \overline{u}}{\partial y} = \frac{u_\tau}{\chi y} \tag{34.4}$$

On integrating we find

$$\overline{u} = \frac{u_\tau}{\chi} \ln y + C \tag{34.5}$$

- Despite the fact that Eq. (34.5) is derived on the basis of the friction velocity in the neighbourhood of the wall because of the assumption that $\tau_w = \tau_t$= constant, we shall use it for the entire region. At *y* = *h* (at the horizontal mid plane of the channel), we have $\bar{u} = U_{max}$. The constant of integration is eliminated by considering

$$U_{\max} = \frac{u_\tau}{\chi} \ln h + C$$

$$C = U_{\max} - \frac{u_\tau}{\chi} \ln h$$

Substituting C in Eq. (34.5), we get

$$\frac{U_{\max} - \overline{u}}{u_\tau} = \frac{1}{\chi} \ln\left(\frac{h}{y}\right) \tag{34.6}$$

Equation (34.6) is known as **universal velocity defect law** of Prandtl and its distribution has been shown in Fig. 34.1

.

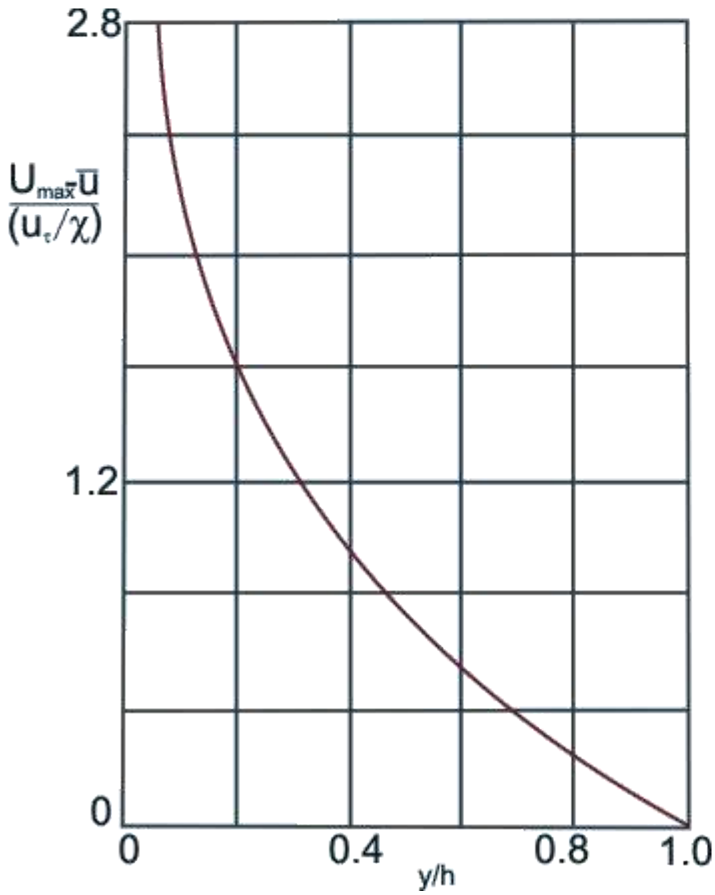

Fig 34.1 Distibution of universal velocity defect law of Prandtl in a turbulent channel flow

Here, we have seen that the friction velocity u_τ is a reference parameter for velocity.Equation (34.5) can be rewritten as

$$\frac{\bar{u}}{u_\tau} = \frac{1}{\chi}\ln y + C'$$

where $c' = \frac{c}{u_\tau}$

- The no-slip condition at the wall cannot be satisfied with a finite constant of integration. This is expected that the appropriate condition for the present problem should be that y_0 at a very small distance $y = y_0$ from the wall. Hence, Eq. (34.5) becomes

$$\frac{\bar{u}}{u_\tau} = \frac{1}{\chi}\left(\ln y - \ln y_0\right) \quad (34.7)$$

- The distance y_0 is of the order of magnitude of the thickness of the viscous layer. Now we can write Eq. (34.7) as

$$\frac{\bar{u}}{u_\tau} = \frac{1}{\chi}\left(\ln y \frac{u_\tau}{\nu} - \ln \beta\right)$$

$$\frac{\bar{u}}{u_\tau} = A_1 \ln \eta + D_1 \quad (34.8)$$

where $A_1 = (1/\chi)$, the unknown β is included in D_1.

Equation (34.8) is generally known as the **universal velocity profile** because of the fact that it is applicable from moderate to a very large Reynolds number.

However, the constants A_1 and D_1 have to be found out from experiments. The aforesaid profile is not only valid for channel (rectangular) flows, it retains the same functional relationship for circular pipes as well . It may be mentioned that even without the assumption of having a constant shear stress throughout, the universal velocity profile can be derived.

- Experiments, performed by J. Nikuradse, showed that Eq. (34.8) is in good agreement with experimental results. Based on Nikuradse's and Reichardt's experimental data, the empirical constants of Eq. (34.8) can be determined for a **smooth pipe** as

$$\frac{\bar{u}}{u_\tau} = 2.5 \ln \eta + 5.5 \quad (34.9)$$

This velocity distribution has been shown through curve (b) in Fig. 34.2

.

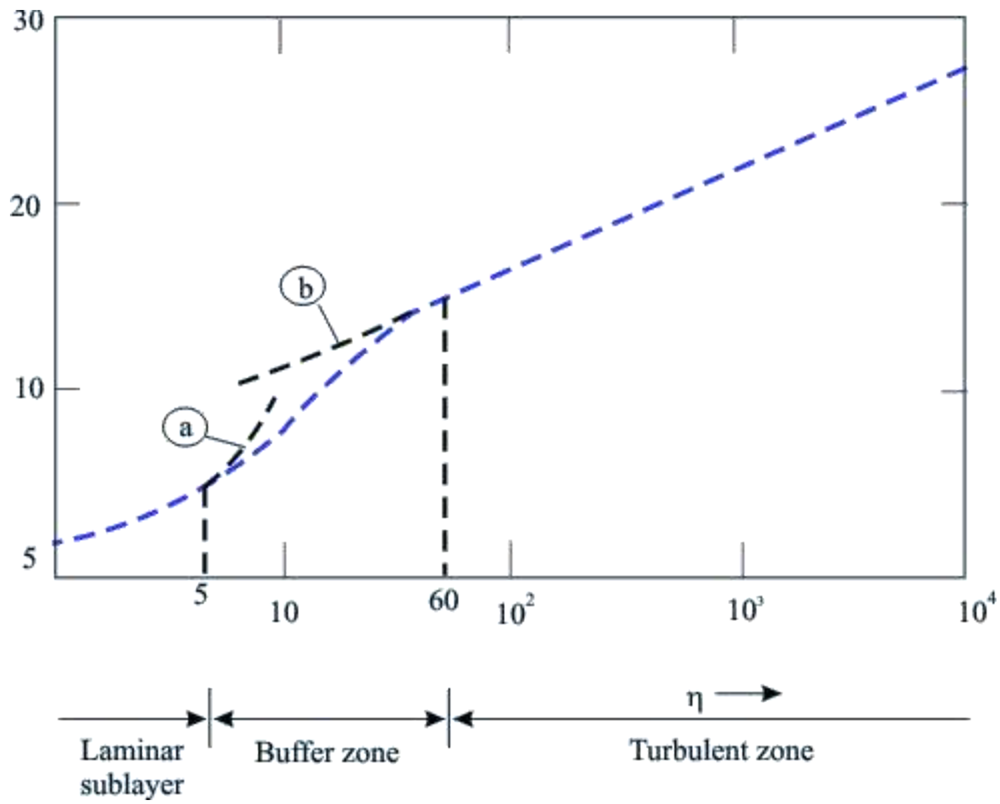

Fig 34.2 The universal velocity distribution law for smooth pipes

- However, the corresponding friction factor concerning Eq. (34.9) is

$$\frac{1}{\sqrt{f}} = 2.0\log_{10}\left(\mathrm{Re}\sqrt{f}\right) - 0.8 \qquad (34.10)$$

the universal velocity profile does not match very close to the wall where the viscous shear predominates the flow.

- Von Karman suggested a modification for the **laminar sublayer** and the **buffer zone** which are

$$\frac{\bar{u}}{u_\tau} = \eta = \frac{u_\tau y}{\nu} \text{for } \eta < 5.0 \qquad (34.11)$$

$$\frac{\bar{u}}{u_\tau} = 11.5\log_{10}\frac{u_\tau y}{\nu} - 3.0 \text{for } 5 < \eta < 60 \qquad (34.12)$$

Equation (34.11) has been shown through curve(a) in Fig. 34.2.

- It may be worthwhile to mention here that a surface is said to be hydraulically smooth so long

$$0 \le \frac{\varepsilon_p u_\tau}{\nu} \le 5 \qquad (34.13)$$

where ε_p is the average height of the protrusions inside the pipe.

Physically, the above expression means that for smooth pipes protrusions will not be extended outside the laminar sublayer. If protrusions exceed the thickness of laminar sublayer, it is conjectured (also justified though experimental verification) that some additional frictional resistance will contribute to pipe friction due to the form drag experienced by the protrusions in the boundary layer.

- In rough pipes experiments indicate that the velocity profile may be expressed as:

$$\frac{\bar{u}}{u_\tau} = 2.5\ln\frac{y}{\varepsilon_p} + 8.5 \qquad (34.14)$$

At the centre-line, the maximum velocity is expressed as

$$\frac{U_{max}}{u_\tau} = 2.5\ln\frac{R}{\varepsilon_p} + 8.5 \qquad (34.15)$$

Note that ν no longer appears with R and ε_p. This means that for completely rough zone of turbulent flow, the profile is independent of Reynolds number and a strong function of pipe roughness .

- However, for pipe roughness of varying degrees, the recommendation due to **Colebrook and White works** well. Their formula is

$$\frac{1}{\sqrt{f}} = 1.74 - 2.0\log_{10}\left[\frac{\varepsilon_p}{R} + \frac{18.7}{\text{Re}\sqrt{f}}\right] \qquad (34.16)$$

where R is the pipe radius

For $\varepsilon_p \rightarrow 0$, this equation produces the result of the smooth pipes (Eq.(34.10)). For $\mathrm{Re} \rightarrow \infty$, it gives the expression for friction factor for a completely rough pipe at a very high Reynolds number which is given by

$$f = \frac{1}{\left(2\log\frac{R}{\varepsilon_p} + 1.74\right)^2} \quad (34.17)$$

Turbulent flow through pipes has been investigated by many researchers because of its enormous practical importance.

Fully Developed Turbulent Flow In A Pipe For Moderate Reynolds Numbers

- The entry length of a turbulent flow is much shorter than that of a laminar flow, J. Nikuradse determined that a fully developed profile for turbulent flow can be observed after an entry length of 25 to 40 diameters. We shall focus to fully developed turbulent flow in this section.
- Considering a fully developed turbulent pipe flow (Fig. 34.3) we can write

$$2\pi R\tau_w = -\left(\frac{dp}{dx}\right)\pi R^2 \quad (34.18)$$

or

$$\left(-\frac{dp}{dx} = \frac{2\tau_w}{R}\right) \quad (34.19)$$

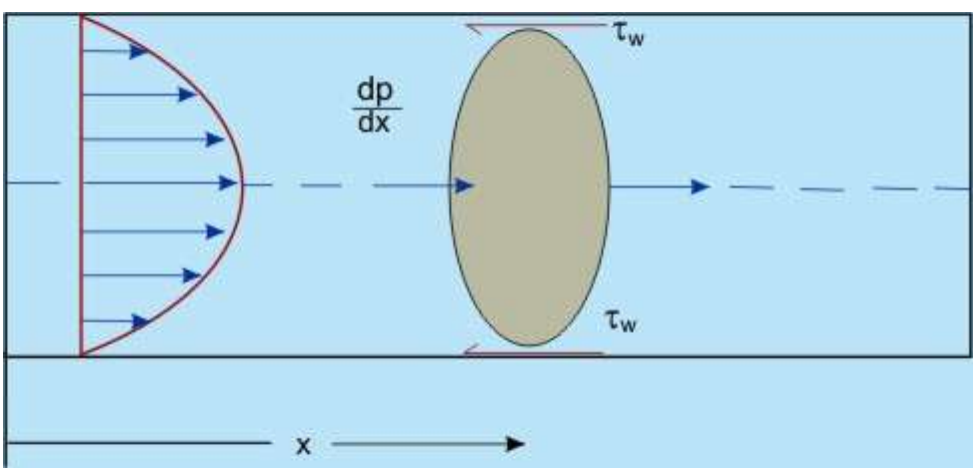

Fig. 34.3 Fully developed turbulent pipe flow

It can be said that in a fully developed flow, the pressure gradient balances the wall shear stress only and has a constant value at any x. However, the friction factor (Darcy friction factor) is defined in a fully developed flow as

$$-\left(\frac{dp}{dx}\right) = \frac{\rho f U_{av}^2}{2D} \qquad (34.20)$$

Comparing Eq.(34.19) with Eq.(34.20), we can write

$$\tau_w = \frac{f}{8}\rho U_{av}^2 \qquad (34.21)$$

H. Blasius conducted a critical survey of available experimental results and established the empirical correlation for the above equation as

$$f = 0.3164\,\mathrm{Re}^{-0.25} \text{ where } \mathrm{Re} = \rho U_{av} D/\mu \qquad (34.22)$$

- It is found that the Blasius's formula is valid in the range of Reynolds number of Re $\leq 10^5$. At the time when Blasius compiled the experimental data, results for higher Reynolds numbers were not available. However, later on, J. Nikuradse carried out experiments with the laws of friction in a very wide range of Reynolds numbers, $4 \times 10^3 \leq \mathrm{Re} \leq 3.2 \times 10^6$. The velocity profile in this range follows:

$$\frac{u}{\bar{u}} = \left[\frac{y}{R}\right]^{1/n} \qquad (34.23)$$

where $\bar{u}$ is the time mean velocity at the pipe centre and y is the distance from the wall . The exponent *n* varies slightly with Reynolds number. In the range of Re ~ 10^5, *n* is 7.

Fully Developed Turbulent Flow In A Pipe For Moderate Reynolds Numbers

- The ratio of $\bar{u}$ and U_{av} for the aforesaid profile is found out by considering the volume flow rate Q as

$$Q = \pi R^2 U_{av} = \int_0^R 2\pi r u\,dr$$

$$r = R - y$$

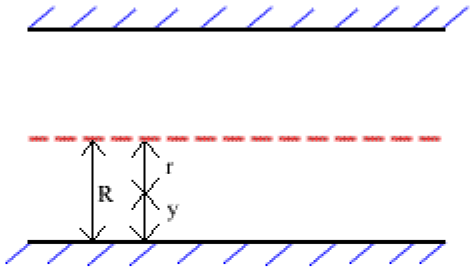

From equation (34.23)

$$\pi R^2 U_{av} = 2\pi \bar{u} \int_0^R (R-y)(y/R)^{1/n}(-dy)$$

or

$$\pi R^2 U_{av} = 2\pi \bar{u}\left[\frac{n}{n+1}\left(R^{\frac{n-1}{n}} y^{\frac{n+1}{n}}\right) - \frac{n}{2n+1}\left(y^{\frac{2n+1}{n}} R^{-\frac{1}{n}}\right)\right]_0^R$$

or

$$\pi R^2 U_{av} = 2\pi \bar{u}\left[R^2 \frac{n}{n+1} - \frac{n}{2n+1} R^2\right]$$

or

$$\pi R^2 U_{av} = 2\pi R^2 \bar{u}\left[\frac{n^2}{(n+1)(2n+1)}\right]$$

or

$$\frac{U_{av}}{\bar{u}} = \frac{2n^2}{(n+1)(2n+1)} \qquad (34.24a)$$

- Now, for different values of *n* (for different Reynolds numbers) we shall obtain different values of $U_{av}/\bar{u}$ from Eq.(34.24a). On substitution of Blasius resistance formula (34.22) in Eq.(34.21), the following expression for the shear stress at the wall can be obtained.

putting $\mathrm{Re} = \rho U_{av} 2R/\mu$

and where $\nu = \mu/\rho$

$$\tau_w = 0.03955 \rho U_{av}^2 \left(\frac{\nu}{2RU_{av}} \right)^{1/4}$$

or

$$\tau_w = 0.03325 \rho U_{av}^{7/4} \left(\frac{\nu}{R} \right)^{1/4}$$

or

$$\tau_w = 0.03325 \rho \left(\frac{U_{av}}{\bar{u}} \right)^{7/4} (\bar{u})^{7/4} \left(\frac{\nu}{R} \right)^{1/4}$$

- For n=7, $U_{av}/\bar{u}$ becomes equal to 0.8. substituting $U_{av}/\bar{u} = 0.8$ in the above equation, we get

$$\tau_w = 0.03325 \rho (0.8)^{1/4} (\bar{u})^{7/4} (\nu / R)^{1/4}$$

Finally it produces

$$\tau_w = 0.0225 \rho (\bar{u})^{7/4} (\nu / R)^{1/4} \qquad (34.24b)$$

or

$$u_\tau^2 \rho = 0.0225 \rho (\bar{u})^{7/4} \left(\frac{\nu}{R} \right)^{1/4}$$

where u_τ is friction velocity. However, u_τ^2 may be spitted into $u_\tau^{1/4}$ and $u_\tau^{7/4}$ and we obtain

$$\left(\frac{\bar{u}}{u_\tau} \right)^{7/4} = 44.44 \left(\frac{u_\tau R}{\nu} \right)^{1/4}$$

or

$$\frac{\bar{u}}{u_\tau} = 8.74 \left(\frac{u_\tau R}{\nu} \right)^{1/7} \qquad (34.25a)$$

- Now **we can assume that the above equation is not only valid at the pipe axis (y = R) but also at any distance** from the wall y and a **general form is proposed as**

$$\frac{\bar{u}}{u_\tau} = 8.74\left(\frac{yu_\tau}{\nu}\right)^{1/7} \qquad (34.25b)$$

- Concluding Remarks :

1. It can be said that (1/7)th power velocity distribution law (24.38b) can be derived from Blasius's resistance formula (34.22) .
2. Equation (34.24b) gives the shear stress relationship in pipe flow at a moderate Reynolds number, i.e $\mathrm{Re} \le 10^5$. Unlike very high Reynolds number flow, here laminar effect cannot be neglected and the laminar sub layer brings about remarkable influence on the outer zones.
3. The friction factor for pipe flows, f , defined by Eq. (34.22) is valid for a specific range of Reynolds number and for a particular surface condition.

Skin Friction Coefficient For Boundary Layers On A Flat Plate

- Calculations of skin friction drag on lifting surface and on aerodynamic bodies are somewhat similar to the analyses of skin friction on a flat plate. Because of zero pressure gradient, the flat plate at zero incidence is easy to consider. In some of the applications cited above, the pressure gradient will differ from zero but the skin friction will not be dramatically different so long there is no separation.
- We begin with the momentum integral equation for flat plate boundary layer which is valid for both laminar and turbulent flow.

$$\frac{d}{dx}\left(U_\infty^2 \delta^{**}\right) = \frac{\tau_w}{\rho} \qquad (34.26a)$$

- Invoking the definition of $C_{fx}\left(C_{fx} = \frac{\tau_w}{1/2\rho U_\infty^2}\right)$, Eq.(34.26a) can be written as

$$C_{fx} = 2\frac{d\delta^{**}}{dx} \qquad (34.26b)$$

- Due to the similarity in the laws of wall, correlations of previous section may be applied to the flat plate by substituting δ for *R* and U_∞ for the time mean velocity at the pipe centre.The rationale for using the turbulent pipe flow results in the situation of a turbulent flow over a flat plate is to consider that the time mean velocity, at the centre of the pipe is analogous to the free stream velocity, both the velocities being defined at the edge of boundary layer thickness.

Finally, the velocity profile will be [following Eq. (34.24)]

$$\frac{u}{U_\infty} = \left[\frac{y}{\delta}\right]^{1/7} \quad \text{for } \mathrm{Re} \le 10^5 \tag{34.27}$$

Evaluating momentum thickness with this profile, we shall obtain

$$\delta^{**} = \int_0^\delta \left(\frac{y}{\delta}\right)^{1/7}\left[1-\left(\frac{y}{\delta}\right)^{1/7}\right]dy = \frac{7}{72}\delta \tag{34.28}$$

Consequently, the law of shear stress (in range of $\mathrm{Re} \le 10^5$) for the flat plate is found out by making use of the pipe flow expression of Eq. (34.24b) as

$$\tau_w = 0.0225\rho\left(\bar{u}\right)^{7/4}\left(\frac{\nu}{R}\right)^{1/4}$$

$$\frac{\tau_w}{\rho\left(\bar{u}\right)^2} = 0.0225\left[\frac{\nu}{R\bar{u}}\right]^{1/4}$$

Substituting U_∞ for $\bar{u}$ and δ for *R* in the above expression, we get

$$\frac{\tau_w}{\rho\left(\bar{u}\right)^2} = 0.0225\left[\frac{\nu}{\delta U_\infty^2}\right]^{1/4} \tag{34.29}$$

Once again substituting Eqs (34.28) and (34.29) in Eq.(34.26), we obtain

$$\frac{7}{72}\cdot\frac{d\delta}{dx} = 0.0225\left[\frac{\nu}{\delta U_\infty^2}\right]^{1/4}$$

$$\delta^{1/4}\frac{d\delta}{dx} = 0.2314\left[\frac{\nu}{U_\infty^2}\right]^{1/4}$$

(34.30)

$$\delta^{5/4} = 0.2892x\left(\frac{\nu}{U_\infty^2}\right)^{1/4} + C$$

- For simplicity, if we assume that the turbulent boundary layer grows from the leading edge of the plate we shall be able to apply the boundary conditions x = 0, δ = 0 which will yield *C* = 0, and Eq. (34.30) will become From Eqs (34.26b), (34.28) and (34.31), it is possible to calculate the **average skin friction coefficient** on a flat plate as

$$\left(\frac{\delta}{x}\right)^{5/4} = 0.2892\left[\frac{\nu}{xU_\infty}\right]^{1/4}$$

or, $$\frac{\delta}{x} = 0.37\left[\frac{\nu}{xU_\infty}\right]^{1/5}$$

or, $$\frac{\delta}{x} = 0.37\left(\mathrm{Re}_x\right)^{-1/5} \qquad (34.31)$$

Where $\mathrm{Re}_x = (U_\infty x)/\nu$

From Eqs (34.26b), (34.28) and (34.31), it is possible to calculate the **average skin friction coefficient** on a flat plate as

$$\overline{C}_f = 0.072\left(\mathrm{Re}_L\right)^{-1/5} \qquad (34.32)$$

It can be shown that Eq. (34.32) predicts the average skin friction coefficient correctly in the regime of Reynolds number below 2×10^6.

- This result is found to be in good agreement with the experimental results in the range of Reynolds number between 5×10^5 and 10^7 which is given by

$$\overline{C}_f = 0.074\left(\mathrm{Re}_L\right)^{-1/5} \qquad (34.33)$$

Equation (34.33) is a widely accepted correlation for the average value of turbulent skin friction coefficient on a flat plate.

- With the help of Nikuradse's experiments, Schlichting obtained the semi empirical equation for the average skin friction coefficient as

$$\overline{C}_f = \frac{0.455}{(\log \mathrm{Re})^{2.58}} \qquad (34.34)$$

Equation (34.34) was derived asssuming the flat plate to be completely turbulent over its entire length . In reality, a portion of it is laminar from the leading edge to some downstream position. For this purpose, it was suggested to use

$$\overline{C}_f = \frac{0.455}{(\log \mathrm{Re})^{2.58}} - \frac{A}{\mathrm{Re}} \qquad (34.35a)$$

where A has various values depending on the value of Reynolds number at which the transition takes place.

- If the trasition is assumed to take place around a Reynolds number of 5×10^5, the average skin friction correlation of Schlichling can be written as

$$\overline{C}_f = \frac{0.455}{(\log \mathrm{Re})^{2.58}} - \frac{1700}{\mathrm{Re}} \qquad (34.35b)$$

All that we have presented so far, are valid for a smooth plate.

- Schlichting used a logarithmic expression for turbulent flow over a rough surface and derived

$$\overline{C}_f = \left(1.89 + 1.62\log \frac{L}{\varepsilon_p}\right)^{2.5} \qquad (34.36)$$

Exercise Problems - Chapter 10

1.Estimate the power required to move a flat plate, 15 m. long and 4 m. wide, in oil $(\rho = 800\mathrm{kg/m^3}, \nu = 10^{-5}\mathrm{m^2/sec})$ at 4m/sec, under the following cases:

a) The boundary layer is assumed laminar over the entire surface of the plate. (Ans. 1665.5 N-m/sec)

b) Transition to turbulence occurs at $\mathrm{Re} = 3\times10^5$ and plate is smooth.(Ans. 9486 N-m/sec)

c) The boundary layer is turbulent over the entire plate which is smooth.(Ans. 10023.94 N-m/sec)

d) The boundary layer is turbulent over the entire rough plate with $\frac{u_\infty \varepsilon_p}{\nu} = 10^3$.(Ans. 17200 N-m/sec)

2. Water $(\rho = 1000\mathrm{kg/m^3}, \nu = 2\times10^{-6}\mathrm{m^2/sec})$ is transported through a horizontal pipeline, 800 m. long, with a maximum velocity of 3m/sec. If the Reynolds number is , find the diameter of the pipe (with and without the use of Moody Diagram).

Also calculate the thickness of laminar sub-layer and the buffer layer, and find the power required to maintain the flow. Calculate your results for a fully rough pipe with $\frac{u_\tau \varepsilon_p}{\nu} = 100$.

(Ans. Diameter of the pipe 0.8 m., laminar sub-layer thickness 0.1 mm, buffer layer thickness 1.3 mm, power required 50250 W)

3. Find the frictional drag on the top and sides of a box-shaped moving van 2.4 m wide, 3.0 m high, and 10.5 m long traveling at 100km/h through air ($\nu = 1.4 \times 10^{-5}$). Assume that the vehicle has a rounded nose so that the flow does not seperate from the top and side. also assume that a turbulent boundary layer starts immediately at the leading edge.

Also, find the thickness of the boundary layer and the shear stress at the trailing edge.

(Ans. Drag = 105.9 N, B.L. = 0.136m, Shear stress = 0.904 Pa)

Applications of Viscous Flows Through Pipes

Introduction

- A complete analytical solution for the equation of motion in the case of a laminar flow is available, even the advanced theories in the analysis of turbulent flow depend at some point on experimentally derived information. Flow through pipes is usually turbulent in practice.
- One of the most important items of information that an hydraulic engineer needs is the power required to force fluid at a certain steady rate through a pipe or pipe network system. This information is furnished in practice through some routine solution of pipe flow problems with the help of available empirical and theoretical information.
- This lecture deals with the typical approaches to the solution of pipe flow problems in practice.
-

Concept of Friction Factor in a pipe flow:

- The friction factor in the case of a pipe flow was already mentioned in lecture 26.
- We will elaborate further on friction factor or friction coefficient in this section.
- Skin friction coefficient for a fully developed flow through a closed duct is defined as

$$C_f = \frac{\tau_w}{(1/2)\rho V^2} \tag{35.1}$$

where, *V* is the average velocity of flow given by $V = Q/A$, *Q* and *A* are the volume flow rate through the duct and the cross-sectional area of the duct respectively.

From a force balance of a typical fluid element (Fig. 35.1) in course of its flow through a duct of constant cross-sectional area, we can write

$$\tau_w = \frac{\Delta p^* A}{SL} \qquad (35.2)$$

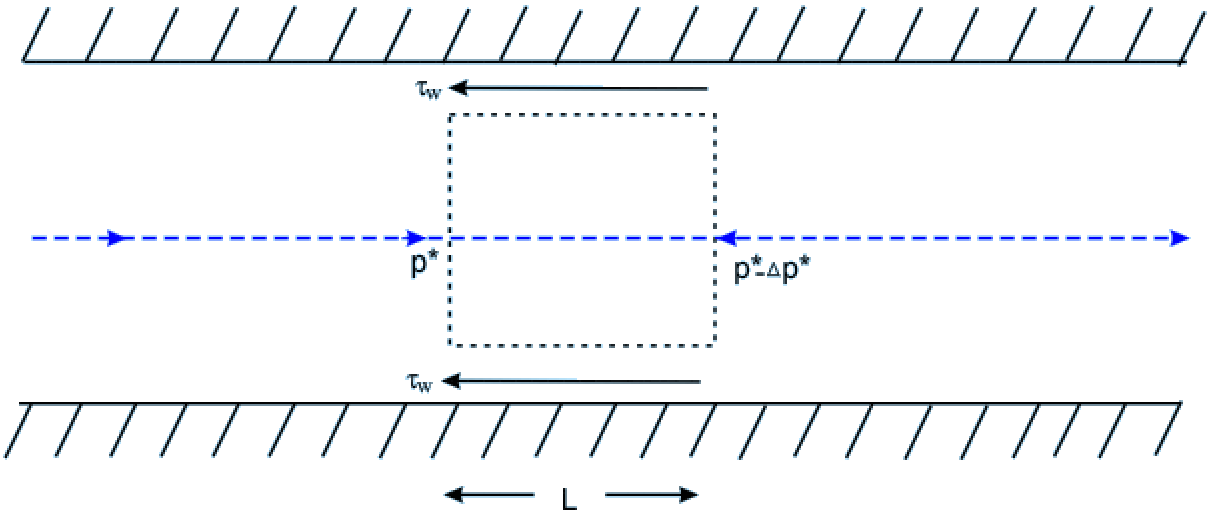

FIG 35.1 Force Balance of a fluid element in the course of flow through a duct

where, τ_w is the shear stress at the wall and Δp^* is the piezometric pressure drop over a length of **L** . **A** and **S** are respectively the cross-sectional area and wetted perimeter of the duct.
Substituting the expression (35.2) in Eq. (35.1), we have,

$$C_f = \frac{\Delta p^* A}{SL(1/2)\rho V^2} = \frac{1}{4}\frac{D_h}{L}\frac{\Delta p^*}{(1/2)\rho V^2} \qquad (35.3)$$

where, $D_h = 4A/S$ and is known as the **hydraulic diameter** .

In case of a circular pipe, D_h=D, the diameter of the pipe. The coefficient C_f defined by Eqs (35.1) or (35.3) is known as **Fanning's friction factor** .

- To do away with the factor 1/4 in the Eq. (35.3), Darcy defined a friction factor **f (Darcy's friction factor)** as

$$f = \frac{D_h}{L}\frac{\Delta p^*}{(1/2)\rho V^2} \qquad (35.4)$$

- Comparison of Eqs (35.3) and (35.4) gives $f = 4C_f$. Equation (35.4) can be written for a pipe flow as

$$f = \frac{D_h}{L} \frac{\Delta p^*}{(1/2)\rho V^2} \tag{35.5}$$

- Equation (35.5) is written in a different fashion for its use in the solution of pipe flow problems in practice as

$$\Delta p^* = f \cdot \frac{L}{D_h} \cdot \frac{\rho}{2} V^2 \tag{35.6a}$$

or in terms of head loss (energy loss per unit weight)

$$h_f = \frac{\Delta p^*}{\rho g} = \frac{f L V^2}{2 g D_h} \tag{35.6b}$$

where, h_f represents the loss of head due to friction over the length L of the pipe.

- Equation (35.6b) is frequently used in practice to determine h_f
- In order to evaluate h_f, we require to know the value of f. The value of f can be determined from Moody's Chart.

Variation of Friction Factor

- In case of a laminar fully developed flow through pipes, the friction factor, f is found from the exact solution of the Navier-Stokes equation as discussed in lecture 26. It is given by

$$f = \frac{64}{\mathrm{Re}} \tag{35.7}$$

- In the case of a turbulent flow, friction factor depends on both the Reynolds number and the roughness of pipe surface.
- Sir Thomas E. Stanton (1865-1931) first started conducting experiments on a number of pipes of various diameters and materials and with various fluids. Afterwards, a German engineer Nikuradse carried out experiments on flows through pipes in a very wide range of Reynolds number.
- A comprehensive documentation of the experimental and theoretical investigations on the laws of friction in pipe flows has been presented in the form of a diagram, as shown in Fig. 35.2, by **L.F. Moody** to show the variation of friction factor, f with the pertinent governing parameters, namely, the Reynolds number of flow and the relative roughness ε / D of the pipe. This diagram is known as **Moody's Chart** which is employed till today as the best means for predicting the values of f .

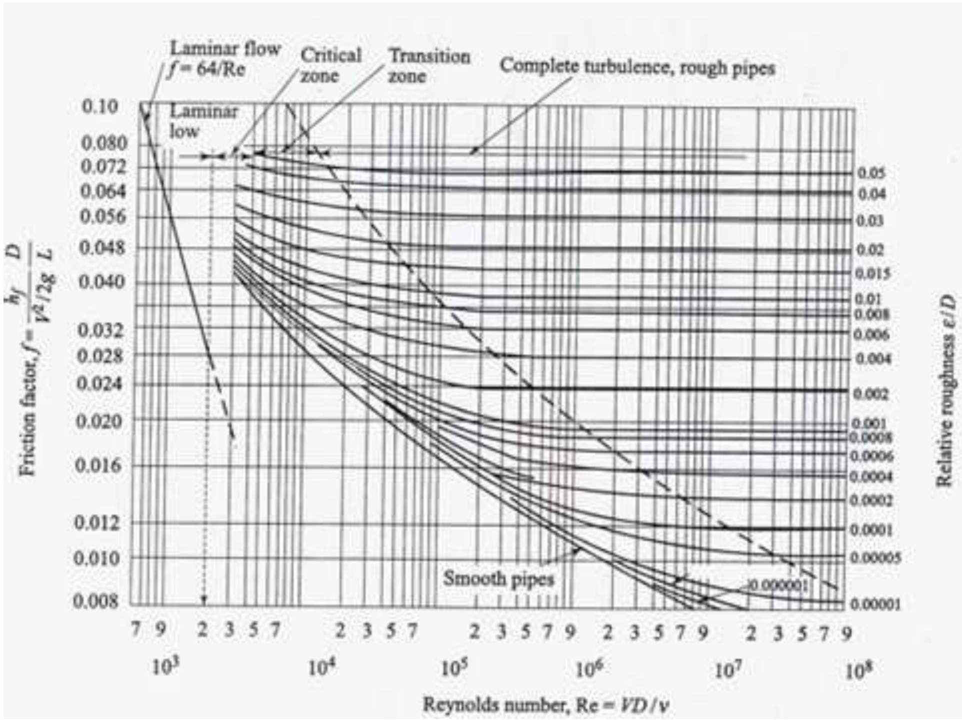

Fig. 35.2 Friction Factors for pipes (adapted from Trans. ASME, 66,672, 1944)

Figure 35.2 depicts that

- The friction factor *f* at a given Reynolds number, in the turbulent region, depends on the relative roughness, defined as the ratio of average roughness to the diameter of the pipe, rather than the absolute roughness.
- For moderate degree of roughness, a pipe acts as a smooth pipe up to a value of Re where the curve of f vs Re for the pipe coincides with that of a smooth pipe. This zone is known as the **smooth zone of flow** .
- The region where f vs Re curves (Fig. 35.2) become horizontal showing that **f** is independent of Re, is known as the **rough zone** and the intermediate region between the smooth and rough zone is known as the **transition zone**.
- The position and extent of all these zones depend on the relative roughness of the pipe. In the smooth zone of flow, the laminar sublayer becomes thick, and hence, it covers appreciably the irregular surface protrusions. Therefore all the curves for smooth flow coincide.
- With increasing Reynolds number, the thickness of sublayer decreases and hence the surface bumps protrude through it. The higher is the roughness of the pipe, the lower is the value of Re at which the curve of f vs Re branches off from smooth pipe curve (Fig. 35.2).

- In the rough zone of flow, the flow resistance is mainly due to the form drag of those protrusions. The pressure drop in this region is approximately proportional to the square of the average velocity of flow. Thus f becomes independent of Re in this region.

In practice, there are three distinct classes of problems relating to flow through a single pipe line as follows:

1. The flow rate and pipe diameter are given. One has to determine the loss of head over a given length of pipe and the corresponding power required to maintain the flow over that length.
2. The loss of head over a given length of a pipe of known diameter is given. One has to find out the flow rate and the transmission of power accordingly.
3. The flow rate through a pipe and the corresponding loss of head over a part of its length are given. One has to find out the diameter of the pipe.

In the first category of problems, the friction factor f is found out explicitly from the given values of flow rate and pipe diameter. Therefore, the loss of head h_f and the power required, P can be calculated by the straightforward application of Eq.(35.6b).

(contd from previous...) Concept of Flow Potential and Flow Resistance

The velocity *V* in the above equation is usually substituted in terms of flow rate *Q* , since, under steady state, the flow rate remains constant throughout the pipe even if its diameter changes. Therefore, replacing V in Eq. (35.11) as $V = 4Q/\pi D^2$ we finally get

$$h_f = \left[8\left(1.5 + f\frac{L}{D}\right)\frac{1}{\pi^2 D^4 g}\right]Q^2$$

or, $$h_f = RQ^2 \qquad (35.12)$$

where $$R = \left[\frac{8}{\pi^2 D^4 g}\left(1.5 + f\frac{L}{D}\right)\right] \qquad (35.13)$$

The term *R* is defined as the **flow resistance** .

In a situation where f becomes independent of **Re**, the flow resistance expressed by Eg. (35.13) becomes simply a function of the pipe geometry. With the help of Eq. (35.10), Eq. (35.12) can be written as

$$\Delta H = RQ^2 \qquad (35.14)$$

- ΔH in Eq. (35.14) is the head causing the flow and is defined as the difference in flow potentials between A and B.

This equation is comparable to the voltage-current relationship in a purely resistive electrical circuit. In a purely resistive electrical circuit, $\Delta V = RI$, where ΔV is the voltage or electrical potential difference across a resistor whose resistance is *R* and the electrical current flowing through it is *I*.

- The difference however is that while the voltage drop in an electrical circuit is linearly proportional to current, the difference in the flow potential in a fluid circuit is proportional to the square of the flow rate.
- Therefore, the fluid flow system as shown in Fig. 35.3 and described by Eq. (35.14) can be expressed by an equivalent electrical network system as shown in Fig. 35.4.

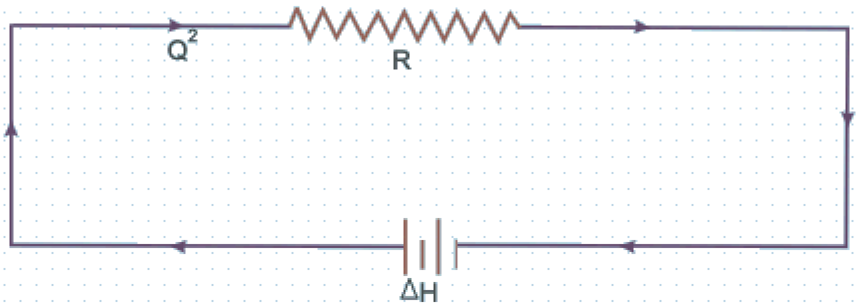

Fig 35.4 Equivalent electrical network system for a simple pipe flow problem shown in Fig.35.3

Flow Through Branched Pipes

In several practical situations, flow takes place under a given head through different pipes jointed together either in series or in parallel or in a combination of both of them.

Pipes in Series

- If a pipeline is joined to one or more pipelines in continuation, these are said to constitute pipes in series. A typical example of pipes in series is shown in Fig. 36.1. Here three pipes *A, B* and *C* are joined in series.

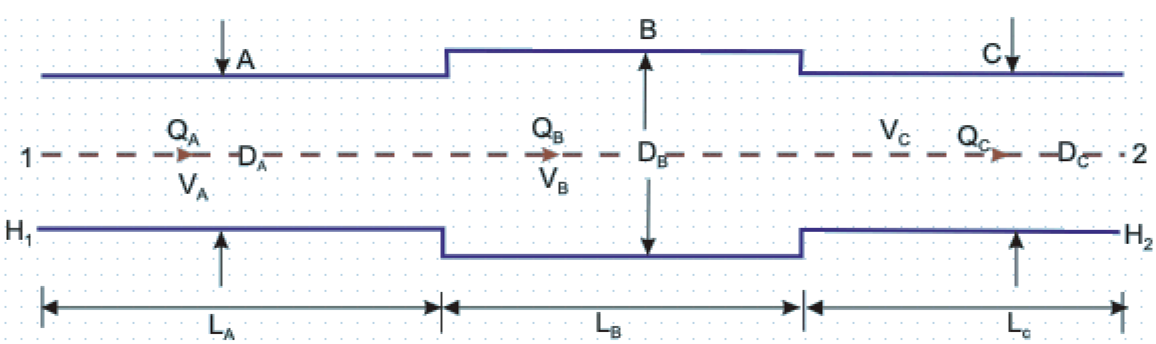

Fig 36.1 Pipes in series

In this case, rate of flow *Q* remains same in each pipe. Hence,

$$Q_A = Q_B = Q_C = Q$$

- If the total head available at Sec. 1 (at the inlet to pipe A) is H_1 which is greater than H_2, the total head at Sec. 2 (at the exit of pipe C), then the flow takes place from 1 to 2 through the system of pipelines in series.
- Application of Bernoulli's equation between Secs.1 and 2 gives

$$H_1 - H_2 = h_f$$

where, h_f is the loss of head due to the flow from 1 to 2. Recognizing the minor and major losses associated with the flow, h_f can be written as

$$h_f = f_A \frac{L_A}{D_A}\frac{V_A^2}{2g} + \frac{(V_A - V_B)^2}{2g} + f_B \frac{L_B}{D_B}\frac{V_B^2}{2g} + \left(\frac{1}{C_C} - 1\right)^2 \frac{V_C^2}{2g} + f_C \frac{LC}{D_C}\frac{V_C^2}{2g} \quad (36.1)$$

Friction loss in pipe A	Loss due to enlargement at entry to pipe B	Friction loss in pipe B	Loss due to abrupt contraction at entry to pipe C	Friction loss in pipe C

The subscripts *A, B* and *C* refer to the quantities in pipe A, B and C respectively. C_c is the coefficient of contraction.

- The flow rate Q satisfies the equation

$$Q = \frac{\pi D_A^2}{A} V_A = \frac{\pi D_B^2}{4} V_B = \frac{\pi D_C^2}{4} V_C \quad (36.2)$$

Velocities V_A, V_B and V_C in Eq. (36.1) are substituted from Eq. (36.2), and we get

$$h_f = \left[\underset{(R_1)}{\frac{8}{g\pi^2} f_A \frac{L_A}{D_A^5}} + \underset{(R2)}{\frac{8}{g\pi^2}\left(1-\frac{D_A^2}{D_B^2}\right)^2 \frac{1}{D_A^4}} + \underset{(R3)}{\frac{8}{g\pi^2} f_B \frac{L_B}{D_B^5}} + \underset{(R4)}{\frac{8}{g\pi^2}\left(\frac{1}{C_C}-1\right)^2 \frac{1}{D_C^4}} + \underset{(R5)}{\frac{8}{g\pi^2} f_c \frac{L_C}{D_C^5}} \right] Q^2 \qquad (36.3)$$

$$h_f = RQ_2$$

$$R = R_1 + R_2 + R_3 + R_4 + R_5 \qquad (36.4)$$

Equation (36.4) states that the total flow resistance is equal to the sum of the different resistance components. Therefore, the above problem can be described by an equivalent electrical network system as shown in Fig. 36.2.

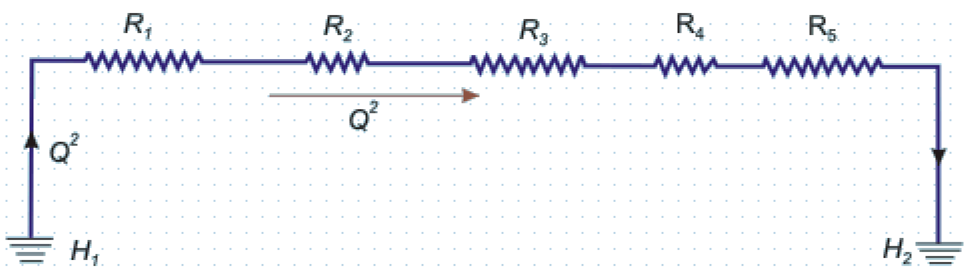

Fig 36.2 Equivalent electrical network system for through pipes in series

Pipes In Parallel

- When two or more pipes are connected, as shown in Fig. 36.3, so that the flow divides and subsequently comes together again, the pipes are said to be in parallel.
- In this case (Fig. 36.3), equation of continuity gives

$$Q = Q_A + Q_B \qquad (36.5)$$

where, *Q* is the total flow rate and Q_A and Q_B are the flow rates through pipes *A* and *B* respectively.

- Loss of head between the locations 1 and 2 can be expressed by applying Bernoulli's equation either through the path 1-A-2 or 1-B-2.
- Therefore, we can write

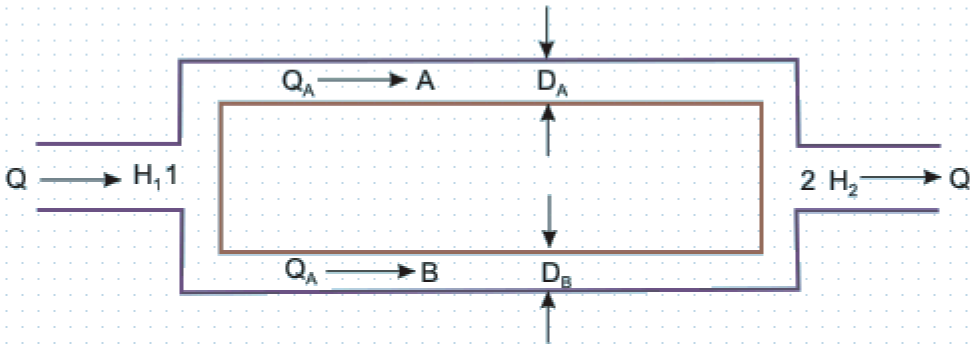

Fig 36.3 Pipes in Parallel

$$H_1 - H_2 = f_A \frac{L_A}{D_A} \frac{V_A^2}{2g} = \frac{8L_A}{\pi^2 D_A^5 g} f_A Q_A^2$$

and $$H_1 - H_2 = f_B \frac{L_B}{D_B} \frac{V_B^2}{2g} = \frac{8L_B}{\pi^2 D_B^5 g} f_B Q_B^2$$

Equating the above two expressions, we get -

$$Q_A^2 = \frac{R_B}{R_A} Q_B^2 \qquad (36.6)$$

where, $$R_A = \frac{8L_A}{\pi^2 D_A^5 g} f_A$$

$$R_B = \frac{8L_B}{\pi^2 D_B^5 g} f_B$$

Equations (36.5) and (36.6) give -

$$Q_A = \frac{K}{1+K} Q, \; Q_B = \frac{1}{1+K} Q \qquad (36.7)$$

where, $K = \sqrt{R_B / R_A}$ (36.8)

- The flow system can be described by an equivalent electrical circuit as shown in Fig. 36.4.

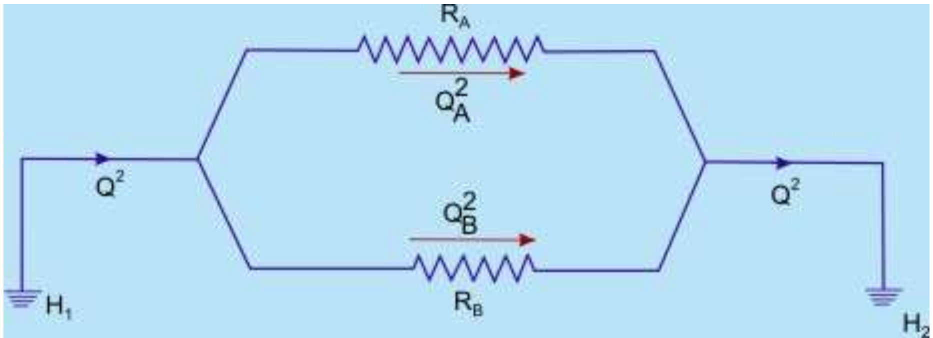

Fig 36.4 Equivalent electrical network system for flow through pipes in parallel

From the above discussion on flow through branched pipes (pipes in series or in parallel, or in combination of both), the following principles can be summarized:

1. The friction equation must be satisfied for each pipe.
2. There can be only one value of head at any point.
3. Algebraic sum of the flow rates at any junction must be zero. i.e., the total mass flow rate towards the junction must be equal to the total mass flow rate away from it.
4. Algebraic sum of the products of the flux (Q^2) and the flow resistance (the sense being determined by the direction of flow) must be zero in any closed hydraulic circuit.

The principles 3 and 4 can be written analytically as

$\sum Q = 0$ at a node (Junction) (36.9)

$\sum R|Q|Q = 0$ in a loop (36.10)

While Eq. (36.9) implies the principle of continuity in a hydraulic circuit, Eq. (36.10) is referred to as pressure equation of the circuit.

Pipe Network: Solution by Hardy Cross Method

- The distribution of water supply in practice is often made through a pipe network comprising a combination of pipes in series and parallel. The flow distribution in a pipe network is determined from Eqs(36.9) and (36.10).

- The solution of Eqs (36.9) and (36.10) for the purpose is based on an iterative technique with an initial guess in *Q*
- The method was proposed by Hardy-Cross and is described below:
    - The flow rates in each pipe are assumed so that the continuity (Eq. 36.9) at each node is satisfied. Usually the flow rate is assumed more for smaller values of resistance *R* and vice versa.
    - If the assumed values of flow rates are not correct, the pressure equation Eq. (36.10) will not be satisfied. The flow rate is then altered based on the error in satisfying the Eq. (36.10).
- Let Q_0 be the correct flow in a path whereas the assumed flow be Q. The error d*Q* in flow is then defined as

$$Q = Q_0 + dQ \qquad (36.11)$$

Let $h = R\,|\,Q\,|\,Q$ (36.12a)

and $h' = R\,|\,Q_0\,|\,Q_0$ (36.12b)

Then according to Eq. (36.10)

$\sum h' = 0$ in a loop (36.13a)

and $\sum h = e$ in a loop (36.13b)

Where *'e'* is defined to be the error in pressure equation for a loop with the assumed values of flow rate in each path.
From Eqs (36.13a) and (36.13b) we have

$$\sum (h - h') = e$$

or, $\sum dh = e$ (36.14)

Where dh (= h - h') is the error in pressure equation for a path. Again from Eq. (36.12a), we can write

$$\frac{dh}{dQ} = 2R\,|\,Q\,|$$

or, $dh = 2R\,|\,Q\,|\,dQ$ (36.15)

Substituting the value of dh from Eq. (36.15) in Eq. (36.14) we have

$$\sum 2R\,|\,Q\,|\,dQ = e$$

Considering the error dQ to be the same for all hydraulic paths in a loop, we can write

$$dQ = \frac{e}{\sum 2R\,|\,Q\,|} \quad (36.16)$$

The Eq. (36.16) can be written with the help of Eqs (36.12a) and (36.12b) as

$$dQ = \frac{\sum R\,|\,Q\,|\,Q}{\sum 2R\,|\,Q\,|} \quad (36.17)$$

The error in flow rate d*Q* is determined from Eq. (36.17) and the flow rate in each path of a loop is then altered according to Eq. (36.11).

The Hardy-Cross method can also be applied to a hydraulic circuit containing a pump or a turbine. The pressure equation (Eq. (36.10)) is only modified in consideration of a head source (pump) or a head sink (turbine) as

$$-\Delta H + \sum R\,|\,Q\,|\,Q = 0 \quad (36.18)$$

where ΔH is the head delivered by a source in the circuit. Therefore, the value of ΔH to be substituted in Eq. (36.18) will be positive for a pump and negative for a turbine.

Flow Through Pipes With Side Tappings

- In course of flow through a pipe, a fluid may be withdrawn from the side tappings along the length of the pipe as shown in Fig. 37.1
- If the side tappings are very closely spaced, the loss of head over a given length of pipe can be obtained as follows:

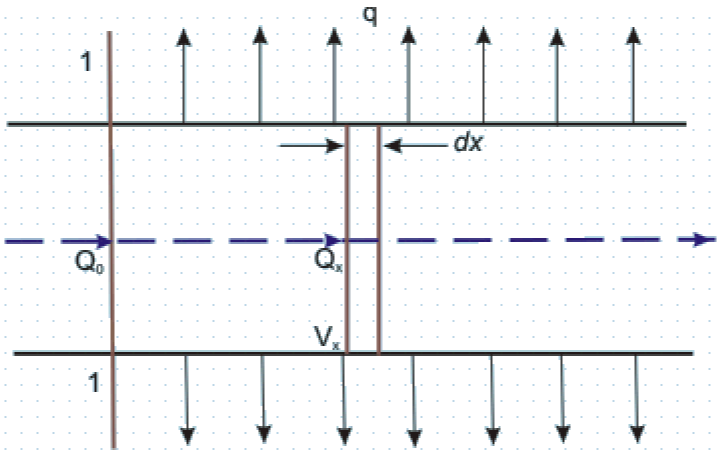

Fig. 37.1 Flow through pipes with side tappings

- The rate of flow through the pipe, under this situation, decreases in the direction of flow due to side tappings. Therefore, the average flow velocity at any section of the pipe is not constant.
- The frictional head loss dh_f over a small length dx of the pipe at any section can be written as

$$dh_f = f\frac{dx}{D}\frac{V_x^2}{2g} \qquad (37.1)$$

where, V_x is the average flow velocity at that section.

- If the side tappings are very close together, Eq. (37.1) can be integrated to determine the loss of head due to friction over a given length L of the pipe, provided, V_x can be replaced in terms of the length of the pipe.
- Let us consider, for this purpose, a Section 1-1 at the upstream just after which the side tappings are provided. If the tappings are uniformly and closely spaced, so that the fluid is removed at a uniform rate *q* per unit length of the pipe, then the volume flow rate Q_x at a distance x from the inlet Section 1-1 can be written as

$$Q_x = Q_0 - qx$$

where, Q_0 is the volume flow rate at Sec.1-1.

- Hence,

$$V_x = \frac{4Q_x}{\pi D^2} = \frac{4Q_0}{\pi D^2}\left(1 - \frac{q}{Q_0}x\right) \qquad (37.2)$$

Substituting V_x from Eq. (37.2) into Eq. (37.1), we have,

$$dh_f = \frac{16Q_0^2 f}{2\pi^2 D^5 g}\left(1 - \frac{q}{Q_0}x\right)^2 dx \qquad (37.3)$$

Therefore, the loss of head due to friction over a length *L* is given by

$$h_f = \int_0^L dh_f = \frac{8Q_0^2 f L}{\pi^2 D^5 g}\left(1 - \frac{q}{Q_0}L + \frac{1}{3}\frac{q^2}{Q_0^2}L^2\right) \qquad (37.4a)$$

- Here, the friction factor *f* has been assumed to be constant over the length *L* of the pipe. If the entire flow at Sec.1-1 is drained off over the length *L* , then,

$$Q_0 - qL = 0 \quad or \quad \frac{q}{Q_0} = \frac{1}{L}$$

Equation (37.4a), under this situation, becomes

$$h_f = \frac{8}{3}\frac{Q_0^2 f L}{\pi^2 D^5 g} = \frac{1}{3} f \frac{L}{D} V_0^2 \frac{1}{2g} \qquad (37.4b)$$

- where, V_0 is the average velocity of flow at the inlet Section 1-1.

  Equation (37.4b) indicates that the loss of head due to friction over a length *L* of a pipe, where the entire flow is drained off uniformly from the side tappings, becomes one third of that in a pipe of same length and diameter, but without side tappings.

Losses In Pipe Bends

- **Bends are provided in pipes to change the direction of flow through it. An additional loss of head, apart from that due to fluid friction, takes place in the course of flow through pipe bend.**
- **The fluid takes a curved path while flowing through a pipe bend as shown in Fig. 37.2.**

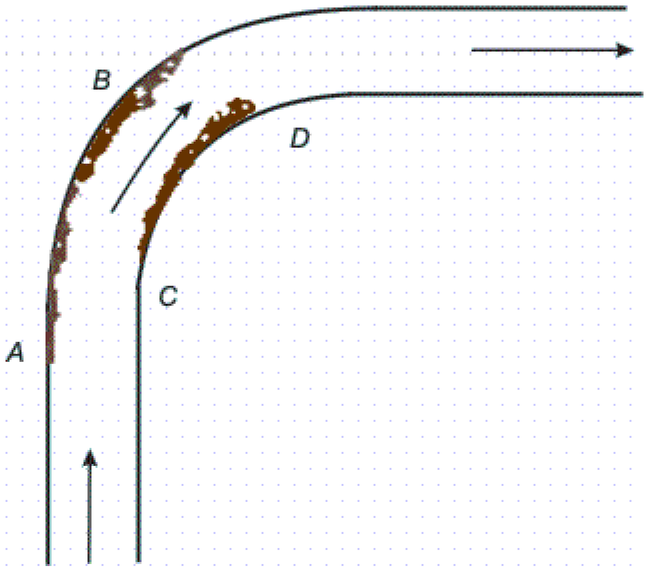

Fig. 37.2 Flow through pipe bend

Whenever a fluid flows in a curved path, there must be a force acting radially inwards on the fluid to provide the inward acceleration, known as centripetal acceleration .

This results in an increase in pressure near the outer wall of the bend, starting at some point *A* (Fig. 37.2) and rising to a maximum at some point *B* . There is also a reduction of pressure near the inner wall giving a minimum pressure at *C* and a subsequent rise from *C* to *D* . Therefore **between *A* and *B* and between C and D the fluid experiences an adverse pressure gradient** (the pressure increases in the direction of flow).

Fluid particles in this region, because of their close proximity to the wall, have low velocities and cannot overcome the adverse pressure gradient and this leads to a separation of flow from the boundary and consequent losses of energy in generating local eddies. **Losses also take place due to a secondary flow in the radial plane of the pipe because of a change in pressure in the radial depth of the pipe.**

This flow, in conjunction with the main flow, produces a typical spiral motion of the fluid which persists even for a downstream distance of fifty times the pipe diameter from the central plane of the bend. This spiral motion of the fluid increases the local flow velocity and the velocity gradient at the pipe wall, and therefore results in a greater frictional loss of head than that which occurs for the same rate of flow in a straight pipe of the same length and diameter.

The additional loss of head (apart from that due to usual friction) in flow through pipe bends is known as **bend loss** and is usually expressed as a fraction of the velocity head as $KV^2/2g$, where *V* is the average velocity of flow through the pipe. The value of *K* depends on the total length of the bend and the ratio of radius of curvature of the bend and pipe diameter *R/D*. The radius of curvature *R* is usually taken as the radius of curvature of the centre line of the bend. The factor *K* varies slightly with Reynolds number Re in the typical range of Re encountered in practice, but increases with surface roughness.

Losses In Pipe Fittings

- An additional loss of head takes place in the course of flow through pipe fittings like valves, couplings and so on. In-general, more restricted the passage is, greater is the loss of head.
- For turbulent flow, the losses are proportional to the square of the average flow velocity and are usually expressed by $KV^2/2g$, where *V* is the average velocity of flow. The value of *K* depends on the exact shape of the flow passages. Typical values of *K* are

Approximate Loss Coefficients, *K* for Commercial Pipe Fittings .

Type and position of fittings	Values of *K*
Globe valve,wide open	**10**
Gate valve, wide open	**0.2**
Gate valve, three-quarters open	**1.15**
Gate valve, half open	**5.6**
Gate valve, quarter open	**24**
Pump foot valve	**1.5**
90°elbow(threaded)	**0.9**
45°elbow(threaded)	**0.4**
Side outlet of T junction	**1.8**

- Since the eddies generated by fittings persist for some distance downstream, the total loss of head caused by two fittings close together is not necessarily the same as the sum of the losses which,each alone would cause.
  These losses are sometimes expressed in terms of an equivalent length of an unobstructed straight pipe in which an equal loss would occur for the same average flow velocity. That is

$$K\frac{V^2}{2g} = f\frac{L_e}{D}\frac{V^2}{2g} \; or \; \frac{L_e}{D} = \frac{K}{f} \qquad (37.5)$$

where, L_e represents the equivalent length which is usually expressed in terms of the pipe diameter as given by Eq. (37.5). **Thus L_e / D depends upon the friction factor *f* , and therefore on the Reynolds number and roughness of the pipe.**

Power Transmission By A Pipeline

- In certain occasions, hydraulic power is transmitted by conveying fluid through a pipeline. For example, water from a reservoir at a high altitude is often conveyed by a pipeline to an impulse hydraulic turbine in an hydroelectric power station. The hydrostatic head of water is thus transmitted by a pipeline. Let us analyse the efficiency of power transmission under this situation.

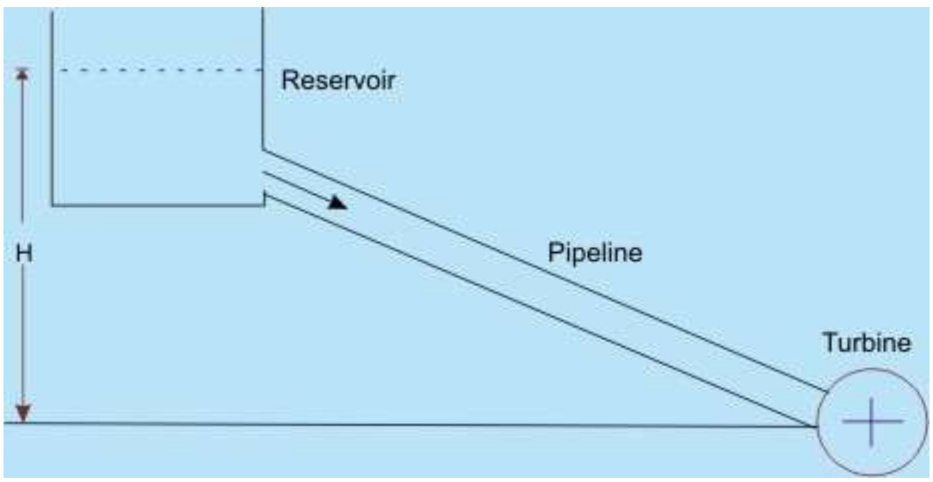

Fig. 37.3 Transmission of hydraulic power by a pipeline to a turbine

The potential head of water in the reservoir = H (the difference in the water level in the reservoir and the turbine center)

The head available at the pipe exit (or at the turbine entry) $= H_E = H - h_f$

Where h_f is the loss of head in the pipeline due to friction.

- Assuming that the friction coefficient and other loss coefficients are constant, we can write

$$h_f = RQ^2$$

Where *Q* is the volume flow rate and *R* is the hydraulic resistance of the pipeline. Therefore, the power available *P* at the exit of the pipeline becomes

$$P = \rho g Q H_E = \rho g Q (H - RQ^2)$$

For *P* to be maximum, for a given head *H*, *dP/dQ* should be zero. This gives

$$H - 3RQ^2 = 0 \quad (37.6)$$

or, $$RQ^2 = h_f = \frac{H}{3}$$

$[d^2 P / dQ^2]$ is always negative which shows that *P* has only a maximum value (not a minimum) with *Q*.

- From Eq. (37.6), we can say that maximum power is obtained when one third of the head available at the source (reservoir) is lost due to friction in the flow.

- The efficiency of power transmission η_p is defined as

$$\eta_p = \frac{\rho g Q \left(H - RQ^2\right)}{\rho g Q H} = 1 - \frac{RQ^2}{H} \quad (37.7)$$

1. The efficiency η_p equals to unity for the trivial case of *Q* = 0.

2. For flow to commence and hence η_p is a monotonically decreasing function of *Q* from a maximum value of unity to zero.

3. The zero value of η_p corresponds to the situation given by $RQ^2 = H \left(or\ ,\ Q = \sqrt{H/R}\right)$ when the head *H* available at the reservoir is totally lost to overcome friction in the flow through the pipe.

- The efficiency of transmission at the condition of maximum power delivered is obtained by substituting RQ^2 from Eq. (37.6) in Eq. (37.7) as

$$\eta_{at\ P = P_{max}} = 1 - \frac{H/3}{H} = \frac{2}{3}$$

Therefore the maximum power transmission efficiency through a pipeline is 67%.

Exercise Problems - Chapter 11

1. Calculate the force F required on the piston to discharge $500\ mm^3/s$ of water through a syringe (see Fig. 37.4), taking into account the frictional loss in the syringe needle only. Assume fully developed laminar flow in the syringe needle. Take the dynamic viscosity of water $\mu = 10^{-3}\ Ns/m^2$.

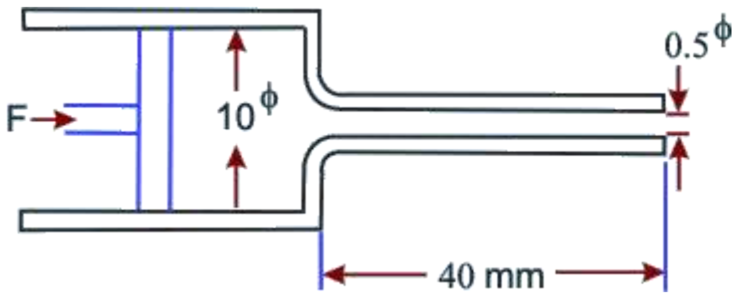

Figure 37.4

2. A hydrocarbon oil (viscosity 0.025 pa-s and density 900 kg/m^3) is transported using a 0.6 m diameter, 10 km long pipe. The maximum allowable pressure drop across the pipe length is 1 MPa. Due to a maintenance schedule on this pipeline, it is required to use a 0.4 m diameter, 10 km long pipe to pump the oil at the same volumetric flow rate as in the earlier case. Estimate the pressure drop for the 0.4 m diameter pipe. Assume both pipes to be hydrodynamically smooth and in the range of operating conditions, the Fanning friction factor is given by:

$$f = 0.079\, Re^{-0.25}$$

3. Two reservoirs 1 and 2 are connected as shown in the Fig 37.5 through a turbine T. Given the friction factor relation

$$\frac{1}{\sqrt{f}} = 2\log_{10}\left(Re\sqrt{f}\right) - 0.8$$

for the connecting pipes, the turbine characteristics $H = 10^3 Q\, m$ of water [Q in m^3/s] and an ideal draft tube at the discharge end, find (a) the volume flow rate between the two reservoirs and (b) the power developed by the turbine. Note:

$$f = \frac{(\Delta p/L)d}{\frac{1}{2}\rho U^2}$$

$$\mathrm{Re} = \rho U d / \mu$$

$$\rho = 1000 kg/m^3$$

$$\mu = 80 \times 10^{-5} pas.$$

Use an initial guess for power developed by the turbine as 1 MW. Show only **two iterations** . Also H is head available at the turbine.

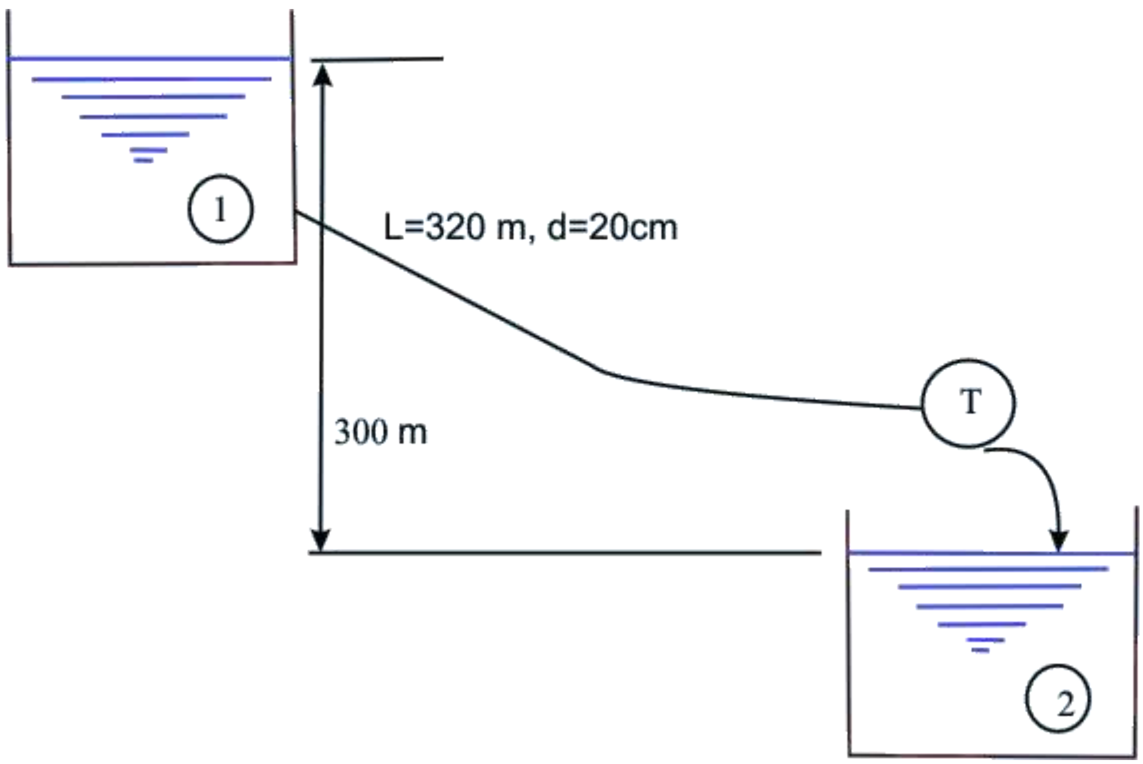

figure 37.5